To the Graduate Council:

We are submitting herewith a dissertation written by Robert Jay Engelbach entitled "Photochemical Investigation of Polycyclic Aromatic Hydrocarbons Vapor-adsorbed on Coal Fly Ash." We have examined the final copy of this dissertation for form and content and recommend that it be accepted in partial fulfillment of the requirements for the degree of Doctor of Philosophy, with a major in Chemistry.

Gleb Mamantov, Major Professor

Earl L. Wehry, Major Professor

We have read this dissertation and recommend its acceptance:

Accepted for the Council:

Vice Provost
and Dean of The Graduate School

PHOTOCHEMICAL INVESTIGATION OF POLYCYCLIC AROMATIC HYDROCARBONS VAPOR-ADSORBED ON COAL FLY ASH

A Dissertation

Presented for the

Doctor of Philosophy

Degree

The University of Tennessee, Knoxville

Robert Jay Engelbach

December 1986

ACKNOWLEDGEMENT

The author wishes to express his deepest appreciation to a host of people who have contributed to this project. This includes co-workers Dr. Robert Yokley and Dr. Arlene Garrison, with whom a large part of the earlier experiments were coordinated; Mr. Jonathan Krueger, who provided much needed "missing data"; Mr. L.H. Norman and Mr. Arthur Pratt, for their mastery in the art of making chromatographic columns; Dr. Don Dunstan, for his additional insights concerning the measurement of the heats of adsorption; Mr. John Taylor and Mr. James Hurley, for their expertise in electronic troubleshooting; and to Mr. Gary Young, for a superb job in typing this dissertation.

Further, this author would like to thank the Department of Energy for financially supporting this research and The University of Tennessee's Department of Chemistry for lending this author its new gas chromatograph when not in classroom use.

Certainly, this author would like to thank Dr. Gleb Mamantov for his overall wisdom and encouragement throughout the course of this research. Finally, I would like to thank Dr. Earl L. Wehry for his expert guidance in resolving many difficult theoretical and laboratory-oriented problems encountered in this work, and for his diligence in thoroughly reviewing an earlier, handwritten draft of this dissertation.

ABSTRACT

Five polycyclic aromatic hydrocarbons (PAHs) were deposited from the vapor phase onto the surfaces of eight different types of coal fly ash. This procedure generated samples of PAH-laden fly ash in a manner which simulated the actual process of adsorption occurring in the gaseous effluent of a coal-fired electric power plant.

Samples were then irradiated with a light source similar in spectral distribution to sunlight. The adsorbed PAHs were extracted from the ash, and the decrease in the PAH concentration on the ash due to irradiation was measured and assumed to be the result of photochemical decomposition. The percentage photochemical decomposition was calculated for each combination of a single PAH compound adsorbed onto a single type of fly ash. The extent of this decomposition was observed to vary from ash to ash. Apparent decomposition of adsorbed PAHs was found to be generally more extensive on ash surfaces which were relatively photo-reflective. In addition, the extent of decomposition was generally suppressed on ashes for which the percentage recovery of pyrene by solvent extraction was lower, and for which the heat of adsorption of pyrene was more exothermic. These results suggested that more strongly adsorbed PAHs were less susceptible to photochemical transformation.

Measurement of the percentage of vapor-deposited pyrene recovered by solvent extraction was obtained with the help of a flame ionization detector to measure the amount of pyrene depositing on the ash. The heat of adsorption was determined by injecting solutions of PAHs onto a gas chromatographic column packed with fly ash, and varying the column

temperature for successive injections at the same PAH concentration; results were improved by using small amounts of fly ash and, in most cases, by diluting the ash six-fold with a nonadsorptive solid particulate substrate.

For samples of PAH deposited on fly ash from the solution phase, the percentage recoveries by solvent extraction were frequently larger than the percentage recoveries for samples deposited from the vapor phase, indicating the possibility of competition of solvent with PAH for the most active adsorption sites in "solution deposition" experiments.

TABLE OF CONTENTS

PAGE

PAGE

LIST OF TABLES

PAGE

LIST OF FIGURES

PAGE

CHAPTER 1

INTRODUCTION

1.1 Environmental Hazard: Potential Oncological Activity

This research concerns itself with two substances which are released into the atmosphere by the combustion of coal, and which may interact to form a potential hazard to the environment. The first substance is a fine particulate residue called coal "fly ash."

Coal fly ash is composed of the non-combustible material present in the original coal which is expelled upward from the coal furnace. Material which is filtered out of the furnace effluent by electrostatic precipitators is sometimes referred to as "precipitator ash," but is often included in the general category of "fly ash."

Coal fly ash escapes into the atmosphere at the rate of millions of tons per year.[1] It accounts for about one fourth the total mass of particulate matter released into the atmosphere in the United States.[2] Emission of coal fly ash is expected to continue increasing along with our increasing consumption of coal as an industrial fuel.

Although coal fly ash has been shown to contain "inorganic" constituents[1-3] such as compounds of chromium, iron, manganese, selenium, mercury and lead, which may be environmentally hazardous, there is considerable concern over the harmful biological effects of certain "organic" constituents found to be present in coal fly ash. Of particular concern is a class of compounds known as polycyclic aromatic hydrocarbons (PAHs).[1,2] These PAHs are produced as an undesirable product of the incomplete combustion of coal and are thought[4,5,6] to

adsorb onto the surfaces of fly ash from the vapor phase at moderate temperatures (100 - 300°C) during emission from a coal furnace.

The oncological (tumor producing) activity of PAHs and related compounds has been well documented.[7,8] Many PAHs and their derivatives formed via air oxidation and metabolism in the body are either direct-acting mutagens or precursors of metabolic products which are direct-acting mutagens. The Ames Salmonella typhimurium assay[9] is a rapid bacterial test for mutagenicity which has been frequently applied to organic extracts of particulate matter. Such extracts of coal fly ashes and other airborne particulates, such as soot and diesel particulates, have been shown to be mutagenic.

A number of independent studies have indicated that the mutagenicity of fly ash extracts is caused by volatile organic compounds rather than less volatile inorganic constituents. One study[10] showed that mutagenicity of the extract did not appear if the fly ash sample was first heated to 350°C prior to extraction. In another experiment,[10,11] samples of ash were taken from an electrostatic precipitator positioned close to the combustion zone of a coal furnace, so that the ash samples had been maintained at a very high temperature. Although extracts of fly ash emitted from the stacks were mutagenic, extracts of the precipitator ash were not. This suggested that the volatile organic compounds passed through the precipitator at high temperatures and deposited on the emitted fly ash at considerably lower temperatures.

In yet another experiment[12] using diesel particulates, the organic extract was separated into acidic, basic, and neutral fractions. The

neutral fraction was further separated into "nonpolar," "moderately polar," and "highly polar" fractions. The "moderately polar" fraction was found to account for over half of the total mutagenicity of the extract, and contained PAH-related compounds (such as oxygenated PAHs, including ketones, ethers, and hydroxyl derivatives) as its most abundant class of species. Furthermore, other researchers[6,12,13] have attributed mutagenicity of particulates to PAHs, PAH derivatives, and PAH oxidation products.

1.2 Environmental Hazard: Stability and Decomposition

The harmful effects of adsorbed PAHs may not only result from the original PAH, but also from interaction of PAH products created by exposure of the adsorbed PAH molecules to atmospheric gases and sunlight. Therefore, it is important to study the chemical stability of adsorbed PAHs.

The high susceptibility of PAHs to photochemical decomposition is well known.[14-18] Efficient photochemical decomposition has been observed for pure solid PAHs, PAHs in solution, and PAHs adsorbed on many common solid substrates such as sand, glass, alumina and silica gel. Korfmacher, et al.[14] and others[19-21] have demonstrated that PAHs adsorbed on many fly ashes exhibit a resistance to photochemical decomposition when compared with PAHs adsorbed on most other solid substrates. Another group,[22] studying photochemical decomposition of benzo[a]pyrene incorporated into smoke, found that the decomposition rate increased with increasing particle surface area. It is evident from these early decomposition studies that the chemical and physical

properties of adsorbent particles have a substantial effect on the stability of adsorbed PAHs to photochemical decomposition.

Such observations are significant from an environmental standpoint, because they imply that the residence times of adsorbed PAHs in the atmosphere depend partly on the characteristics of the adsorbent carriers. Thus, estimates of atmospheric residence times of PAHs obtained from laboratory observations of non-adsorbed PAHs (or of PAHs on adsorbents different from the actual atmospheric particulate matter) may not be applicable.

Irradiation in air of benzo[a]pyrene adsorbed on silica was observed to produce a large variety of oxidation products which were known mutagens.[23] When PAHs adsorbed on glass fiber filters were exposed to nitrogen dioxide and ozone, extremely potent direct-acting mutagens were formed.[13,24] These experiments demonstrated the potential for a distribution of environmentally hazardous compounds to be formed photochemically or nonphotochemically on particulate surfaces during transport through the atmosphere.

When maintained in the dark and exposed to air, several PAHs have been observed to decompose on coal fly ash, but not on the common adsorbents such as silica gel, alumina and glass.[21,25] Relative to these common adsorbents, the fact that coal fly ash suppresses photochemical decomposition of some PAHs and accelerates nonphotochemical decomposition on others suggests the existence of strong adsorbate/adsorbent interactions. Behymer and Hites[26] recently reported that fifteen different PAHs had nearly identical photolytic half-lives when adsorbed on a coal fly ash and subjected to

illumination, compared with a very large range of half-lives for the same compounds adsorbed on silica gel and alumina. These results were interpreted as demonstrating that the photolytic process on the fly ash was independent of the structure of the PAH, but strongly dependent on the physical and chemical nature of the substrate.

In addition to adsorbate/adsorbent interaction, photon/adsorbent interactions have also been postulated. Güsten, et al.[27] observed that the photochemical decomposition of PAHs adsorbed on metal oxides was accelerated if the metal oxides were also photoconductive in the spectral range of incident radiation. It is conceivable that certain metal oxides in the fly ash surface may thus act as sensitizers, absorbing light energy and releasing it in the form of excited electrons that are transported to adsorbed PAH molecules, thereby inducing or facilitating chemical oxidation or degradation.

Another photon/adsorbent interaction which may effect the susceptibility of adsorbed PAHs to phototransformation is the "inner filter" effect, as suggested by Korfmacher, et al.[14] The "inner filter effect" may be defined generally as a decrease in the apparent efficiency of a photochemical reaction caused by absorption of incident light by some constituent of the sample other than the intended reactant. In terms of the PAH/fly ash samples, an "inner filter" effect can occur by direct absorption of incident light by the ash, decreasing the number of incident photons that can interact with adsorbed PAH molecules. Such an effect is likely to be significant if (a) the ash absorbs strongly in the spectral regions in which PAHs absorb, and if

(b) the ash contains pore structure that permits adsorbed PAH molecules to be situated some distance from the "surface" of the ash particle.

Occurrence of an "inner filter" effect would result in slower decomposition rates for fly ashes that are dark (absorb strongly) in the region of the spectrum where the PAH molecule absorbs strongly, and for ashes that have an abundance of "cave-like" pores which are readily accessible to adsorbate molecules, but not to radiation.

These reported studies have shown that some of the factors determining the environmental impact of adsorbed PAHs--such as the potential for generation of additional hazardous products by photochemical or non-photochemical transformation--may be strongly influenced by a variety of chemical and/or physical phenomena associated with the nature of the particulate surfaces upon which these compounds are adsorbed. A study of the apparent decomposition of PAHs adsorbed on a variety of coal fly ashes is reported in this dissertation, with the primary objective being to elucidate these characteristics of coal fly ashes (and other solid adsorbents) that can affect the photochemical reactivity of adsorbed PAHs.

1.3 Research Plan and Outline of Dissertation

For the purpose of elucidating which characteristics of PAHs and fly ashes were significant in affecting decomposition, we decided to study the decomposition of five PAH compounds, using eight dissimilar varieties of fly ashes as adsorbents. Additional adsorbents such as silica gel and flaked graphite were studied for comparison. Samples were prepared, each containing one PAH compound adsorbed onto one

variety of fly ash (i.e., no attempt was made to examine the photoysis of adsorbed PAH mixtures).

The PAHs studied are listed in order of increasing molecular size with abbreviations in parenthesis: anthracene (An), phenanthrene (Ph), pyrene (Py), benz[a]anthracene (BaA), and benzo[a]pyrene (BaP). Molecular backbone structures are shown in Figure 1- 1.

Samples of PAH adsorbed on substrates were produced artificially by allowing vapor phase PAHs to adsorb onto the surfaces of substrates at moderately high temperatures (100 - 200^{o}C). These conditions simulated the adsorption process in gaseous coal plant effluents. Therefore, we considered these "vapor deposited" samples to be more like actual environmental samples than those produced by allowing PAHs to adsorb onto substrates from the liquid phase, producing "solution-deposited" samples. (This aspect is discussed in more detail in Section 2.2).

A modification of the vapor deposition apparatus described by Korfmacher and Miguel[28,29] was used to produce the PAH/adsorbent samples. This equipment utilized a stream of nitrogen to carry vaporized PAH through a bed of adsorbent material. The bed was maintained at a temperature above the melting point of the PAH in order to minimize condensation of the PAH. PAH was deposited onto the adsorbent surface from the vapor phase as the stream passed through the bed.

After preparing the PAH/fly ash samples, our major effort focused on investigating the photochemical decomposition of the adsorbed PAH. A portion of a PAH/fly ash sample was exposed to a light source, the

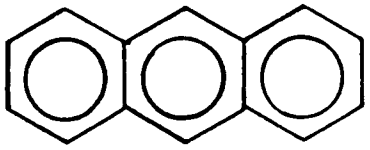

ANTHRACENE

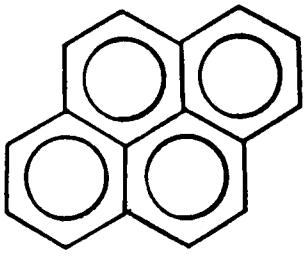

PYRENE

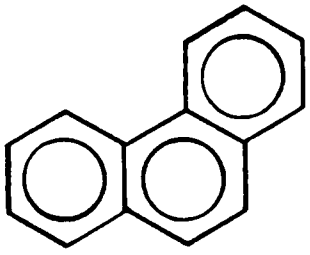

PHENANTHRENE

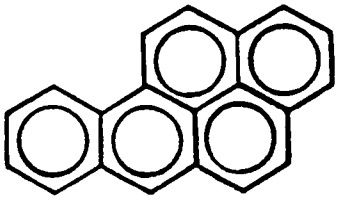

BENZO [A]PYRENE

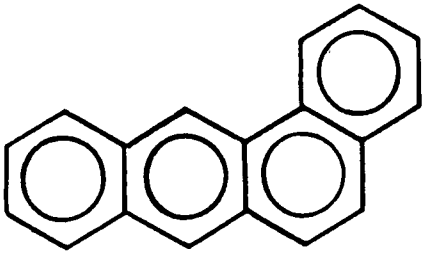

BENZ[A]ANTHRACENE

FIGURE 1-1. Molecular structures of PAHs

output of which exhibited a spectral distribution similar to sunlight. The PAH content of the exposed portion was then compared with that of the unexposed portion of the sample. The difference in PAH content between the exposed and unexposed portions was presumed to indicate the amount of PAH that decomposed upon illumination. Analysis of PAH content was accomplished by extracting the sample portions with methanol and then quantifying the PAH content of the extracts using UV/VIS absorption spectrophotometry.

Very few photochemical decomposition products were found in the extracts by Fourier transform infrared spectroscopy or gas chromatography. Therefore, the assumption that the decrease in extractable PAH after irradiation was due entirely to photochemical decomposition has not been conclusively verified. It is possible to postulate that alternative mechanisms may have contributed to the decrease in extractable PAH. For instance, photo-excitation of adsorbed PAH molecules may have induced migration of these molecules to more active adsorption sites, from which the adsorbed PAH molecules were unextractable.

Strong evidence indicating the occurrence of photochemical decomposition of anthracene or benz[a]anthracene adsorbed on silica gel and TX ash consisted of observations that the surfaces of these samples turned red upon irradiation, similar to the color change observed for the process of photochemical decomposition in solution of these two PAHs. Traces of anthraquinone, reflecting a very small fraction of the total amount of anthracene lost due to irradiating, were detected in the extract of irradiated samples containing silica gel originally deposited

with anthracene, but no products were detected in the extracts for anthracene adsorbed on TX ash.

The surfaces of the extracted substrates retained their original color after extraction with methanol. This suggested that polar products of photochemical decomposition, such as anthraquinone, were very strongly adsorbed on the substrate. Such behavior was assumed to occur on all fly ashes, although most ashes were too dark for any color change on their surfaces to be detected by manual inspection.

Nevertheless, the occurrence of photochemical decomposition remains to be verified conclusively. Therefore, the term "photochemical decomposition" as used in this dissertation is to be regarded as a tentative cause for the decrease in extractable PAH due to irradiation.

The first part of Chapter 2 contains a detailed description of sample preparation, irradiation and analytical procedures. It includes an explanation of why these methods were selected. The results for these experiments are reported in the remainder of Chapter 2, along with some correlations between decomposition behavior and chemical/physical properties of PAHs and fly ashes. Some properties of fly ash surfaces were previously reported by Yokley[19,30]; these data are used where necessary in this dissertation with appropriate attribution. Some additional data obtained by Dr. Arlene Garrison and Jonathan Krueger also are cited where necessary, again with attribution.

Another major effort discussed in the dissertation involves the quantification of the amount of PAH on ash samples. The reason for initially proceeding with this work arose from indications that our solvent extraction procedures do not quantitatively remove all the

adsorbed PAH from fly ashes.[31] We thus needed a quantitative method to accurately measure the total amount of PAH depositing on our ash samples, and to assess the efficiencies of the solvent extraction procedures. This objective was accomplished by placing a flame ionization detector (FID) into the N_2/PAH vapor flow path in the sample-preparation apparatus directly downstream from the ash bed. The FID was of the kind commonly used to measure mass flow rates of vaporized organic samples in a gas chromatograph. Refinements in the original vapor deposition apparatus were made to facilitate such quantitative measurements. The techniques used in these investigations and corresponding results are described in detail in Chapter 3.

By examining a variety of chemical and physical characteristics of the fly ashes, we were able to correlate some of these characteristics with the extent of apparent photochemical decomposition of the adsorbed PAHs. These results strongly suggested that an examination of the parameters that described the "interaction" of PAH with the fly ash surfaces, rather than individual characteristics of either the PAHs or the fly ashes, was needed. Two such "interaction" parameters--the heat of adsorption (ΔH_a) of PAH for the surface, and the distribution coefficient (K_D) for the ratio of the concentration of adsorbed PAH to the concentration remaining in the vapor phase at equilibrium--were investigated by gas-solid chromatographic methods, using various fly ashes as the chromatographic stationary phases.

Solutions of PAHs in a presumably inert organic solvent were injected into a chromatographic column packed with fly ash. The retention times of these PAH samples on the column were combined with

temperature and surface area data to obtain the thermodynamic parameters, which in turn were examined for empirical relationships to the photochemical reactivity of adsorbed PAHs. The theory, adaptation and results of these measurements are described in Chapter 4.

Finally, Chapter 5 contains a discussion of aspects of the previous three chapters as they interrelate to each other.

CHAPTER 2

APPARENT PHOTODEGRADATION OF PAHS ADSORBED ON COAL FLY ASH

2.1 Preliminary

The objective of these studies was to examine the apparent photochemical decomposition of PAHs adsorbed on the surfaces of a variety of fly ashes. In these experiments, a PAH was deposited from the vapor phase onto a solid substrate and then a portion of this PAH/substrate sample was irradiated. Portions of non-irradiated and irradiated samples were extracted with methanol and analyzed quantitatively via optical spectroscopic methods. The decrease, due to irradiation, in the quantity of PAH (per gram of substrate) detected in the extract was used to calculate the percentage photochemical decomposition of PAH adsorbed on the substrate. The percentage decomposition of adsorbed PAHs was obtained for eight coal fly ashes and four conventional laboratory adsorbents listed along with their abbreviations in Table 2-1.

In this chapter and ensuing chapters, attempts have been made to correlate these data with chemical and physical properties of the PAHs and substrates.

2.2 Sample Preparation

The large number of PAH compounds contained in an environmental particulate sample is such that the concentration of any one PAH is usually very small. Thus, it is generally impractical to study decomposition of individual PAHs as they occur in environmental

TABLE 2-1

Coal fly ashes and model substrates

Abbrev.	Substrate Name and Source
	COAL FLY ASHES
KA	Kaneb Coal (McIntosh power plant, Lakeland, Fla.)
EA	East Appalachian bituminous coal[32]
NM	New Mexico subbituminous coal[32]
ET	East Tennessee bituminous coal[32]
TX	Texas lignite[32]
WK	Western Kentucky bituminous coal[32]
IL	Illinois bituminous coal[32]
AR	Alpha Resources Inc., lot no. 720-1, Stevensville, MI.
	MODEL SUBSTRATES
Silica	Silica Gel, 70-230 mesh, Brinkman Instruments, Inc., Westbury, NY
Alumina	Alumina, neutral, Brockman Activity I, 80-200 mesh, Fisher Scientific, Inc.
Glass	Controlled porosity glass, 37-74 μm dia., 100 Å avg., pore radius, Pierce Chemical Co., Rockford, IL
Carbon	Flaked graphite, Southwestern Graphite Co., Burnet, TX

samples; accordingly, samples prepared in the laboratory were used in this work.

We deposited PAHs on samples of coal fly ash which had been degassed with nitrogen at moderate temperatures (100 - 200°C). Several of these degassed ash samples had been analyzed previously for detectable organic residues using a Soxhlet extraction technique described in Section 2.3. No detectable organic residues were found, indicating that these degassed ash samples were relatively free of adsorbed organic constituents. We deposited at conditions similar to those occurring in a coal furnace effluent, namely, moderate temperatures[4,5,6] of 100 - 200°C with PAH absorbing from the vapor phase. Only one PAH was deposited on any particular adsorbent, thereby eliminating interactions between PAHs and the problems of simultaneous detection of several PAHs. In addition, the concentration of PAH depositing on each sample could be carefully controlled.

Our method of sample preparation was a "vapor deposition" technique rather than "solution deposition." "Solution depositions" are commonly performed by placing a weighed amount of particulate substrate into a solution containing a known concentration of PAH in a volatile solvent. The solvent is evaporated to dryness, allowing all the PAH to deposit on the substrate from the evaporating solution phase. The speed and convenience of the solution deposition method has made it a popular technique. In a recent publication[25] it is referred to as "static doping" and is described in detail.

Our major objection to solution deposition is that the conditions in a solution or suspension are presumably radically different from

those in a coal plant exhaust, where temperatures are much higher and there are no chemical interferences from solvent molecules competing with PAH molecules for adsorption sites. Vapor depositions were accomplished using a modified version of the apparatus employed by Miguel and Natusch[29] and Korfmacher.[21] Yokley[30] included a description of the diffusion cell (PAH generator), adsorption cell (expanded bed reactor), and 4-port valve used in this apparatus, with an emphasis on the physical construction of these elements rather than an explanation of how the apparatus works as a whole. Therefore, an explanation is briefly presented here and step by step procedures are described in Appendix 2.1.

In the apparatus shown in Figure 2-1 a steady stream of nitrogen gas enters the PAH generator in Oven 1. With Oven 1 "off" (at room temperature), the nitrogen continues through glass tubing to a 4-port valve (Valco Instruments Company, Houston, Texas, model V-4- HT) in Oven 2. When the temperature of Oven 1 is raised (to a temperature below the melting point of the PAH), PAH vapor forms above the solid and is drawn into the stream of nitrogen above it. The mass flow rate (MFR) of PAH, measured in μg/hr, has been shown by experimentation to remain virtually constant (±2%) for a given set of operating conditions (nitrogen flow rate, backpressure, temperature, surface area of solid PAH exposed). The MFR can be easily increased or decreased by increasing or decreasing the temperature of Oven 1.

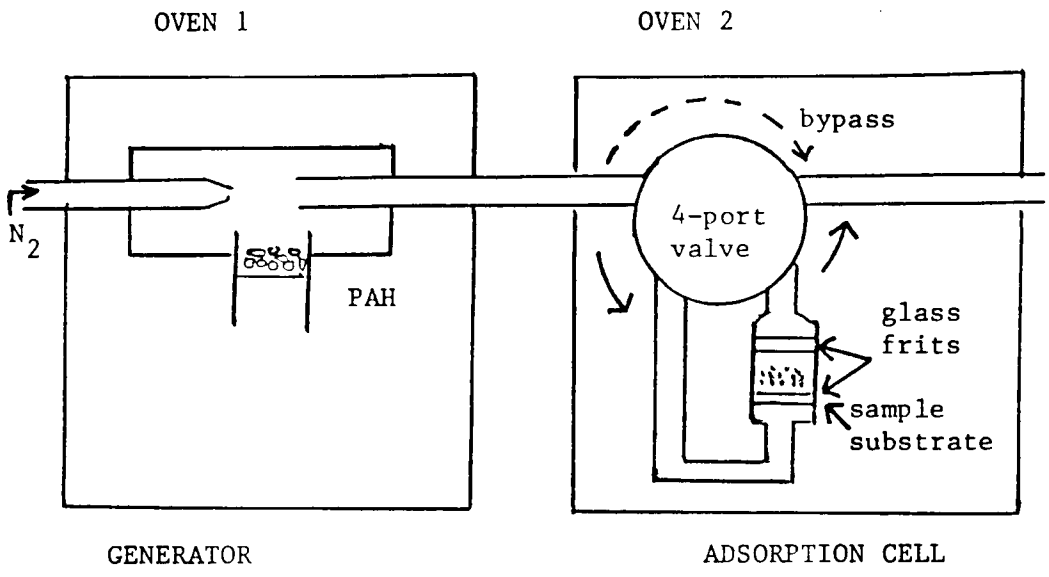

FIGURE 2-1. Simplified diagram of vapor deposition apparatus

The 4-port valve in Oven 2 may be set in either of two positions:

(1) in the "bypass" position, which allows the vapor flow to be shunted directly to the exit, thus bypassing the adsorption cell; or

(2) in the "cell" position, in which the flow stream is directed through the sample, contained in the adsorption cell, before looping back to the exit.

PAH is deposited on the sample according to the detailed procedure set forth in Appendix 2.1. Analysis of the quantity of PAH deposited on the previous sample was used to estimate the deposition time required to deposit a desired quantity of PAH on the next sample.

2.3 Analysis of Samples

Direct analysis of adsorbed PAHs on fly ash substrates has not been developed successfully to this date. Therefore, all analysis performed in this work entailed solvent extraction of PAHs from an adsorbent, followed by quantification of the PAH concentration in each extract. In comparison with several extraction techniques that we tested (described on pages 19 through 21), Soxhlet extraction using methanol as solvent produced the best combined performance of efficiency and reproducibility. As in virtually any extraction process, the recovery of adsorbed PAH may be less than 100%, and the extraction efficiency may vary from one PAH to another, and from one fly ash surface to another. However, we believe that the Soxhlet extractions, although not necessarily quantitative, were sufficiently efficient and reproducible to detect significant changes in adsorbed PAH concentrations due to chemical decomposition.

We used a miniaturized version of a conventional Soxhlet system known as a micro-soxhlet extractor (Fisher Scientific Company, #20-650). We weighed 50-75 mg portions of sample with cellulose thimbles, placed them into micro-soxhlet extractors which were kept in a darkened hood, and extracted with methanol for 24 hours. Reproducibility was maximized by adjusting the temperature of the Soxhlet flask so that the Soxhlet reservoir would empty every 7-12 minutes. At cycle times shorter or longer than this, the efficiency of extraction was observed to decrease and also to vary from extractor to extractor. The extract was later quantitated for PAH spectroscopically.

Methanol yielded the highest extraction efficiency among a group of non-hazardous solvents which did not exhibit appreciable absorbance in the visible and near UV spectral region. This group included toluene and acetonitrile, giving extraction yields of 99 μg/g and 124 μg/g respectively, compared to 149 μg/g using methanol to extract pyrene from ET ash.

In an attempt to improve the recoveries of the extractions, a variation of the Soxhlet extraction was constructed after a design by Aue, et al.[33] This design allowed solvent to flow continuously instead of in cycles, a feature which improved Aue's extraction efficiency and speed. However, when adapted to our smaller-sized extractors, it was impossible to obtain a constant flow without continuously adjusting a flow valve. This required too much attention to be practical.

Several other extraction techniques were attempted and compared. Yokley[30] mentioned an acid etching technique and a method using

ultrasonic stimulation (using a sonicator commonly used to emulsify biological suspension). Neither of these produced acceptable results.[27]

We also tried high-temperture extraction (HTE) as described by Renkes, et al.[34] wherein PAHs were extracted from particulate matter with a high-boiling solvent at moderately high temperatures (240°C) and short extraction times (5 min). The extraction procedure consisted of suspending 50-100 mg of sample in 2 ml of solvent in a test tube. The tube was placed in a molten salt bath (containing an equimolar mixture of $NaNO_3$ and KNO_3) maintained at 240°C. The tube was positioned in the bath for a heating time of 5.00 minutes and then its contents were filtered through a glass microfiber filter (Whatman 934-AH). Samples of phenanthrene adsorbed on KA and carbon substrates were extracted with decyl alcohol. The filtered solutions were then quantified by UV absorption. The amount of phenanthrene that was extracted from the KA sample increased with heating time, yielding 107% of the Soxhlet value after ten minutes of heating. The amount extracted from carbon decreased from 10% to 0% of the Soxhlet value when the heating time was increased from five to ten minutes. The filtered residues from the HTE of the carbon sample were extracted with methanol via Soxhlet, to see if any phenanthrene had been left unextracted on the carbon. No detectable phenanthrene was found. Originally this was interpreted as meaning that the phenanthrene decomposed thermally at 240°C. There is also the possibility that phenanthrene may have diffused more readily into micropores at the higher temperatures, from which desorption (and therefore extraction) would be slower[35]. Because of the low recovery of phenanthrene from carbon by HTE, in addition to low yields from

additional tests using pyrene, and tests using other solvents (hexadecane and diphenylmethane), further development of this technique was abandoned.

Another method of extraction investigated was the elution of samples with solvent at room temperature. This technique was used by Behymer and Hites[26] and Soltys, et al.[25] to extract PAHs from fly ash. In our procedure, elution was accomplished by plugging the narrow end of a Pasteur pipet with a portion of a glass microfiber filter (Whatman 934-AH).

About 50-100 mg of sample was placed above the plug and 50-100 ml of methanol was forced through the pipet using 5 psi of nitrogen, as shown in Figure 2-2. Flow rates were on the order of 10 ml/min. A volume of 200 ml of methanol was required for elution to be complete, as evidenced by the absence of detectable PAH in subsequent eluent. A value of 764 ± 12 mg/g of pyrene on KA ash was obtained, compared with a Soxhlet determined value of 813 ± 41 mg/g; thus the elution technique was slightly less efficient than the Soxhlet technique at high adsorbate concentrations using methanol as solvent. Experiments with 1,2 dichloroethane as eluting solvent yielded virtually the same results. Compared with the Soxhlet method, this method was much faster, and would probably be advantageous in extracting unstable compounds; however, each sample would require more personal attention than the Soxhlet method and a large volume of solvent would be needed.

After Soxhlet extracts were obtained they were analyzed for PAH concentration using UV/VIS absorption spectrophotometry. Fluorescence

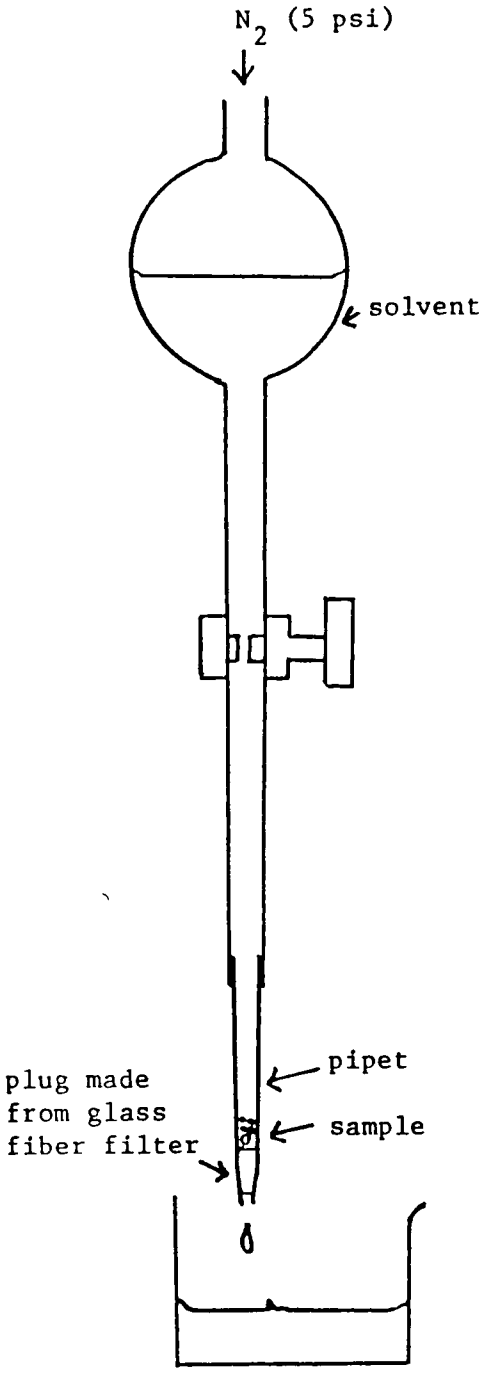

FIGURE 2-2. Elution at room temperature

detection was used for PAH concentrations too small to detect by UV absorption.

Because Beer's-law plots were linear with virtually zero intercepts, only a single standard in the approximate concentration range of the samples was necessary for absorption measurements. Very low concentration determinations having noisy absorption spectra, as well as all fluorescence determinations, were performed using two standards of different (known) PAH concentration.

2.4 Illumination Techniques

Approximately 300-400 mg of fly ash on which a PAH had been deposited was placed in a quartz irradiation cell (Figure 2-3) and exposed to radiation from a Cermax Xenon Illuminator (ILC Technology, Sunnyvale, California, model LX300UV), which, according to the manufacturer, exhibited a fairly uniform output of about 0.04 to 0.08 W/nm over the 250 nm to 750 nm wavelength range. The cell was positioned 34-38 cm from the lamp and inserted into the vacuum port of a rotary evaporator, where it was held in place by a partial vacuum from a water aspirator. The cell was rotated about its long axis by the rotary evaporator motor. The motor life was prolonged by allowing cold water to run through copper tubing coiled around its exterior.

A 20 cm filter, containing distilled water was placed between the lamp and the irradiation cell. The filter had quartz windows at both ends and was cooled by a water jacket. The purpose of the water filter was to eliminate near infrared radiation from the lamp which would otherwise heat the sample and possibly induce thermal decomposition of

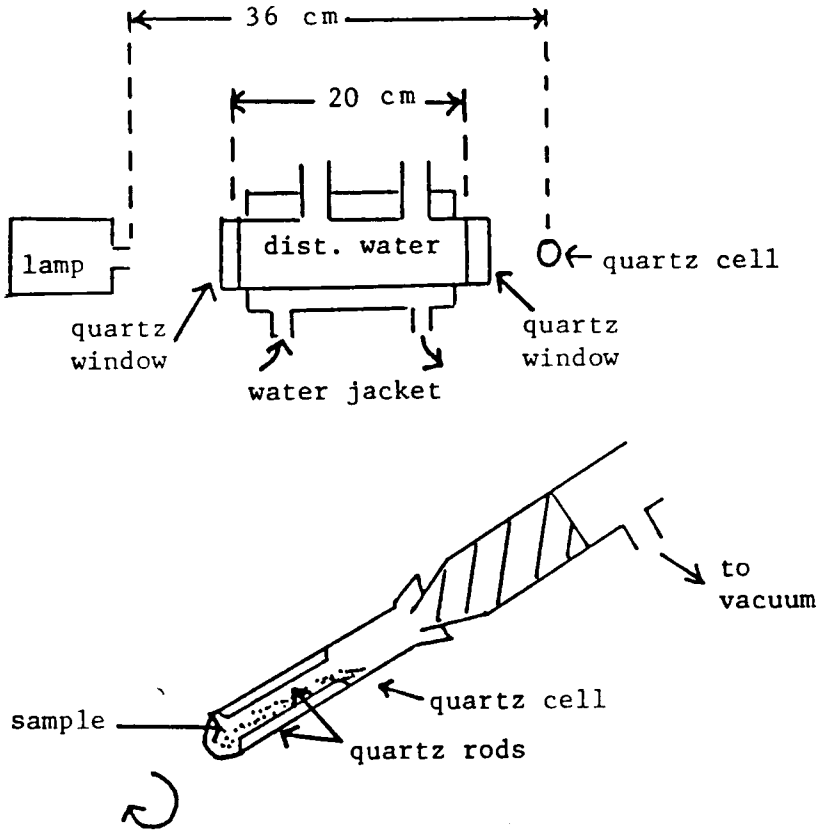

FIGURE 2-3. Irradiation apparatus

adsorbed PAH. Further details of the irradiation cell were described by Yokley.[30]

The nonphotochemical contribution to decomposition was measured by rotating an identical sample portion in the irradiation cell, but with the lamp off, the room darkened, and the irradiation cell covered with aluminum foil.

2.5 Observations

2.5.1 Data for Apparent Photochemical Decomposition

Approximately one gram of sample substrate was degassed overnight with nitrogen at the temperature intended to be used for deposition. Approximately 50-500 mg of PAH was then deposited on the sample. A portion of this sample was later analyzed by Soxhlet extraction, giving a value of the adsorbate concentration for the "untreated sample." A second portion was placed in an irradiation cell and rotated in the absence of light for 24 hours; it was then analyzed, giving a value for the "rotated" sample. A third portion was simultaneously illuminated and rotated for 24 hours, giving a value for the "rotated and illuminated" sample.

Tables 2-2 and 2-3 contain data for the apparent photo- and nonphotochemical decomposition for phenanthrene and benz[a]anthracene, respectively. The percentages of photo-and nonphotochemical decomposition for each sample were later calculated as:

$$\% \text{ nonphoto} = \frac{\text{rotated - untreated}}{\text{untreated}} \times 100\% \qquad (2\text{-}1)$$

$$\% \text{ photo} = \frac{\text{rot. \& ill. - rotated}}{\text{untreated}} \times 100\% \qquad (2\text{-}2)$$

TABLE 2-2

Photo- and nonphotochemical decomposition of phenanthrene on coal fly ash[a] and model adsorbents.

1	2	3	4
Substrate	Untreated	Rotated	Rot. & ill.
KA	532 ± 25	456 ± 56	509 ± 75
EA	345 ± 29	327 ± 49	342 ± 34
NM	753 ± 69	732 ± 16	607 ± 49
ET	222 ± 5	181 ± 2	189 ± 8
ET	228 ± 18	148 ± 8	159 ± 9
ET	141 ± 8	103 ± 2	106 ± 10
TX	442 ± 12	416 ± 12	353 ± 26
WK	na[c]	na	na
IL	na	na	na
AR	142 ± 14	125 ± 7	119 ± 7
Silica	220 ± 10	238 ± 10	60 ± 6
Alumina	2508 ± 81	2362 ± 154	1808 ± 65
Alumina[b]	204 ± 11	205 ± 7	38 ± 21
Alumina[b]	213 ± 86	na	nd[d]
Glass	na	na	na
Carbon[b]	246 ± 18	241 ± 9	258 ± 38

[a] All data expressed as μg of PAH extracted per gram substrate.
[b] Data obtained by Jonathan Krueger.
[c] na = not available.
[d] nd = not detected.

TABLE 2-3

Photo- and nonphotochemical decomposition of benz[a]anthracene on coal fly ash and model adsorbents[a]

1	2	3	4
Substrate	Untreated	Rotation	Rot.& ill.
KA	57 ± 7	47 ± 4	53 ± 12
EA[b]	324 ± 53	260 ± 72	304 ± 47
EA[b]	29 ± 3	na[c]	24 ± 5
NM	726 ± 19	700 ± 16	739 ± 13
ET	236 ± 5	231 ± 1	211 ± 4
TX	142 ± 4	137 ± 5	64 ± 1
TX	288 ± 5	295 ± 18	173 ± 5
TX[b]	324 ± 7	310 ± 6	152 ± 13
WK[b]	11 ± 1	na	9 ± 1
IL	33 ± 8	34 ± 10	39 ± 17
AR[b]	197 ± 74	198 ± 62	na
AR[b]	38 ± 2	na	30±1
Silica	na	na	na
Alumina[b]	882 ± 40	828 ± 10	<40
Alumina[b]	236 ± 21	231 ± 14	nd[d]
Glass	na	na	na
Carbon	46 ± 10	na	53 ± 15

[a]All data expressed as μg of PAH extracted per gram substrate.
[b]Data obtained by Jonathan Krueger.
[c]na = not available.
[d]nd = not detected.

Adsorbate concentrations were determined by Soxhlet analysis and reported in micrograms PAH per gram substrate. Uncertainties in the results in Tables 2-2 and 2-3 are expressed as 95% confidence intervals.

To facilitate comparisons of apparent PAH decompositions for a large number of samples, the percentages of decomposition were converted into semi-quantitative designations, called "reactivity categories." There were three categories of substrate associated with varying degrees of reactivities of PAH adsorbed on them: they were "++" for very reactive (greater than 50% decomposition), "+" for moderately reactive (between 10 and 50% decomposition) and "0" for little or no reactivity (less than 10% decomposition), all based on 24 hr illuminations.

Eight coal fly ashes and four model substrates were studied in this manner, using five PAHs. Approximately one gram of sample substrate was first degassed overnight with N_2 at 100-200°C and then deposited with about 50 to 500 μg of PAH. The resultant reactivity categories for photochemical decomposition of all PAH/substrate samples are presented in Table 2-4.

The "overall reactivity" (OR) in Table 2-4 was computed for each substrate by adding the number of "pluses" in the corresponding column. It is intended to serve as a relative estimate of the photochemical reactivity of PAHs adsorbed on each substrate. Thus, PAHs adsorbed on alumina (OR = 10) are more reactive than PAH adsorbed on Texas (OR = 8).

2.5.2 Correlation with Substrate Color & Reflectance

Munsell soil color charts were used to describe the color of all substrates.[19] The substrates on which PAHs were very photochemically reactive generally were lighter in color than the substrate on which

TABLE 2-4

Photochemical reactivity[c,d] of adsorbed PAHs

PAH	KA	EA	NM	ET	TX	WK	IL	AR[a]	Silica	Alumina	Glass	Carbon
An	0	0	+	+	++	+	0	+	++	++	++	0
Ph	0	0	+	0	+	na	na	0	++	++	na	0
Py	0	0	0	0	+	0	0	+	++	++	++	0
BaA	0	0	0	0	++	0	0	+	na[e]	++	++	0
BaP	0	0	0	0	++	+	0	+	++	++	na	0
OR[b]	0	0	2	1	8	3±1	1±1	4	9±1	10	8±2	0

[a]Sample lot no. 720-2, also designated as "AB" ash.

[b]Overall reactivity obtained by adding the number of pluses in each column. For each "na" entry, 1±1 was added to represent the range from the lowest (0) to the highest (++) possible value for the entry.

[c]Reactivity designations are:
"0" for low reactivity (0-10% decomposition over 24 hours)
"+" for moderate reactivity (10-50% decomposition over 24 hours)
"++" for high reactivity (50-100% decomposition over 24 hours)

[d]Data for An by A.A. Garrison. Data for Py and BaP by R.A. Yokley. Data for Ph and BaA by R.J. Engelbach (except for Ph on Alumina and Carbon, and BaA on EA and WK by J. Krueger).

[e]na = not available.

the PAHs were less reactive. The major exception to this general trend was ET ash, which is relatively light in color but was a substrate on which adsorbed PAHs were generally less reactive. This observation suggested that a correlation existed between the optical properties of the substrate and photochemical decomposition of adsorbed PAHs. However, it was not known whether this relationship was due to an "inner filter effect" (as defined on page 5) or to the adsorbate being affected by variations in chemical composition, rather than the colors themselves.

Evidence for the "inner filter effect" was provided by observations of diffuse reflectance spectra of the substrate over the 250-400 nm wavelength range in which the PAHs typically absorbed light. In the case for adsorbed pyrene and benzo[a]pyrene, substrates KA, WK, IL, and carbon, on which lower apparent photochemical reactivity occurred, also had low reflectances. Substrates TX, AR, silica, glass and alumina, on which higher apparent photochemical reactivities occurred, had high reflectances. Two exceptions to this trend, ET and NM, on which low photochemical reactivity occurred, had high reflectances.[30]

In Table 2-5, the overall photochemical reactivity observed on all five PAHs is compared with substrate reflectance. These data show that not only are ET and NM ashes exceptional cases, but the reactivities on AR and WK are exceptionally high considering their relative reflectances. This observation implies that, if the substrate reflectance does indeed have a major influence on photochemical decomposition, then there must be one or more additional factors which

TABLE 2-5

Diffuse reflectance of substrates compared to photochemical reactivity of adsorbed PAHs

Arranged in order of decreasing average reflectance

Substrate	Substrate absorbance[a]			Overall reactivity[b] (OR)
	300 nm	350 nm	400 nm	
Alumina	-0.2	-0.18	-0.06	10
Glass	-0.09	-0.03	0.01	8±2
Silica	-0.065	0	0.05	9±1
ET	0.82	0.38	0.2	1
TX	0.86	0.56	0.35	8
NM	0.98	0.69	0.58	2
AR	1.15	0.87	0.6	4
EA	1.18	0.92	0.68	0
KA	1.17	1.05	0.97	0
Carbon	1.7	0.79	0.87	0
IL	1.28	1.19	1.09	1±1
WK	1.13	1.23	1.16	3±1

[a] Data from R.A. Yokley's dissertation.[30]

[b] From Table 2-4.

cause a suppression of reactivity on ET and NM ashes and an enhancement of reactivity on AR and WK ashes.

2.5.3 Correlation with Chemical Composition and BET Measurements

In considering chemical composition of the substrate to be a factor that could possibly influence photochemical reactivity, data containing the bulk elemental composition of eight major constituents of the various fly ash were examined. Resistance to photochemical decomposition was found to occur in ashes with a high percentage of carbon or iron content.[19] However, these results were considered inconclusive for several reasons. First, ET ash, on which resistance to photochemical reactivity was large, had neither high carbon or iron content. Second, surface concentrations of elements could be radically different from their bulk concentrations. Finally, the oxidation state of the element present could greatly affect reactivity; iron is obviously an element that can exist in different oxidation states.

Previous BET (N_2) measurements indicated that the range of macropore sizes, pore volumes, and pore shapes were rather similar for the various fly ashes.[19] Differences were observed in specific surface areas, hysteresis of adsorption-desorption isotherms, and shapes of t plots; but none of these appeared to be correlated with photochemical reactivity.[19,30]

However, the BET parameter called the "C" constant did have a possible relationship to photochemical reactivity. A low value for the "C" constant for AR (Table 2-6) implied that adsorbate molecules were nonlocalized (mobile) on the substrate surface;[35] therefore, exposure of these molecules to light would be more probable and photochemical

TABLE 2-6

Surface area, pore size and "C" constant of coal fly ashes and carbon[a]

	Substrate	Particle diameter (μm)	Specific surface area[b] (M^2/g)	C[b]
1.	KA	<45	3.15	432
2.	ET	<45	4.01	890
3.	TX	<45	2.61	148
4.	AR	<45	0.84	30
5.	Carbon	<45	4.43	115
6.	KA	38-45	3.34	na[c]
7.	NM	38-45	2.30	na
8.	TX	38-45	2.19	na
9.	ET	125-150	3.85	na

[a]Data for substrates 1-5 reported by Yokley.[15,25]

[b]Measured by BET method using nitrogen at 77°K.

[c]na = not available.

decomposition would be expected to increase. High values for the "C" constant on KA and ET (Table 2-6) implied that one or more the following three processes occurred: (1) adsorption into micropores (pores less than 20 $\overset{o}{A}$ in diameter), (2) adsorption onto very active sites, or (3) chemisorption (although, experimentally, it is difficult to distinguish which of these processes may actually be occurring). These three processes might be expected to stabilize the adsorbed molecule towards photochemical attack. In addition, vertical stacking of molecules during the first two processes could block underlying molecules from radiation. Thus, on the basis of various phenomena indicated by the "C" constant, enhancement of reactivity on AR ash and suppression of reactivity on ET and KA ashes could perhaps be rationalized.

2.5.4 Nonphotochemical Decomposition

Of particular interest was the nonphotochemical decomposition of phenanthrene adsorbed on ET ash (see Table 2-2, page 26). This sample had a moderate reactivity, whereas phenanthrene adsorbed on all other substrates had little or no nonphotochemical reactivity. Moreover, photochemical reactivities on ET ash were generally low and the photochemical reactivities of phenanthrene were generally the lowest of the five PAHs studied in this work. These observations suggested that a unique process may have been influencing the nonphotochemical decomposition of phenanthrene on ET ash which did not occur as strongly for other PAHs or other adsorbents. It seems highly likely that this process involved a very specific adsorbate-adsorbent interaction and may have possibly been dependent on the structure of the adsorbate. Further

investigation of nonphotochemical decomposition was not pursued because the likelihood of reaching conclusions that would be environmentally relevant was much lower than for studies of photochemical processes.

2.5.5 Comparison with Solution-Deposited Samples

Some significant differences in apparent photochemical decomposition were observed between solution-deposited samples and vapor-deposited samples. Solution-deposited samples containing 60 μg/g pyrene were prepared from dichloromethane as described on page 15. Table 2-7 compares the photochemical reactivities of samples prepared by solution-deposition and vapor-deposition methods. In going from vapor- to solution-deposited samples, an increase in photochemical reactivity occurred on ET ash, but no major differences in reactivities were observed for other substrates.

According to Gregg and Sing,[30] it is thought that the passage of an adsorbate molecule through a constriction slightly larger than a molecular diameter is a process which requires a certain activation energy. Like any activated process, the rate of this process increases with temperature. In the event that the high "C" constant of ET ash was due primarily to microporosity, it is possible that deposition at vapor phase temperatures (155°C) induced more extensive penetration into the microporous structure, making a larger fraction of adsorbate molecules less accessible to light, than for solution phase deposition (25°C). Thus, vapor deposited samples would be less susceptible to photochemical decomposition. Less microporous substrates would not exhibit this constriction effect as strongly.

TABLE 2-7

Photochemical decomposition of pyrene on vapor-deposited and solution-deposited samples

Substrate	Vapor-deposited[a]			Solution-deposited[b]		
	Untreated[d]	Irradiated[d]	category	Untreated[d]	Irradiated[d]	category
KA	96±5	89±3	0	36±8	34±5	0
EA	212±7	241±24	0	40±5	36±3	0
NM	176±11	180±17	0	47±4	43±3	0
ET	44±2	42±9	0	41±6	24±2	+
TX	375±2	244±8	+	55±5	23±3	+
IL	449±29	420±10	0	53±6	54±6	0
NM	176±11	180±17	0	47±4	43±3	0
AR[c]	141±3	120±3	+	42±6	35±4	+
Silica	317±41	68±6	++	65±5	0	++
Glass	318±10	45±3	++	62±3	0	++
Carbon	583±5	580±12	0	60±9	69±5	0

[a]Data from R.A. Yokley.

[b]Data from A.G. Garrison.

[c]Sample lot no. 720-2 (also designated as AB ash).

[d]Concentration of adsorbate in μg pyrene extracted per gram substrate.

It is also possible that competition of solvent molecules with pyrene molecules for adsorption sites might have a significant effect on solution deposition. The distribution of pyrene over the adsorption sites on the ash surface would be, in the presence of a solvent, perturbed, as the most "active" adsorption sites would tend to be occupied by solvent molecules.

From the data available to date it is not yet possible to reach any definite conclusions concerning the constriction effect, the influence of solvent competition, or any other contributing factors. However, it is evident that the method of sample preparation can affect the susceptibility of adsorbed PAH to decomposition. Since vapor-deposited PAHs more accurately reflected the manner in which environmental samples were produced than did solution-deposited PAHs, vapor deposition should be employed for any studies relevant to the atmospheric reactivity of adsorbed PAHs.

2.5.6 Dependence of Apparent Reactivity on PAH Structure

It can be seen in Table 2-4 (page 29) that there is a tendency for apparent PAH reactivities on a particular adsorbent to decrease in the order

$$A > BaA, BaP > P > Ph$$

In contrast to these observed reactivities, Behymer and Hites[26] observed little difference in the photolytic half-lives of 15 PAHs adsorbed on a single variety of coal fly ash. However, large differences in photochemical half-lives were observed for different PAHs adsorbed on conventional adsorbents such as silica gel, alumina, and carbon blacks. From these observations they concluded that, whereas the large

differences in reactivities on the conventional substrates resulted from structural differences in the PAHs, the small differences on the coal fly ash sample indicated that the same structural effects were not taking place on this sample. Therefore, the reactivity of the PAH was independent of PAH structure and dependent entirely on the characteristics of the fly ash.

Whether our observations contradicted their observations is not absolutely clear. The possibility exists that our illumination conditions simply amplified small differences in reactivities on the ashes we tested.

There were two other differences between the design of our experiment and their design. First of all, they prepared their samples by solution deposition. Secondly, they used only one coal fly ash, which may conceivably have been atypical in its effects on PAH photoreactivity. It seems clear that measurements using a variety of coal fly ashes are necessary to draw conclusions about fly ashes in general.

2.6 Conclusions

The photochemical decomposition of PAHs adsorbed on a variety of coal fly ashes was observed to vary with the nature of the ash. The rate of PAH photochemical decompositions was generally lower for fly ash adsorbents than for silica, glass and alumina, but higher (or equal to) the rate observed for PAH photolysis on carbon. There was a relationship between photochemical reactivity and reflectance of the substrate, supporting the hypothesis of an "inner filter effect." However, there were a few exceptions to this correlation which suggested

the involvement of additional factors in determining the resultant reactivity.

Most data for bulk elemental composition of the ashes showed little correlation to reactivities. There was a possible association of high iron and carbon content with stability of adsorbed PAHs towards decomposition. Nevertheless, there is still a need for accurate determinations of surface compositions, including the chemical oxidation states of the elements present.

A significant differences between the pyrene decomposition rates for solution-deposited and vapor-deposited ET ash implied that substantial errors might be introduced by using solution-deposited samples to predict behavior of environmental samples.

A variation in photochemical decomposition rates was observed for five PAHs adsorbed on the same coal fly ash. This, along with the observation of unique nonphotochemical reactivity of phenanthrene on ET ash, suggested that photodecomposition may not be totally independent of PAH structure.

Differences in photochemical reactivity may potentially result from nonlocalization of adsorbate and microporosity. It is possible to rationalize the high reactivity on AR ash and low reactivity on ET ash on these bases. The evidence for the occurrence of an "inner filter" effect on fly ash is thereby strengthened by determining the causes of these exceptional reactivities. Nevertheless, the reactivity of PAHs adsorbed on NM ash (OR = 2) was much lower than on TX ash (OR = 8), despite similarities in reflectance spectra for these two substrates. Also, the rather high reactivity for the least reflective substrate, WK

ash (OR = 3±1), remains to be explained. It seems clear that more information is needed regarding the energetics of interactions of PAHs with coal fly ash surfaces. These matters are considered in more detail in Chapters 3 and 4.

CHAPTER 3

QUANTIFICATION OF VAPOR DEPOSITIONS VIA FID

3.1 Preliminary

In the course of studying the decomposition of adsorbed PAHs, the extracts of two ashes, WK and IL, were found to contain an abnormally low concentration of PAH. Increasing the time interval over which deposition of PAH vapor was carried out had little effect on the concentration of PAH in the subsequent extract. This observation suggested either that these two ashes had a very low capacity for PAH, or that they were absorbing large quantities of PAH that were unextractable. This result also stimulated our interest in determining the percentage of PAH recovered by extraction from all ashes--not just WK and IL. For this purpose, a technique was required that would measure the amount of PAH depositing onto the adsorbent from the vapor phase.

In theory, by using a gas-phase detector to measure the mass flow rate (MFR) of PAH entering the fly ash bed and an identical detector to measure the MFR of PAH exiting the fly ash bed, the difference in the two MFRs (multiplied by the time of measurement) would yield the amount of PAH depositing on the bed during that measurement period. In practice, because the MFR of PAH entering the bed could be maintained virtually constant (± 2%), only one detector was necessary: it was used to measure the entrance MFR before deposition began and then to measure the exit MFR during the course of the deposition.

A flame ionization detector (FID) was a suitable detector for this purpose because it could operate in a flowing stream and was sensitive enough to detect the vapor concentrations of PAHs which we would be using (down to 0.1 μg/cc). Furthermore, the FID has a linear response function (pg. 52) which greatly simplified its calibration, allowing integration of the MFR difference over time to be calculated via area measurements described in Section 3.2.2 (pg. 46).

For this purpose, an FID (model 12-800, GOW-MAC Instruments Co., Bridgewater, N.J.) was installed inside the adsorption cell oven. Thus, the detector and connective tubing could be maintained at a constant temperature (±1°C). It was wired to one channel of a dual/differential electrometer scavenged from an inoperative Series 800 Gas Chromatograph (Varian Aerograph) and a chart recorder (OmniScribe model A5210-15, Houston Instruments, Austin, TX).

In initial studies, a major source of error arose because the entrance MFR and the detector sensitivity both changed when the flow stream was directed into the substrate bed, thus offsetting the calibration obtained in the "bypass" flow mode before deposition. This error was avoided by allowing each deposition to proceed until no more PAH was adsorbed by the substrate. The sample was then considered "saturated" or "deposited to capacity." The entrance MFR was then determined by measuring the exit MFR in the "through-cell" flow mode after the sample was saturated, assuming it to be equal to the entrance MFR during deposition. Later improvements in pressure and flow rate control as described in Section 3.3.1 (pg. 55) eliminated the previous

source of error, enabling measurements to be made for depositions of PAH which did not "saturate" the adsorbent.

To evaluate the utility of the FID technique to measure recoveries by extraction of PAHs from the coal fly ashes and model substrates, one PAH compound, pyrene, was used for a series of substrates. Pyrene was chosen because many of its characteristics (melting point, vapor pressure, molecular weight, and decomposition rates) have intermediate values compared with the values for other PAHs of interest. Measurements for the remaining PAHs (phenanthrene, anthracene, benz[a]anthracene) were performed for only one fly ash (KA) of which we had an especially abundant supply.

3.2 "Saturation" Depositions

3.2.1 Apparatus and Procedure

Figure 3-1 is a diagram of the vapor deposition apparatus equipped with an FID at point "I". The apparatus is similar to that described in Chapter 2 (pg. 16), but now contains the FID and also an additional switching valve, SV2, which can channel the flow stream either to the "FID" or the "outlet."

The adsorption cell used by Yokley was modified (Figure 3-2) by making it more compact and equipping the inlet and outlet with self-sealing connectors (Swagelok SS-QC4-B-200 quickconnect bodies). These changes were made when it was discovered that the adsorption cell, itself, adsorbed up to 300 μg of pyrene during deposition (using a MFR of 300 μg/hr). Therefore the surface area of the cell was minimized and the empty cell was allowed to adsorb PAH until adsorption reached a

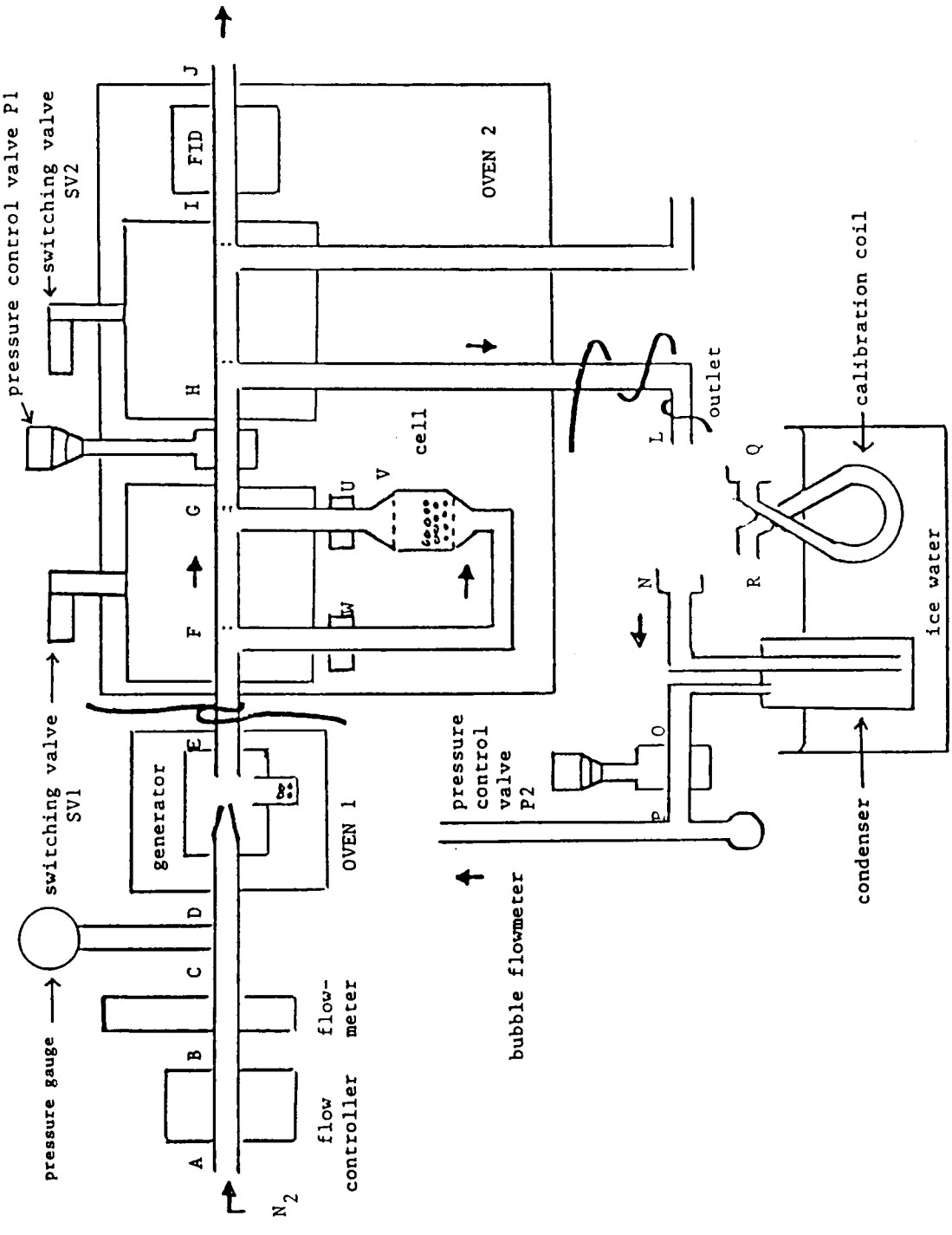

FIGURE 3-1. PAH vapor deposition apparatus

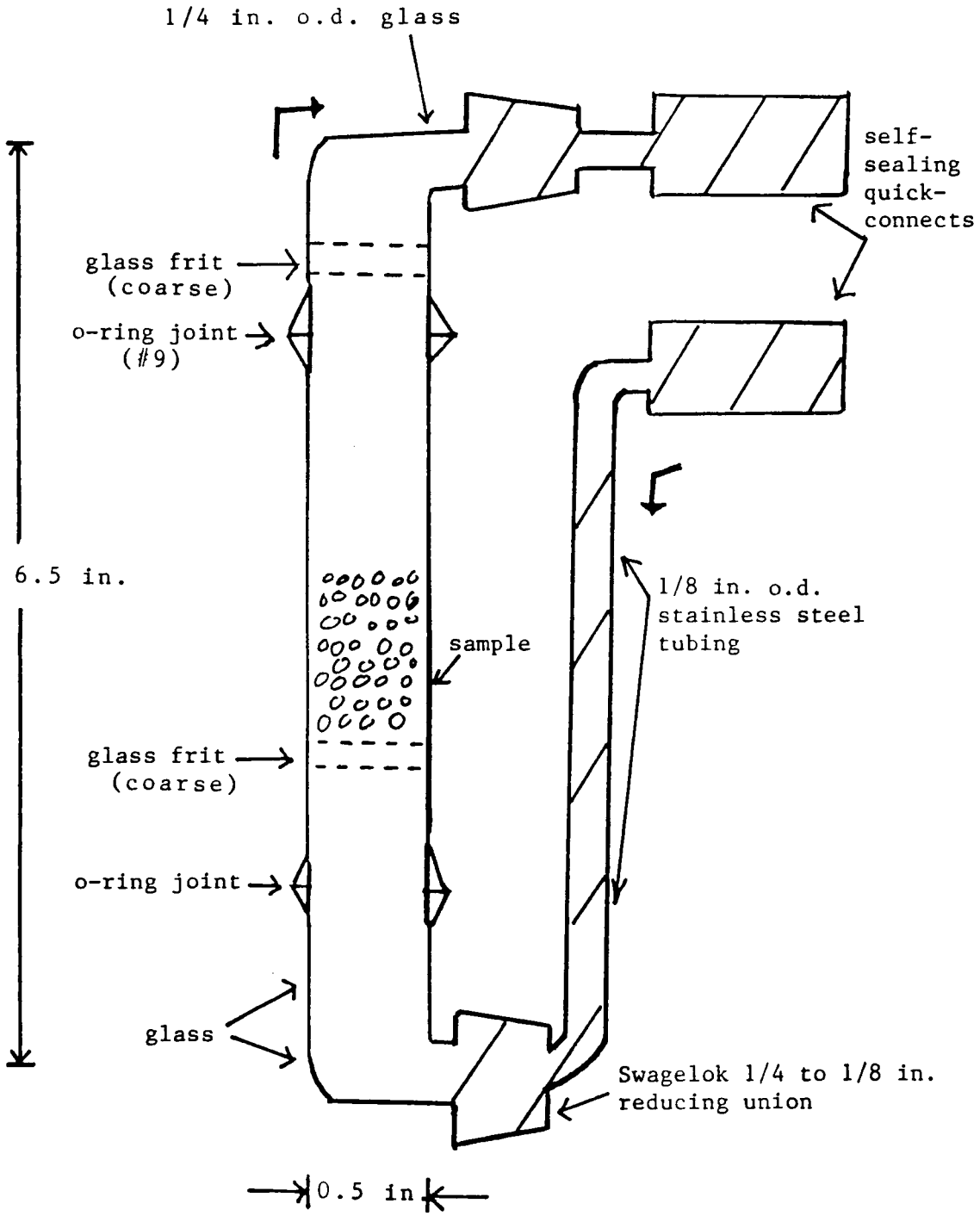

FIGURE 3-2. Adsorption cell

small steady rate, as evidenced by a constant detector signal. This procedure was intended to ensure that adsorption by the cell surfaces themselves would be small relative to that of the fly ash or other adsorbent.

This procedure, however, did not allow the sample to be degassed in the cell as described in Appendix 2-1. Instead, the sample was degassed in a similar cell maintained in an oven which was external to the vapor deposition equipment. Sample was then transferred in a dry box from the degassing cell to the predeposited adsorption cell. The self-sealing ends on both cells protected the substrate from exposure to the atmosphere.

To deposit a substrate with PAH to "capacity", switching valve SV1 (Figure 3-1) was switched to "cell," allowing the PAH vapor to permeate the substrate bed. A decrease in the PAH MFR, as evidenced by a decrease in the detector signal, then occurred due to adsorption of PAH by the substrate. As the deposition proceeded, the FID signal increased until, as shown in Figure 3-3, a plateau was reached at point b where $y = y_p$. Beyond point b, the substrate no longer adsorbed PAH and could be considered "saturated" with PAH.

3.2.2 Calculation of Adsorbate Concentration

Upon "saturation", the detector chart deflection y_p was proportional to the MFR of PAH exiting the cell after saturation, which was equal to the MFR of PAH entering the cell after subtraction of the small and constant rate of PAH adsorbing onto the cell surface. By integrating y_p over the time of deposition, area "abcd" was obtained.

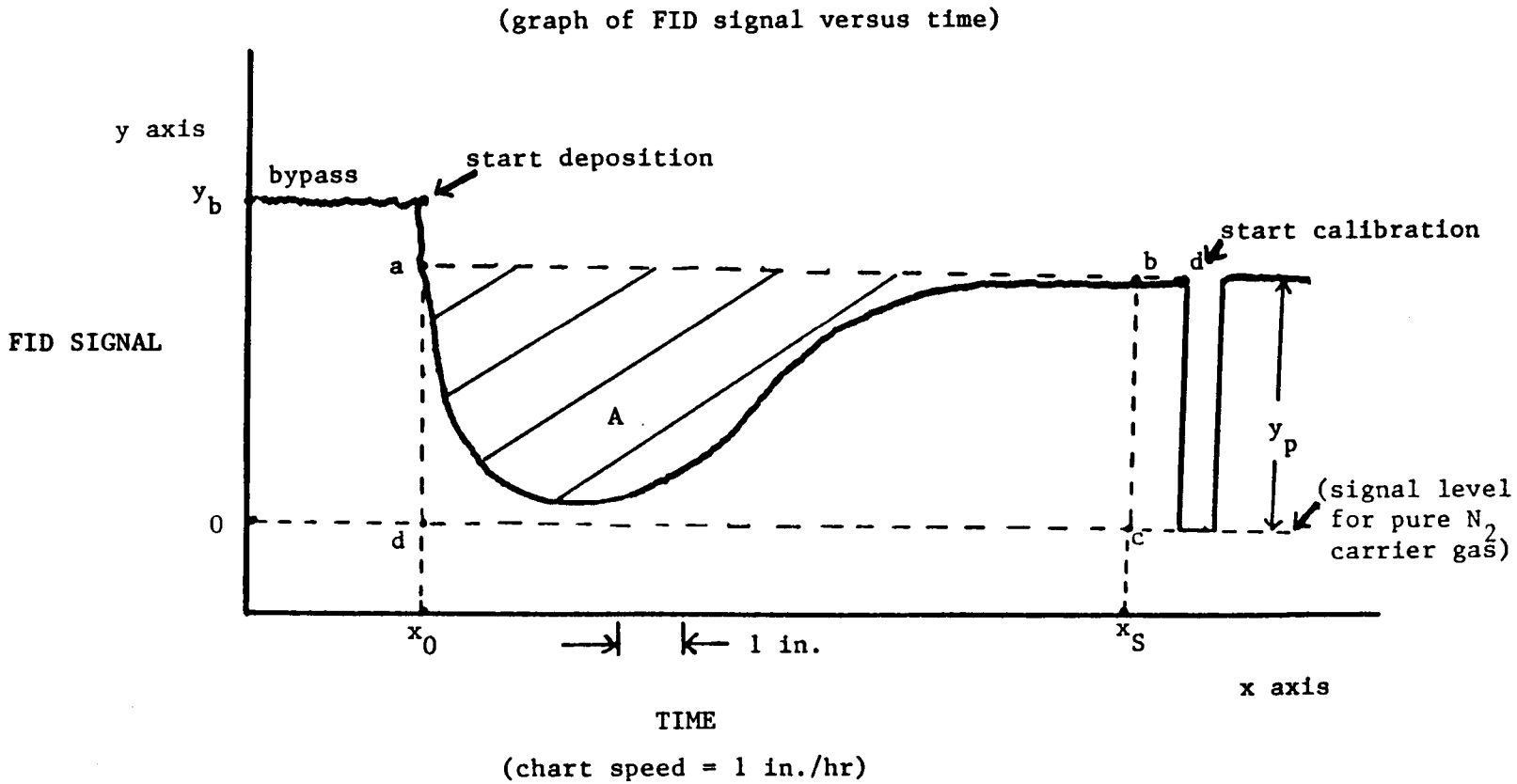

FIGURE 3-3. "Saturated" deposition of pyrene on KA ash

This rectangular area was presumed to be proportional to the quantity of PAH which entered the cell after subtracting the amount that was adsorbed by the cell surface. Area "A," representing a fraction of area "abcd," was proportional to the amount of PAH adsorbed by the substrate.

Area "A" was measured in square inches using a planimeter (Type 16, OTT, West Germany). To convert the area to mass of PAH, the FID signal had to be calibrated to correspond to MFR units. This calibration was accomplished at point d (Figure 3-3), at some time after the plateau was reached, by switching the flow stream from "FID" to "outlet" and collecting the PAH that condensed in a cold trap during a timed period. The amount of PAH collected was determined by dissolving it in solvent (as described in Section 3.2.3) and quantitating the solution via UV absorption spectrophotometry.

The MFR in the plateau region, MFR_p, was then calculated as:

$$MFR_p = \frac{\text{Mass of PAH collected}}{\text{Collection time period}} \quad \{\text{units in } \mu g/hr\} \qquad (3\text{-}1)$$

The mass of PAH adsorbed, M, was then related to area A by:

$$M = k_x k_y A \qquad (3\text{-}2)$$

$$\text{where } k_x = (\text{chart speed})^{-1} \quad \{\text{units in hr/inch}\}$$

$$\text{and } k_y = \frac{MFR_p}{y_p}$$

Finally, the adsorbate concentration was calculated as:

$$C = \frac{M}{w} \quad \{\text{units in } \mu g/g\} \qquad (3\text{-}3)$$

where w = mass of sample substrate in grams

3.2.3 Calibration

Calibrations were accomplished using a 30 to 40 cm length of 1/8-inch i.d. stainless steel tubing, coiled to fit into an ice bath, with teflon tubing at the ends providing thermal insulation, as shown in Figure 3-4. Before connecting the coil to the outlet, it was necessary to allow the outlet tubing to equilibrate to the PAH vapor stream for at least 45 minutes; otherwise, PAH would later be lost via condensation onto the inner surfaces of the outlet tubing. The flow stream (Figure 3-1) was then switched to "FID" and the coil, cooled in ice water, was connected to the outlet. Heating tape was placed over the outlet-to-coil connection. The flow stream was then switched to "outlet" and the PAH collected in the cold trap coil for a specified time (usually 15.0 minutes). The stream was then switched back to "FID" and the coil detached immediately (to prevent further diffusion of PAH from the outlet tubing to the coil).

The coil end Q (Figure 3-4) was attached to a solvent reservoir holding 45 ml of methanol. A pressure of 5 psi of nitrogen was used to force the methanol through the coil and into a 50-ml volumetric flask. The eluent was diluted to 50 ml and later analyzed for its PAH content by UV/VIS absorption spectrophotometry. The coil was eluted with a methanol rinse and allowed to dry under nitrogen flow for 5 minutes prior to subsequent use.

To check the efficiency of PAH collection, an experiment was performed using a second coil immersed in liquid nitrogen and connected to the outlet of the first coil. The absence of detectable quantities

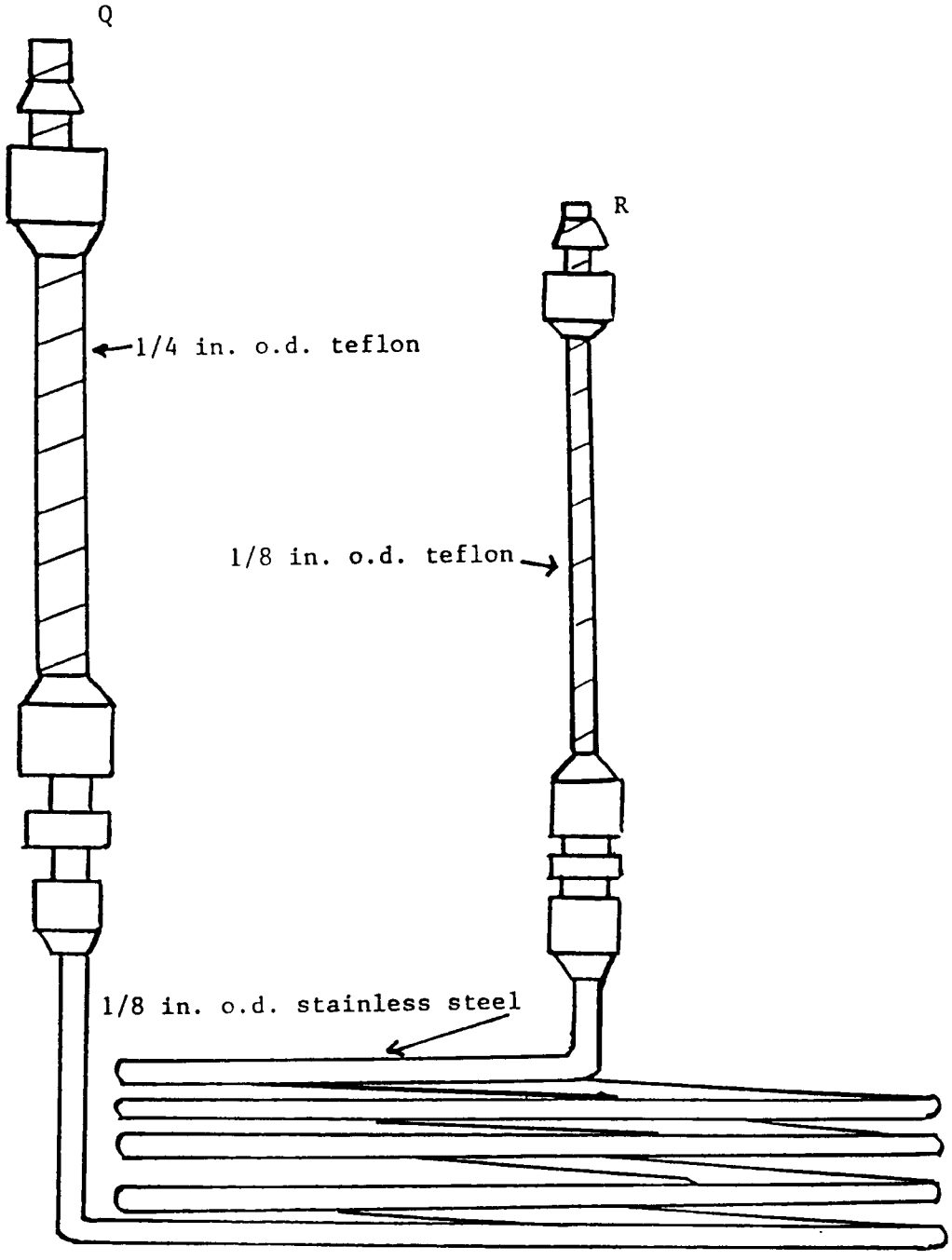

FIGURE 3-4. Calibration coil

of PAH in methanol eluted from the second coil was interpreted as meaning that virtually all PAH had been removed by the first coil.

When not in use for a long time, the coil was conditioned by repeated collections and elutions before an actual calibration measurement was made. This procedure eliminated the possibility of a low measurement in case there was irreversible adsorption of PAH in the coil.

To check the efficiency of elution from the first coil, a second volume of methanol was eluted through it. The absence of detectable PAH in the second volume of eluent likewise demonstrated that virtually all elutable PAH had been eluted in the first volume of eluent.

The possibility existed that there may have been a loss of PAH due to leakage or ongoing condensation in the tubing and valves between points "G" and "L" in Figure 3-1 (page 44). This possibility was examined by removing the cell and connecting two teflon tubes, one to the switching valve at point W and the other to the switching valve at point "U". These tubes were led through holes in Oven 2 (the adsorption cell oven) to the cold trap coil immersed in ice water. Mass flow rates obtained by this method matched those obtained by other methods within ±5%. This second method was not suitable to use routinely, however, because it required Oven 2 to be opened frequently, causing long delays in temperature equilibration. Linearity of the detector response was checked by comparing the detector chart deflection with the MFR of PAH generated at various temperatures of Oven 1. Figure 3-5 shows that the detector response was relatively linear for phenanthrene and pyrene.

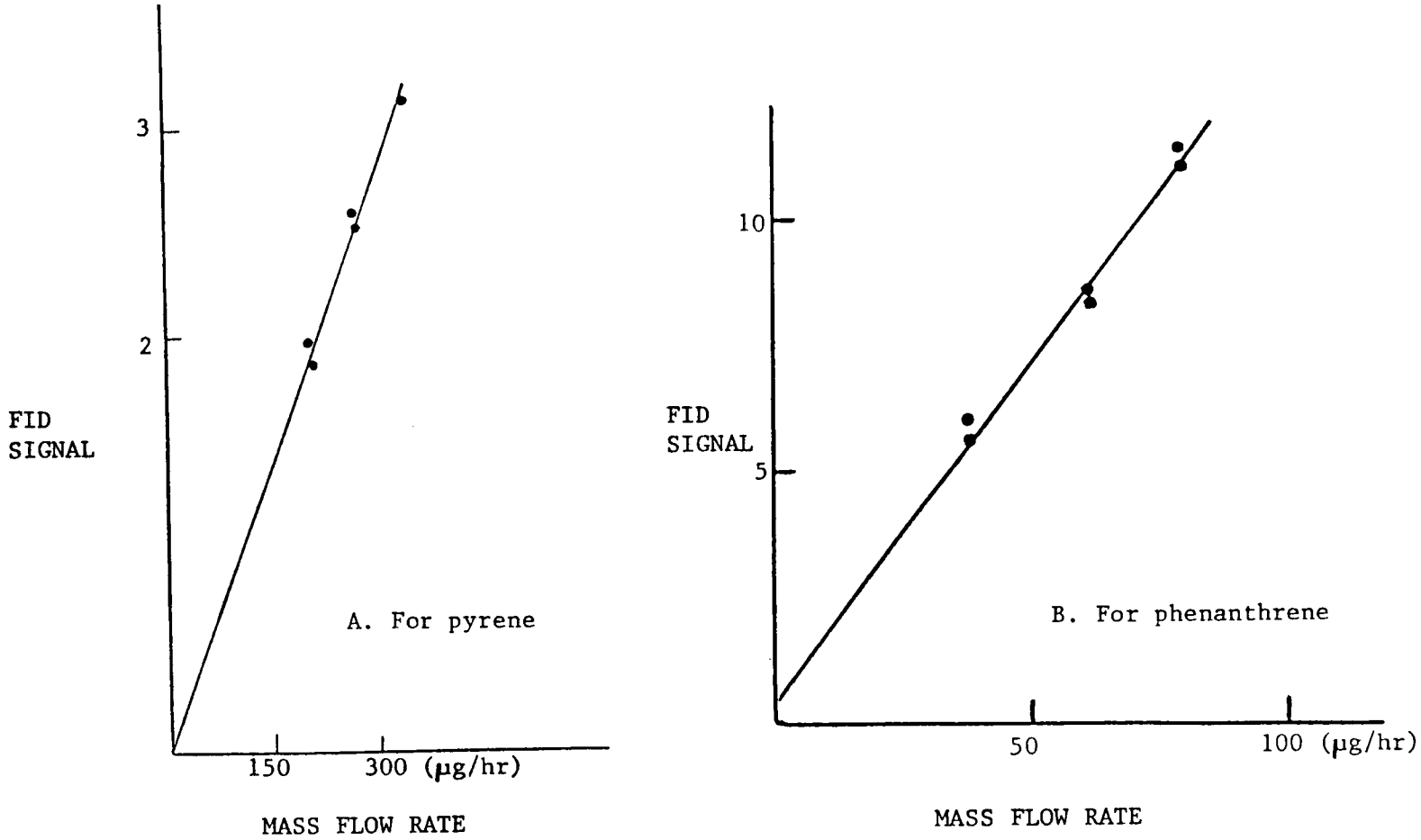

FIGURE 3-5. Linearity of detector response

3.2.4 Results

The results of successive measurements of pyrene depositions on KA ash are shown in Table 3-1. Samples of degassed ash were weighed in a dry box and transferred to the adsorption cell. Although the deposited ash samples were exposed to the atmosphere when weighing out portions for Soxhlet analysis, there was no appreciable error in weight due to potential adsorption of atmospheric vapors (such as water vapor).

Comparison of columns 2 and 3 of Table 3-1 show that depositions made at lower plateau MFRs required more time for the ash to saturate. The data indicated that the FID values for adsorbed PAH concentration were consistently larger than the Soxhlet values. Assuming the FID values to be an accurate measure of the total amount of PAH deposited on the ash, a percentage recovery of 82 ± 2% by Soxhlet extractions of the five KA samples was obtained. This result implied that both the FID determinations and Soxhlet extractions were quite reproducible and that the Soxhlet extractions were moderately efficient at removing pyrene from KA ash at these concentration levels.

On the other hand the results show that approximately 180 μg of pyrene per gram of KA ash was unextracted when the ash was "saturated" with pyrene. This observation suggested that there was a large number of very strong adsorption sites on the ash. If this was the case, then percentage recoveries might decrease if smaller amounts of pyrene were deposited, because the PAH would presumably adsorb preferentially on the most strongly retentive adsorption sites. Efforts were thereafter focused on depositions in which the ash was not "saturated."

TABLE 3-1

"Saturation" depositions of pyrene on KA ash

Sample weight (g)	Plateau MFR (μg/hr)	Hours to saturation	FID conc. (μg/g)	Soxhlet conc. (μg/g)	% Rec.*
1.1523	289	13	1060	875	82
1.1410	341	13	1048	850	81
1.0640	387	9	1082	879	81
0.5561	372	8	1083	880	81
1.0760	206	27	948	741	78

*$\%\ \text{recovery} = \frac{\text{Soxhlet conc.}}{\text{FID conc.}} \times 100\ \%$

Considering that these "saturated" depositions represented an upper limit for the amount of pyrene deposited on KA ash, it was interesting to observe how these capacities related to the surface area of KA ash measured by the B.E.T. method (using nitrogen) which yielded a value of 3.15 m^2/g. Based on an area of 90 $\mathring{A}^2$ for one molecule of pyrene,[36] the capacity of KA ash for pyrene would be 1174 μg/g, assuming monolayer coverage and the validity of the BET (N_2) surface area for pyrene. This value is somewhat larger than that measured via FID (950 - 1080 μg/g). Assuming validity of the monolayer capacity calculation, this observation shows that "saturation" of KA ash with pyrene occurs at less than "monolayer" surface coverage.

3.3 Subcapacity Depositions

3.3.1 Technique

Calibration in the "bypass" flow mode prior to subcapacity depositions was made possible by maintaining the nitrogen flow rate and pressure within the generator constant during an entire deposition experiment. Previously, additional flow resistance from the sample substrate decreased the flow rate and increased the generator pressure, causing changes in the PAH MFR and detector sensitivity in switching valve SV1 (Figure 3-1, page 44) from "bypass" to "cell."

To remedy this problem, a flow controller (model 57-000285-00 Milliflow Controller, Varian) was installed at point "A" in Figure 3-1; it maintained a constant flow rate (about 40 ml/min) despite changes in downstream pressure. In addition, a pressure gauge (11-281A Pressure gauge, 60 torr capacity, Fisher Scientific) was installed at point "B"

(Figure 3-1) and a pressure control valve P1 (SS-2SG fine metering valve, Nupro Co., Willoughby, Ohio) was placed at point "H." The valve could be adjusted to maintain the gauge pressure at 55 ± 1 torr above atmospheric pressure. Upon switching valve SV1 from "bypass" to "cell," valve P1 was opened until the gauge pressure was restored to 55 torr. An additional pressure control valve P2 was installed downstream from the calibration coil at point "O" (Figure 3-1, page 44) to ensure that there would be no significant pressure change in switching valve SV2 from "FID" to "outlet."

Additional modifications included the following. Points "N" and "L" were directly connected when using the bubble flowmeter to measure the outlet flow rate. The condenser prevented escape of PAH from the bubble flowmeter. During calibration, the coil was inserted between points "L" and "N." The system could be checked for leaks, even when hot, by comparing readings of the two flowmeters at points "B" and "O," a lower flow rate at point "O" signifying a leak.

A sample FID plot for the subcapacity deposition of pyrene on KA ash is shown in Figure 3-6; the MFR was 60 μg/hr. Calibration was performed at point "x_3." Deposition was carried out between "x_4" and "x_5," during which time there were three simultaneous processes occurring in the cell: (1) a small degree of adsorption of pyrene at a constant rate, apparently by the cell surface of pyrene represented by area A_4; (2) adsorption of pyrene onto the substrate surface; and (3) desorption of pyrene from the cell and tubing surfaces downstream from the substrate bed.

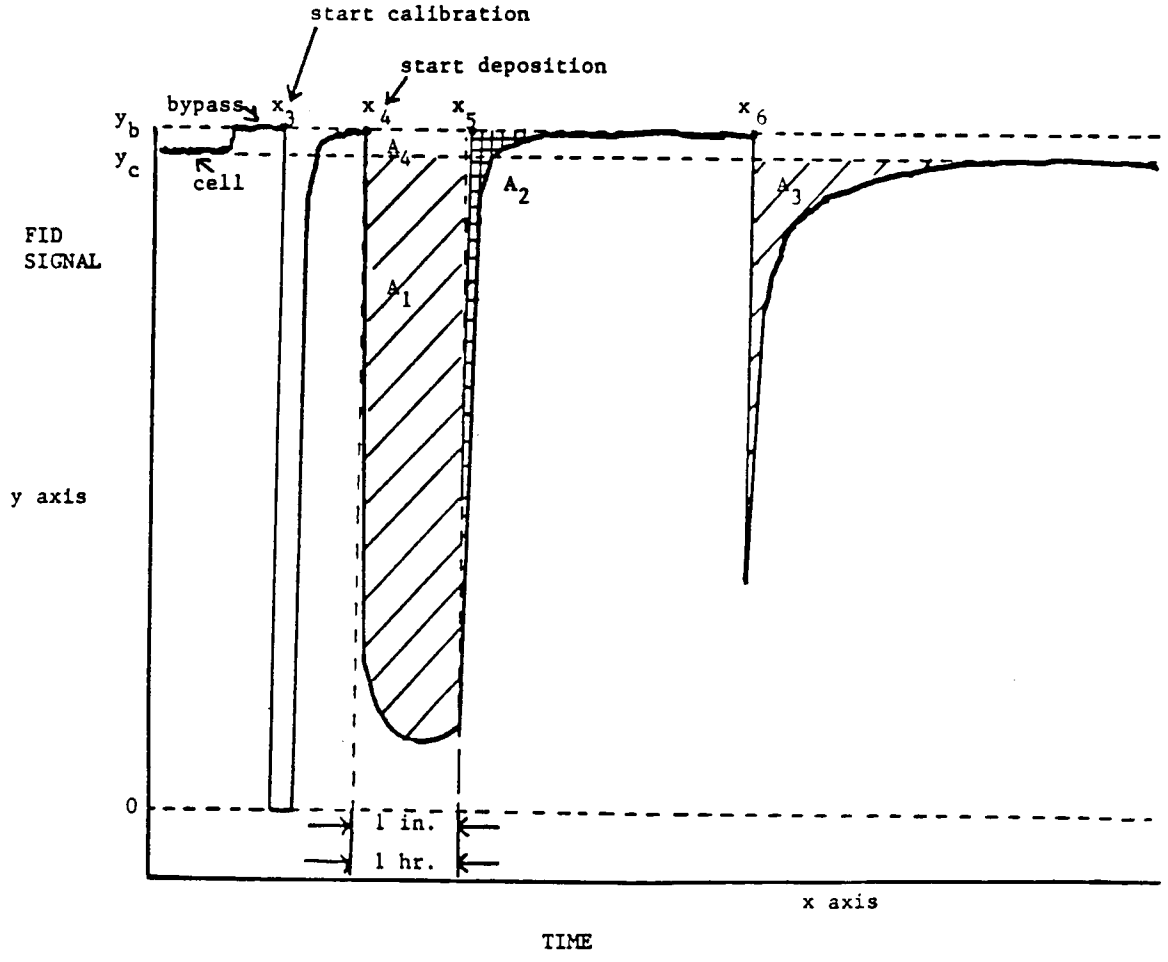

FIGURE 3-6. Subcapacity depositions of pyrene on KA ash

The desorption process was presumed to occur because a large fraction of the PAH content was removed from the vapor stream due to adsorption by the fly ash. Therefore, the layer of condensed PAH on the walls downstream from the substrate probably released some PAH to re-establish equilibrium with the smaller concentration of PAH vapor in contact with it. The last two processes - adsorption on the substrate and desorption from the walls - opposed each other, so that their net contribution to the overall adsorption of PAH was represented by area "A_1."

Readsorption was presumed to occur in the tubing (where desorption previously occurred) when the "bypass" vapor concentration was restored at "x_5." Area A_2 represented the amount of PAH required to restore the deposition layer on the tubing, which was assumed equal to the amount previously desorbed during deposition on the substrate.

After completion of an experiment, the contents of the cell were removed carefully and the cell was replaced in the adsorption oven. At "x_6," after switching to "cell" re-adsorption of PAH occurred on the cell, represented by "A_3," which was assumed equal to the amount previously desorbed during deposition on the substrate.

The net adsorption represented by "A_1" was then related to the adsorption onto the substrate, represented by "A_{sub}," and the amounts desorbed from the tubing and cell, represented by "A_2" and "A_3" respectively:

$$A_1 = A_{sub} - A_2 - A_3 \qquad (3\text{-}4)$$

$$\text{or} \quad A_{sub} = A_1 + A_2 + A_3 \qquad (3\text{-}5)$$

From calibration of the detector signal "y_b" with the measured bypass MFR, the mass of PAH adsorbed and the resulting adsorbate concentration was calibrated in the same manner as in the "saturated" depositions.

It was necessary to demonstrate that areas "A_2" and "A_3" were entirely due to desorption of PAH and not due to dispersion of PAH molecules at the boundary between the gaseous phase containing pure nitrogen and the gaseous phase containing a mixture of PAH and nitrogen (such dispersion possibly occurring due to gaseous diffusion or laminar flow). The absence of observable dispersion was demonstrated experimentally by substituting a nitrogen/methane mixture (54 ppm by weight) for the PAH/nitrogen mixture entering the adsoption cell oven between points E and F (Figure 3-1, page 44). The adsorption cell was detached and a stream of pure N_2 was directed into switching value SV1 at point U. Thus by switching back and forth from "bypass" to "cell," a boundary between the two gas phases was created which moved through the tubing towards the FID. Methane was chosen because it did not adsorb or desorb appreciably on the inner walls of the tubing; thus, if any spreading of the boundary between phases were observed it would have to be due to dispersion. No spreading of the boundary was observed, as evidenced by the square corners on the FID plot (Figure 3-7) which resulted from switching from "bypass" to "cell."

At a given temperature, diffusion effects for methane, having a lower molecular weight than pyrene, were expected to be greater than for pyrene, while laminar flow effects were expected to be about the same (diffusion and laminar flow effects are calculated in Appendix 3-1). It

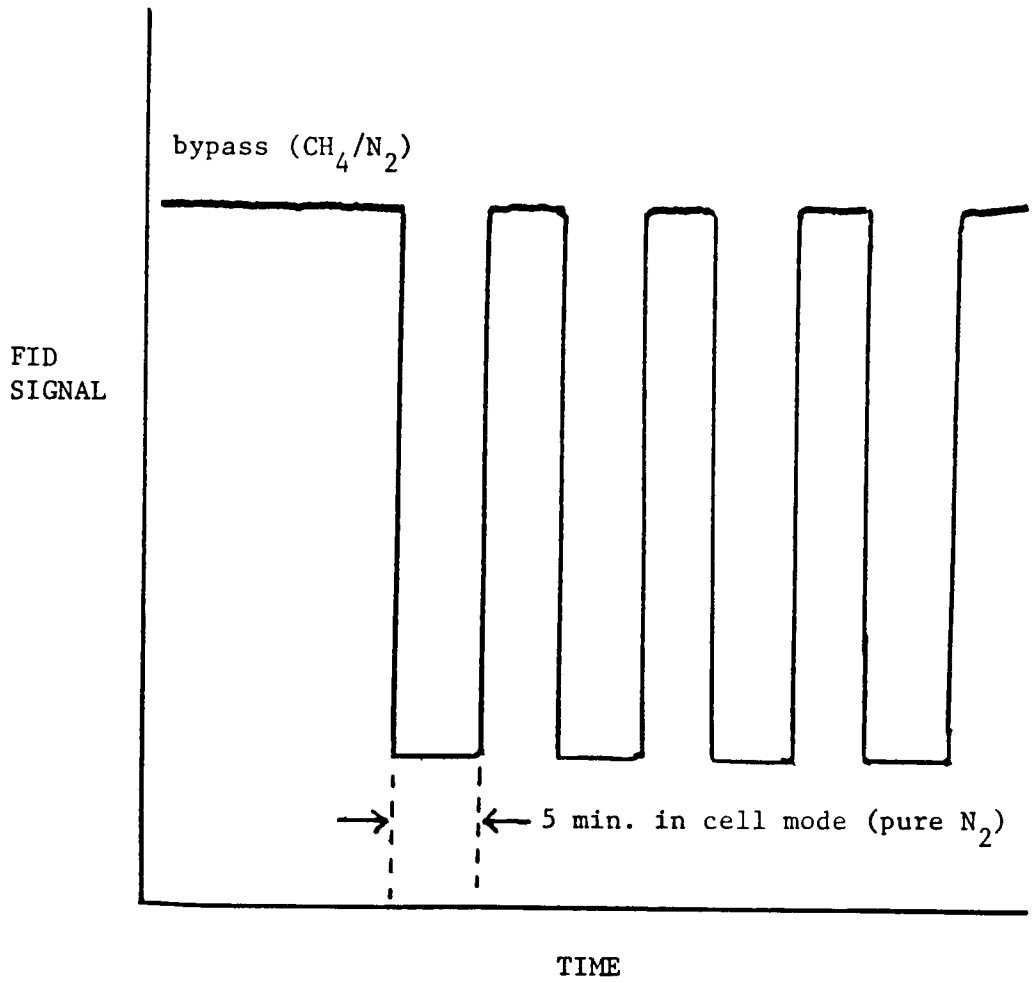

FIGURE 3-7. FID plot of a moving gaseous boundary

was therefore reasonable to conclude that, if dispersion did not occur for methane, then these effects were also insignificant for PAHs.

Quantification of PAH at low adsorbate concentration was thus carried out using the procedure described in this section to correct for desorption from the tubing and cell walls. Contributions to desorption during one-hour depositions at 60 μg/hr pyrene amounted to about 2 ± 1 μg from the tubing and about 10 ± 3 μg from the cell walls. In addition, when the empty predeposited cell was removed from the oven, opened, and then replaced, approximately 1 μg of pyrene was readsorbed by the cell before chart deflection y_c in Figure 3-5 was reached. Therefore, a blank of 1 μg was subtracted from the mass of pyrene corresponding to "A_1" and another 1 μg was subtracted corresponding to "A_3." Thus a total of 2 μg was subtracted from the mass corresponding to "A_{sub}," yielding the corrected mass of pyrene adsorbed as the substrate.

During "saturated" depositions, any surface adsorbing at the beginning of the deposition should have readsorbed approximately the same amount of PAH by the time saturation was reached. There were probably some small differences in the equilibrium conditions before and at the end of deposition in the tubing and cell walls, but the result would be a very small error in comparison with the amount of PAH adsorbed by the substrate. Therefore, the "saturated" depositions automatically compensated for any significant error due to desorption.

3.3.2 Results

Approximately 1.0 gram of degassed substrate (except carbon which was 0.60 g) was weighed inside a dry box and placed into a presaturated

adsorption cell. Then the sample was deposited for 60 minutes with pyrene at 155°C and a MFR of 60 μg/hr. The nitrogen source pressure was 40 psi and the flow rate was 40 ml/min. The pressure of the flow stream in the generator was maintained at 55 ± 1 torr above atmospheric pressure. The silica, after being removed from the adsorption cell, gained nearly 30% of its weight in water upon exposure to air; therefore the weights of the portions for Soxhlet analysis had to be corrected by subtracting for the amount of water adsorbed, so the weights would be consistent with the original degassed sample weight. This was done by weighing the entire sample immediately after removing it from the adsorption cell, then allowing it to attain a constant weight upon exposure to air (requiring about 24 hours). The percentage increase in weight due to water, designated "I%," was then determined. The weights for the Soxhlets were then multiplied by 100/(100 + I%) to reduce them to be consistent with the degassed sample weight.

Results for vapor depositions on nine substrates are shown in Table 3-2. Results were for particles of less than 45 μm diameter, unless otherwise stated. Column two lists the adsorbate concentrations of these samples as determined by Soxhlet extraction. Column three contains adsorbate concentrations determined by the FID technique which are assumed to be the actual amounts of pyrene vapor deposited on the substrates. In column four, the percentage recoveries for Soxhlet extractions of the vapor deposited samples are listed.

TABLE 3-2

Subcapacity deposition of pyrene on various substrates

1	2	3	4
Sub-strate	Conc.[a] Soxhlet	Conc.[a] FID	% Rec.[b] vapor
KA	28	59	47
KA	32	60	53
KA	29	59	49
ET	10	53	19
TX	64	62	103
WK	23	31	74
IL	"0"[c]	47	"0"[c]
AR	41	45	91
Silica	60	58	103
Carbon	91	54	52
Avg. dev.[d]	±3	±2	±4

[a]In μg pyrene per gram substrate.

[b]Equal to (Conc. Soxh./Conc FID) x 100%.

[c]"0" means no detectable pyrene was found in the extract.

[d]Absolute deviations were for the 95% confidence interval and were approximately equal in value over all substrates. Value shown represents the average over all substrate.

In Table 3-3, recoveries for Soxhlet extractions of samples which were solution-deposited with about the same quantity of pyrene (60 μg/g) are compared to the vapor-deposited recoveries. Table 2-7 (page 36) compared the photochemical decomposition for the vapor and solution depositions. The following observations were made from these data:

(1) Good agreement of the data was observed for the three different KA samples.

(2) For silica, extraction of both the solution-deposited and vapor-deposited samples appeared to be virtually 100% complete.

(3) For vapor deposition, the photoreactivity of adsorbed pyrene increased with percentage recovery by extraction. Pyrene adsorbed on substrates AR, TX and Silica had both high photochemical reactivities and high extraction recoveries. Substrates for which pyrene exhibited lower recoveries tended to correspond to those on which pyrene exhibited little or no photoreactivity. However, for solution deposition recoveries and reactivities there was no apparent correlation of this type.

(4) Most of the samples prepared by vapor depositions, except for AR, clearly had lower recoveries than those prepared by solution deposition.

(5) In going from vapor to solution-deposited samples, the recoveries clearly increased for ET, IL, and carbon substrates.

TABLE 3-3

Comparison of recoveries of solution-deposited versus vapor-deposited pyrene on various substrates

1	2	3
Sub-strate	% Rec[a] vapor	% Rec[d] solu.
KA	49	61
NM	na[c]	77
ET	19	69
TX	103	93
WK	74	na[c]
IL	"0"[b]	88
AR	91	70
Silica	103	109
Carbon	52	101
Avg. dev.[e]	±4	±10

[a]Equal to (conc. Soxh./conc. FID) x 100%.

[b]"0" means no detectable pyrene was found in the extract.

[c]Not available.

[d]Equal to (conc. Soxh./conc. solution-deposited) x 100%.

[e]Absolute deviations were for the 95% confidence interval and were approximately equal in value over all substrates. Value shown represents the average over all substates.

We can conclude from observations (1) and (2) that the quantitative technique via FID was reproducible and yielded reasonable results.

Important differences in the recovery and decomposition behaviors for the solution versus the vapor-deposited samples in observations (3), (4) and (5) raise doubts about the environmental relevance of solution deposited samples in studies of either analytical recovery or chemical transformation of adsorbed PAHs. The lower recoveries for the vapor deposited samples may have resulted from interference from solvent molecules; possibly solvent molecules competed with PAH molecules for the more active adsorption sites. The lower temperature used during solvent deposition may also have allowed PAH to deposit on a greater proportion of less active sites. Lower recoveries for adsorbed PAHs were usually accompanied by lower apparent reactivities, which may signify that strongly adsorbed PAHs are stabilized towards photochemical decomposition.

The most significant conclusion was that we now had a parameter, percentage recovery for extraction of vapor deposited samples, that seemed to be related to photochemical reactivity of adsorbed PAHs. For ashes that were fairly reflective but had low reactivities, such as ET, we now had another measurable characteristic which seemed to be associated with low reactivity.

In answer to the question about WK and IL ashes which originally prompted this investigation of recoveries, we can conclude that unusually low amounts of PAH were extracted from IL because most of the adsorbed PAH was not extractable, whereas for WK the observation was due to its low capacity for PAH.

The recoveries for ET and IL, when vapor-deposited, were unexpectedly low. The fact that major portions of the deposited PAH did not extract introduces a new potential problem--what if a portion of the unextractable PAH underwent photochemical decomposition? Any photoreaction would be undetected under these circumstances. This problem warrants further investigation.

Finally, Yokley, et al.[19] have reported that the bulk carbon content was high for both IL and KA ashes, but low for ET ash. Griest and Tomkins[31] have attributed the low extraction recoveries of solution-deposited BaP from fly ash to be due to high sorptivity of carbonaceous particles. It may therefore be possible for carbonaceous particles to be responsible for the low extraction recoveries of vapor-deposited pyrene from carbon-rich IL and KA ashes. However, the low extraction recovery of vapor-deposited pyrene from the relatively low carbon-containing ET ash suggests that, on some fly ashes, another mechanism for strong retention of PAH on fly ash may occur besides the one associated with carbonaceous particles.

CHAPTER 4

HEATS OF ADSORPTION

4.1 Theory

4.1.1 Preliminary

Two thermodynamic parameters which measure the affinity of an adsorbate molecule for the adsorbate surface are the heat of adsorption (ΔH_a) and the distribution coefficient (K_D). This chapter describes the application of a gas chromatographic technique to measure these parameters at low surface coverages of PAH adsorbed on coal fly ashes. As in the measurement of extraction recoveries in Chapter 3, most measurements were made using pyrene because the thermodynamic behavior of pyrene was intermediate between that of the smaller PAHs--phenanthrene and anthracene--and larger PAHs--benz[a]anthracene and benzo[a]pyrene.

The heat of adsorption is the amount of thermal energy released during adsorption per unit mass of adsorbate, usually expressed in kilojoules per mole. Since adsorption of a PAH on coal ash is an exothermic process, ΔH_a values are negative; however, reference to a heat of adsorption as "high" or "low" in this dissertation pertains to the absolute magnitude of ΔH_a, irrespective of its sign.

Heats of adsorption measured by calorimetry are usually obtained as "integral" heats of adsorption,[37] meaning that the measurement represents the average heat of adsorption for the total amount of solute adsorbed on the surface. Chromatographic methods usually measure a "differential" heat of adsorption, which is a measure of the thermal

energy released per unit mass of solute adsorbed when a small increment of solute is adsorbed onto the surface. Formally, the differential heat of adsorption is defined as the heat released when one mole of adsorbate is adsorbed by an infinite amount of solid without change in the fraction of surface covered by adsorbate.[37]

4.1.2 Isosteric Heats of Adsorption

Differential heats of adsorption can be measured indirectly from adsorption isotherms. The isotherms are plots of the solute concentration on the surface versus solute concentration in the vapor phase when the solute is in equilibrium between surface and vapor at some specific temperature. Data from a series of isotherms at various temperatures can be used to construct "isosteres" -- plots of ln p versus 1/T--at a given adsorbate concentration (where p is the partial pressure of solute in the gas phase and T is the absolute temperature). According to the Clapeyron-Clausius equation[37]

$$\frac{dp}{dT} = \frac{\Delta H_a}{T\Delta V} \qquad (4\text{-}1)$$

where ΔV is the change in volume of one mole of solute in going from vapor to adsorbed phase. Except at very low temperatures and high pressures, ΔV is equal to the volume of vapor in the gas phase which, by applying the ideal gas law is

$$\Delta V = \frac{RT}{p} \qquad (4\text{-}2)$$

so that

$$\frac{dP}{dT} = \frac{\Delta H_a P}{T^2 R} \qquad (4\text{-}3)$$

equivalent to $$\frac{d \ln p}{d(1/T)} = \frac{-\Delta H_a}{R} \qquad (4\text{-}4)$$

which in integrated form becomes

$$\ln p = \frac{-\Delta H_a}{R} \frac{1}{T} + c \qquad (4\text{-}5)$$

Therefore plots of isosteres are straight lines as described by equation 4-5, having slopes equal to $-\Delta H_{ST}/R$.

The heats of adsorption obtained from isosteres are appropriately called "isosteric heats of adsorption" and denoted in this dissertation as ΔH_{ST}. The original adsorption isotherms used to indirectly determine ΔH_{ST} can sometimes be obtained by special gas chromatographic techniques such as "Elution at Characteristic Point" (ECP) and "Frontal Analysis" (FA).[37,38] However, many of these techniques require special conditions for adsorption or dramatic adaptations in GC hardware, so that simpler chromatographic methods may often be preferable.

4.1.3 Limiting Isosteric Heats of Adsorption

The limit of ΔH_{ST} when the adsorbate concentration approaches zero is called the "limiting isosteric heat of adsorption," denoted in this dissertation as ΔH^0_{ST}. This value can be measured directly from chromatographic retention data by applying a formula similar to equation 4-5, which has been derived[12,39-43] as

$$\ln V_g = -\Delta H^0_{ST}/RT + C \qquad (4\text{-}6)$$

where V_g (the "specific retention volume") is defined as the retention

volume of adsorbate per unit weight of adsorbent. It is important to stress that this equation is considered valid for adsorbate concentrations within the linear portions of adsorption isotherms, which is considered to be below 1% surface coverage.[42]

In this technique, one proceeds by injecting small concentrations of PAH onto a column packed with fly ash. By varying the temperature of the column for a series of injections at the same concentration, the slope of a plot of ln V_g verses 1/T should yield a value of $-\Delta H^0_{ST}/R$. This technique has been used by Ross[12,43] to determine heats of adsorption of PAHs on diesel particulate and by Eiceman and Vandiver[5] to find the heats of adsorption of PAH on municipal and incinerator fly ashes. We have used this technique for PAHs on a variety of coal fly ashes, obtaining measurements for surface coverages as low as 0.07%. This limit represented the coverage below which reproducible measurements could not be obtained.

4.1.4 Distribution Coefficient

The distribution coefficient is defined[44] as the ratio of the equilibrium solute concentration on the adsorbent surface to the equilibrium solute concentration in the mobile (vapor) phase:

$$K_D = \frac{q}{c} \qquad (4\text{-}7)$$

where q = solute conc. on surface (mol/m^2)

c = solute conc. in gas (mol/cm^3)

The value of K_D normally varies with temperature. A large K_D indicates that a large fraction of the total available amount of adsorbate is adsorbed on the surface. For the linear region of an adsorption isotherm, K_D is simply the slope of the isotherm. Under these

conditions the specific retention volume is related to the distribution coefficient by[37,44]

$$V_g = K_D A_s \qquad (4\text{-}8)$$

where A_s is the specific surface area of adsorbent (m^2/g). Thus K_D at a given temperature can be evaluated from the specific retention volume obtained by GC when the column is at that temperature.

The specific retention volume used in determining ΔH^0_{ST} and K_D actually refers to the volume for conditions prevailing within the column. Since the flow rate is measured under conditions of atmospheric pressure and room temperature at the column outlet, the retention volume obtained from this flow must be corrected to correspond to the temperature and pressure in the column. The retention volume observed at the column outlet is

$$V_0 = F(t_r - t_0) \qquad (4\text{-}9)$$

where F = flow rate at column outlet (mg/min)

t_r = retention time of peak maximum (min)

t_0 = retention time of nonadsorbed solute (min) (beginning of solvent peak)

The value of V_0 when corrected to the conditions of column temperature and pressure adsorbent is[37]

$$V^{corr} = \frac{V_0}{} \left(\frac{T_c}{T_F}\right)^2 \frac{(P/P_0)^2 - 1}{(P/P_0)^3 - 1} \qquad (4\text{-}10)$$

T_c = absolute temperature of column

T_F = absolute temperature of flowmeter

P = total pressure at column inlet

P_0 = atmospheric pressure at column outlet

The specific retention volume, V_g, then is given by

$$V_g = V^{corr}/W_s \qquad (4\text{-}11)$$

where W_s = mass of adsorbent

The pressure term in equation 4-10 is a conventional expression[37] for correcting to the average pressure of a compressible gas through a pressure drop $\Delta P = P - P_0$.

4.1.5 The Patch Model for Adsorption

The "patch model" is often used to describe adsorption of gases onto heterogeneous surfaces.[45] In this model, a surface that is energetically heterogeneous can be considered to be composed of small areas or "patches", within which adsorption is energetically homogeneous, but between which the energetics of adsorption vary. According to the model, adsorbate molecules adsorb onto patches with sites having the highest adsorption energies first, each patch being filled before adsorption onto the patch with the next highest adsorption site energy occurs. The differential heats of adsorption on heterogeneous surfaces have been observed experimentally to decrease gradually with increasing adsorbate concentration, thus confirming the hypothesis that higher energy sites tend to be filled first. It seems reasonable that adsorption on the very heterogeneous surfaces of fly ashes would tend to follow a model of this type.

4.2 Apparatus and Procedures

4.2.1 Columns

A Hewlett-Packard 5890A Gas Chromatograph, which came equipped with a split/splitless capilary inlet port, was modified to accept a 1/4 inch outer diameter glass column, varying in length from 8-50 cm. The glass column extended into the inlet port where an airtight connection from column to port was made using a silicone o-ring seal. The 50 cm columns were bent in a semi-circle to exactly fit into the detector and injector ports. Smaller columns were connected to the detector port using 1/16-inch o.d. stainless steel tubing and appropriate Swagelok fittings. Flexible graphite ferrules (M-4 ferrules, Supelco, Inc., Bellefonte, PA) were substituted for stainless steel ferrules in many fittings to avoid permanent locking of steel ferrules with steel Swagelok bodies (which frequently occurs at high temperatures).

In order to make a one-piece glass column fit between injection inlet and detector outlet, first a 50 cm segment of 1/8-inch o.d. stainless steel tubing was bent to an exact fit into inlet and detector ports. From this steel column, a template was traced onto a flat board to be used as a guide to bend glass columns.

Glass columns were made from 1/4-inch o.d., 2 mm i.d., borosilicate glass (LG-86005, Lab Glass, Kingston, TN). The 50-cm columns were bent nearly to the desired shape by starting with a 90-cm segment of straight tubing and passing the middle 50-cm back and forth along the column length through a wide flame. When uniformly soft, the center of the column was then bent approximately to the template curve. The column ends were then cut at appropriate points corresponding to the template.

Columns were packed using plugs of silanized glass wool (2-0411 Glass wool, Supelco, Bellefonte, PA). The column was packed with adsorbent by gravity using an electronic vibrating device (Vibro-Graver, model V-74, Burgess Vibrocrafters, Inc., Grayslake, IL) to facilitate particle movement. About 10 cm of column was left empty at the column inlet to allow for sample volatilization.

Prior to packing, fly ashes were sieved to obtain a 38-45 μm particle diameter range where possible. This range corresponded to the approximate range of samples used in the decomposition experiments (i.e., < 45 μm), but excluded smaller particles which tended to increase pneumatic impedance. For WK and AR ash, which were in short supply, it was necessary to use the entire < 45 μm fraction. The pneumatic impedance of ET ash was so high that a larger 125-150 μm fraction had to be used to obtain sufficient flow through the column.

4.2.2 Detection and Injection

A flame ionization detector (FID) was used to measure the amounts of PAH exiting the column. The detector signal was processed by a Hewlett-Packard 3392A Integrator which automatically recorded net retention times along with chromatograms (detector signal vs. time). The detector temperature was maintained at 250°C (260°C for column temperatures above 350°C). The injection inlet was maintained at 200°C (the maximum temperature for the silicone o-ring).

Originally, solutions of PAHs in dichloromethane were injected onto the columns; however, doing so caused the detector to short circuit after repeated use. This occurrence was attributed to a buildup of conductive chloride salts produced by the reaction of the hot

dichloromethane vapor with the lead shielding surrounding the FID. Solutions of PAHs in hexane (Hexane-UV, Burdick and Jackson, Muskegon, MI) were thereafter substituted without occurrence of detector problems.

Injections were made using a 1 µl syringe (#7101, Hamilton Co., Reno, NV) or 10 µl syringe (#1701, gastight, Hamilton Co., Reno, NV) from stock solutions of 50.0×10^{-3}, 2.00×10^{-3} and 0.400×10^{-3} M PAH in hexane.

4.2.3 Conditioning

Helium (High purity Helium, MG Industries, Valley Forge, PA) was used as the carrier gas. Before initial use, columns were conditioned overnight at 350°C. Most chromatographic peaks exhibited considerable tailing at higher retention times and lower concentrations. Under these conditions, PAHs could not be completely removed from the column after injections simply by allowing elution to proceed at the temperature of injection. In some cases, elution for several hours brought the detector signal level back to the baseline. However, reproducibility of successive injections was very poor.

Good reproducibility (±5%) could be obtained by reconditioning the column at a temperature above the injection temperature, usually 350°C, for a short period (usually 10 minutes). For injections at temperatures higher than 350°C, 400°C was used as the conditioning temperature. The conditioning time was chosen so that the chromatogram would return to the original baseline value. It was assumed that virtually all the desorbable PAH was removed by conditioning, and that successive injections would thus be carried out with the column containing the same distribution of available adsorption sites.

For injections of PAHs on columns containing adsorbent material that had not been previously exposed to PAHs, the retention volumes decreased for several replicate injections until a reproducible retention volume was observed. This phenomenon was attributed to irreversible adsorption of PAH on the most active adsorption sites of the adsorbent. As irreversible adsorption sites became gradually filled by successive injections, the total number of adsorption sites would decrease. As a result, peaks would begin to elute earlier and with a larger peak area (since less adsorbate would be left behind in the column). Eventually, all irreversible sites would be filled, so that, in subsequent injections, the condition of the column would no longer change, and the retention time would be influenced only by reversible sites.

4.2.4 Flow Rate, Pressure, and Column Temperature

Carrier gas flow rates in the 5-15 ml/min range were used, as measured by a soap bubble flowmeter at the column outlet. The flowmeter temperature was assumed to be 25°C and the ambient pressure was assumed to be 760 torr. Errors in flow rate measurements due to the vapor pressure of the soap solution[37] were considered negligible (<3%). The pressure at the column inlet was maintained between 0-30 psi above atmospheric pressure, larger pressures being required to ensure sufficient flow rates through adsorbents having higher pneumatic impedances. The pressure was maintained constant by allowing the split vent associated with the split/splitless injector to be partially open; therefore, the "column head pressure" reading on the pressure gauge of the gas chromatograph remained constant during insertion of a syringe

into the injection septum, during actual injection of a sample, and during changes in column temperature.

The pressure gauge on the instrument, however, underestimated the true column pressure when the split vent was partially open. Therefore, an external pressure gauge connected to a needle adapter (inlet pressure gauge 86806, Alltech Associates, Inc., Deerfield, IL) was inserted through the injector septum to accurately measure the column pressure. Pressure readings were obtained periodically between injections.

Column temperatures between 150°C and 333°C were used for injections in which the column was conditioned at 350°C. The temperature range was extended to 390°C for columns conditioned at 400°C. Temperature intervals for each determination of ΔH^0_{st} were typically about 50°C, using three to five data points for each determination, spacing the points at uniform intervals of reciprocal temperature.

Higher temperatures were necessary to obtain solute peaks for cases in which retention was high. These cases occurred when the heat of adsorption was large or when injections of PAH were made onto columns containing large weights of adsorbent.

4.2.5 Experiments

In initial experiments, large amounts of adsorbent (0.5-1.3g) were packed to fill 50 cm columns. The heats of adsorption were measured for several PAHs on TX ash (see pg. 14 for definitions of symbols for the ashes) and silica over a range of adsorbate concentration. Note that the term "adsorbate concentration" is defined as the total quantity of PAH injected per gram of adsorbate. It is the average concentration of

solute considered in equilibrium with the entire amount of adsorbent at the moment of injection onto the column.

Two other adsorbents, AR and WK, were also used successfully in these 50 cm columns. However, such long columns could not be used to obtain satisfactory data for other adsorbents. Adsorbents such as KA and NM were so retentive that no PAH elution peaks from columns with large adsorbent weights could be observed, even after hours of elapsed time. Adsorbents such as ET had such high pneumatic impedances, that a sufficient flow rate could not be established which would allow the peak to elute before it became unrecognizably broadened due to axial diffusion in the gas phase.

In later experiments, it was found that, by using much smaller amounts of adsorbent in the columns (0.05 to 0.3 g), observable chromatographic peaks were obtained for even the most retentive ashes. The problem of high pneumatic impendance was alleviated by mixing the adsorbent with about 0.3 g of a nonadsorbent solid, porous substrate designated as "CW" (Chromosorb W-HP 100/120 mesh, stock number 2364A, Alltech Associates, Arlington Heights, IL) and filling a 50 cm. column with this mixture. The nonadsorbent CW not only facilitated flow, but also allowed reproducible determinations of retention volume at lower surface coverings in comparison to columns without CW but containing the same amount of adsorbent.

4.3 Observations and Conclusions

4.3.1 Chromatograms

Some sample chromatograms are shown to give a general idea of the retention times, peak broadening, and degree of peak asymmetries observed in the heats of adsorption measurements. In Figure 4-1, the peaks for phenanthrene on silica can be seen to be much more symmetrical than the peaks for phenanthrene on TX ash shown in Figure 4-2. In general, peaks for injections on the fly ashes were asymmetrical, with relatively vertical front boundaries and tailing rear boundaries. Such behavior is characteristic of adsorption in an adsorbate concentration range in which the adsorption isotherm is not linear[37] and is also indicative of a large degree of energetic homogeneity, as would be expected because of its more uniform chemical and physical composition. As shown in Figure 4-3 for injections of pyrene on various fly ashes, the degree of asymmetry, and thus the energetic heterogeneity, increased in the order

$$ET, TX < AR < NM, KA$$

In Figure 4-2, the larger retention time for pyrene, compared to phenanthrene and anthracene injected onto TX ash under the same concentration, temperature, and flow rate conditions, is indicative of a greater affinity of pyrene for the ash surface. This is evident from equation 4-8 (pg 72) where A_s is constant for experiments on the same substrate and the retention volume is a mathematical product of the retention time and the flow rate. Thus pyrene has a larger distribution coefficient than the other two PAHs.

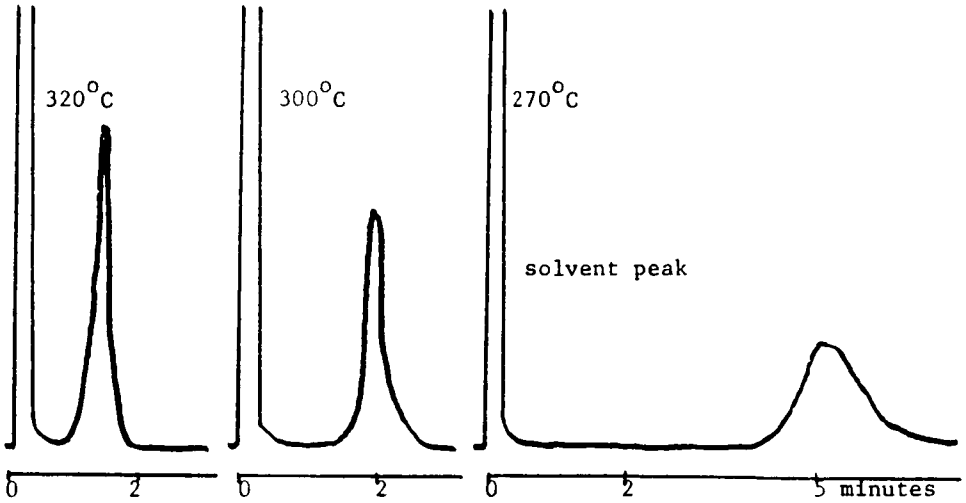

FIGURE 4-1. Chromatograms of phenanthrene on silica (0.03 μmol/g)

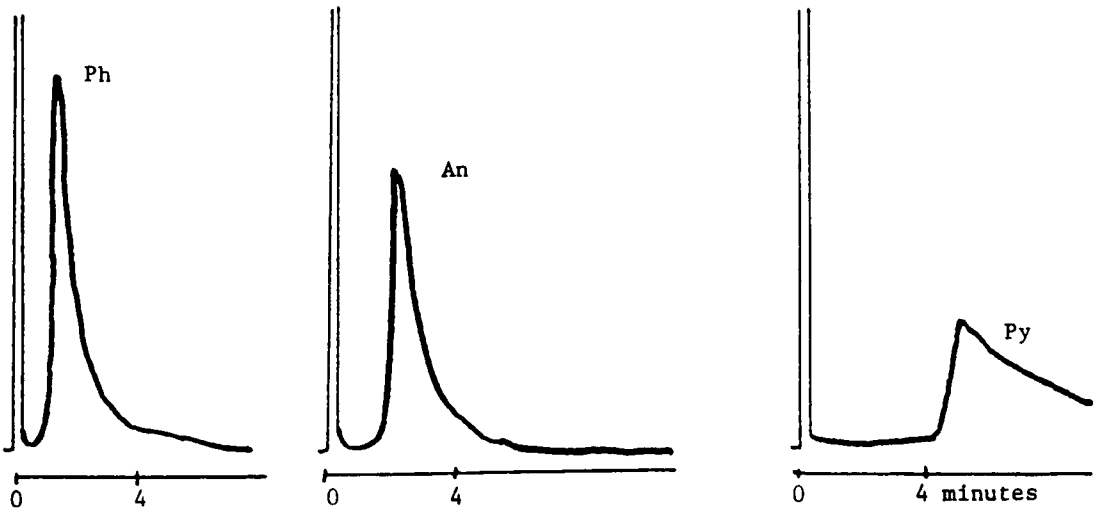

FIGURE 4-2. Chromatograms of PAHs on TX ash (0.08 μmol/g, 315°C)

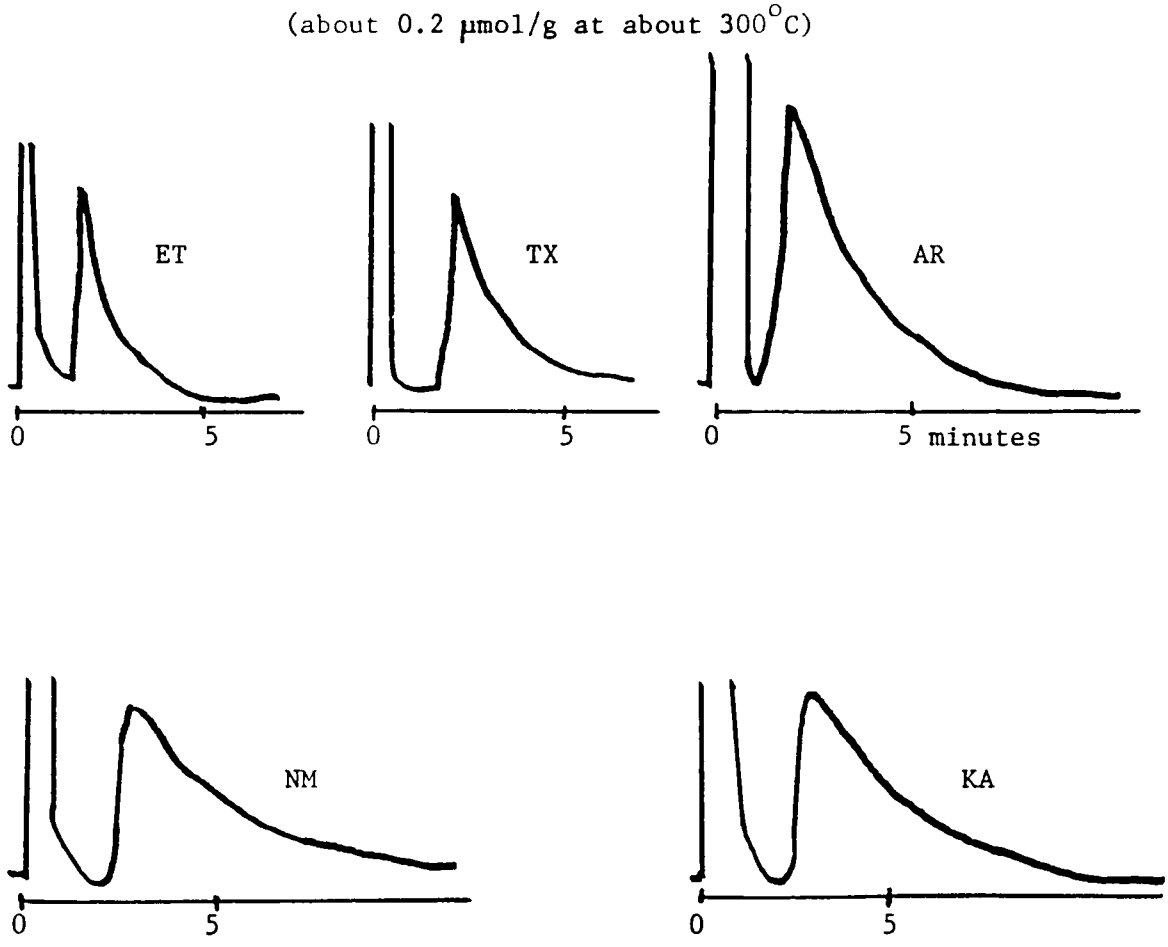

FIGURE 4-3. Chromatograms of pyrene on ET, TX, AR, NM, and KA ashes

4.3.2 Log Vg Versus 1/T Plots

Plots of log specific retention volume versus 1/T are shown in this section, from which heats of adsorption are calculated and discussed in succeeding sections. Figures 4-4 through 4-9 contain plots for pyrene on various fly ashes. Figure 4-10 A, B, C contains plots for phenanthrene, anthracene, pyrene, and benzo[a]anthracene on TX ash. In Figures 4-4 through 4-10, often plots for more than one type of column containing the same adsorbent have been included together. Each plot is identified by a plot number, followed by the adsorbate concentration in μmol/g enclosed in parenthesis, and often followed by a column identification number. Columns having identification numbers followed by the letter "c" were composed of a mixture of adsorbent and the nonadsorbent substrate CW. These plots contain the retention information from which ΔH^{o}_{ST} and K_D were calculated.

Table 4-1 contains a complete listing of the heats of adsorption calculated from the slopes of all plots in this section and includes the standard deviations in the heats of adsorption calculated for at least one plot per substrate.

Figure 4-4 is illustrative for examining the effect of adsorbate concentration on the slopes, and thus the heats of adsorption, associated with log V_g vs. 1/T plots; this Figure was singled out because it contains plots for the same column using a large number of adsorbate concentrations. For this particular figure, data have been listed immediately below the graph showing the heat of adsorption calculated from

$$-\Delta H^{o}_{ST} = \text{slope} \times 2.303\ R \qquad (4\text{-}12)$$

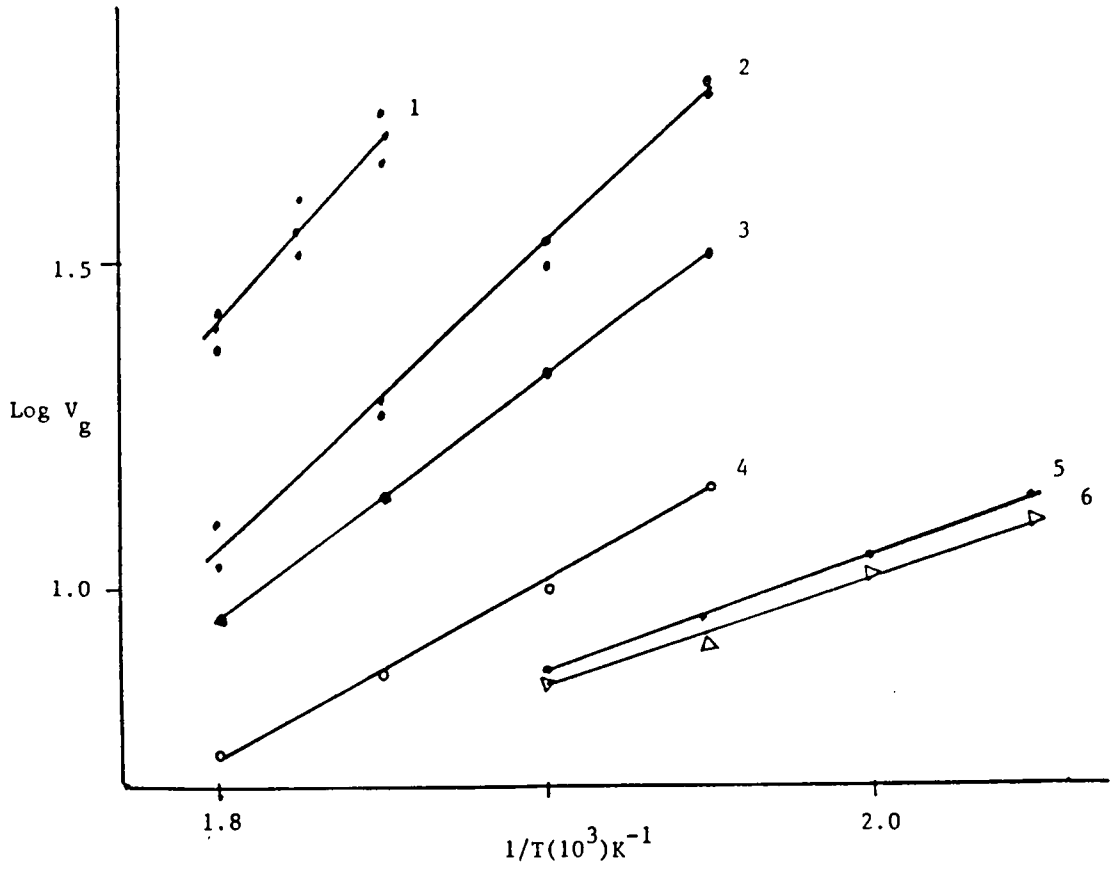

Plot	Py conc[a]	Corr coef	$-\Delta H^{\circ}_{ST}$ (kJ/mol)
1	0.00399	0.9686	102.9 ± .2
2	0.0176	0.9921	87.6 ± .5
3	0.0403	0.9998	69.4 ± .1
4	0.117	0.9975	52.6
5	0.229	0.9926	36.7 ± .2
6	0.403	0.9955	32.0 ± .6

FIGURE 4-4. Log V_g versus 1/T for pyrene on WK ash

a: in μmol/g

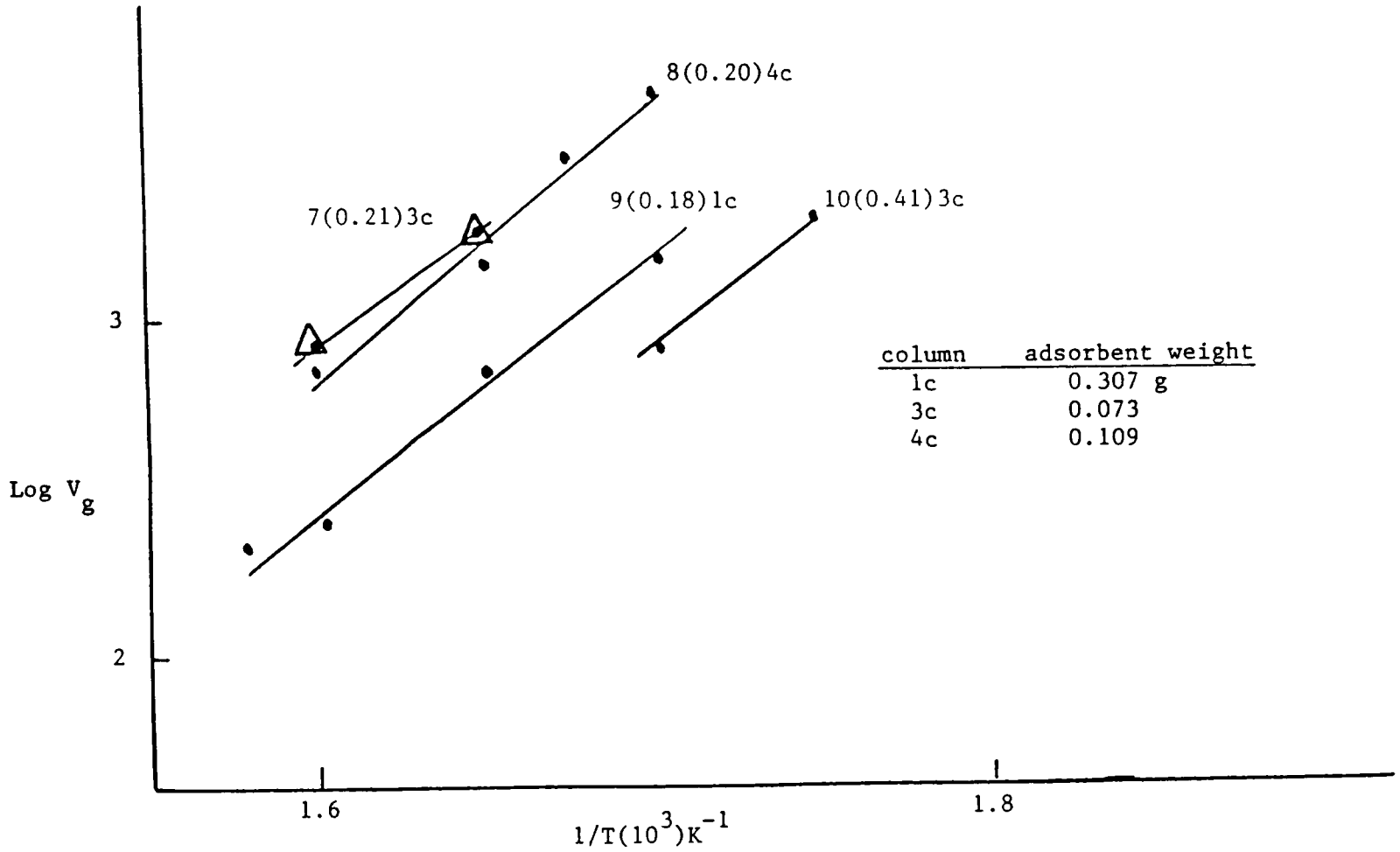

FIGURE 4-5. Log V_g versus 1/T plots for pyrene on NM ash

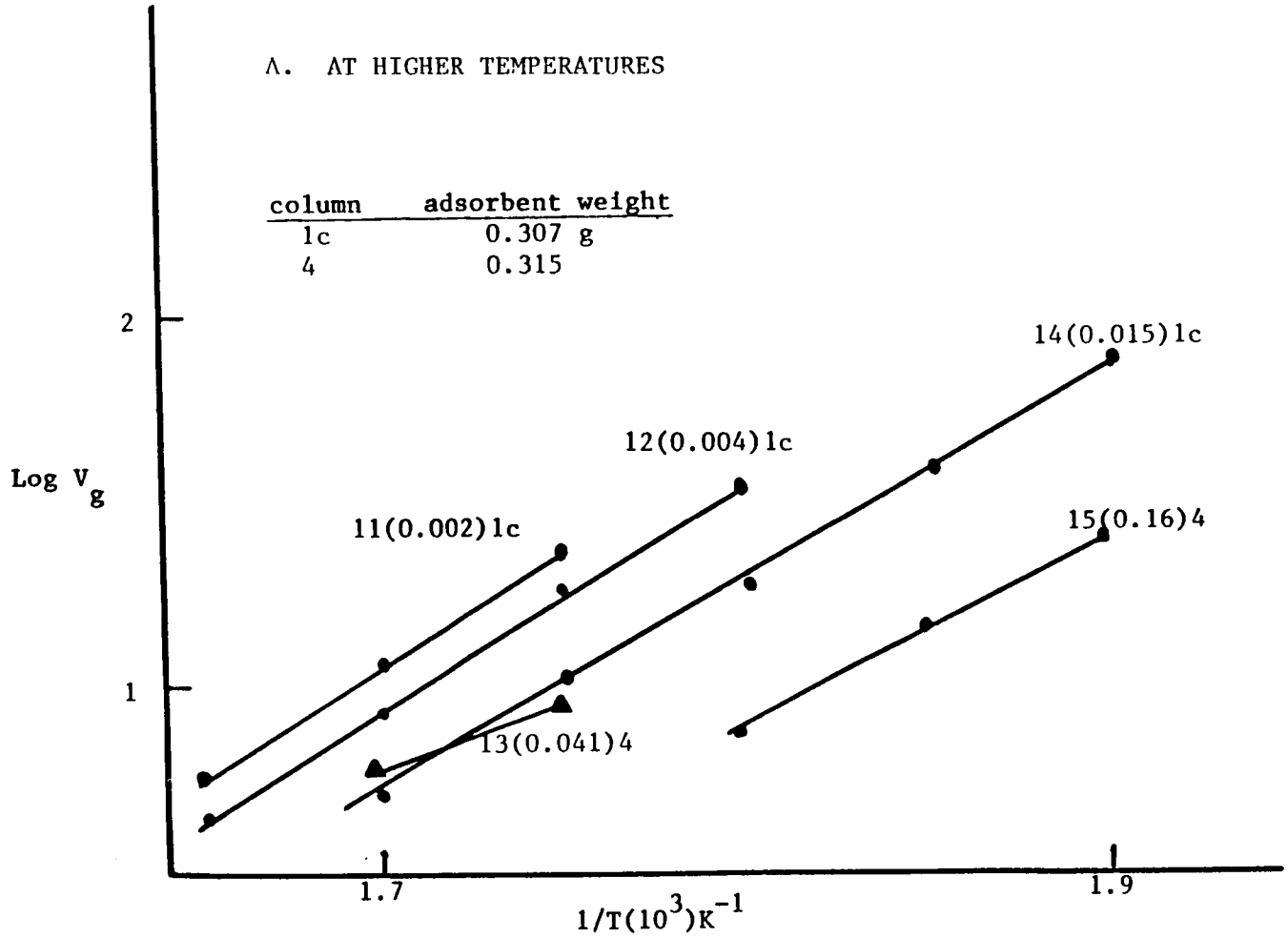

FIGURE 4-6 Log V_g versus 1/T for pyrene on TX ash

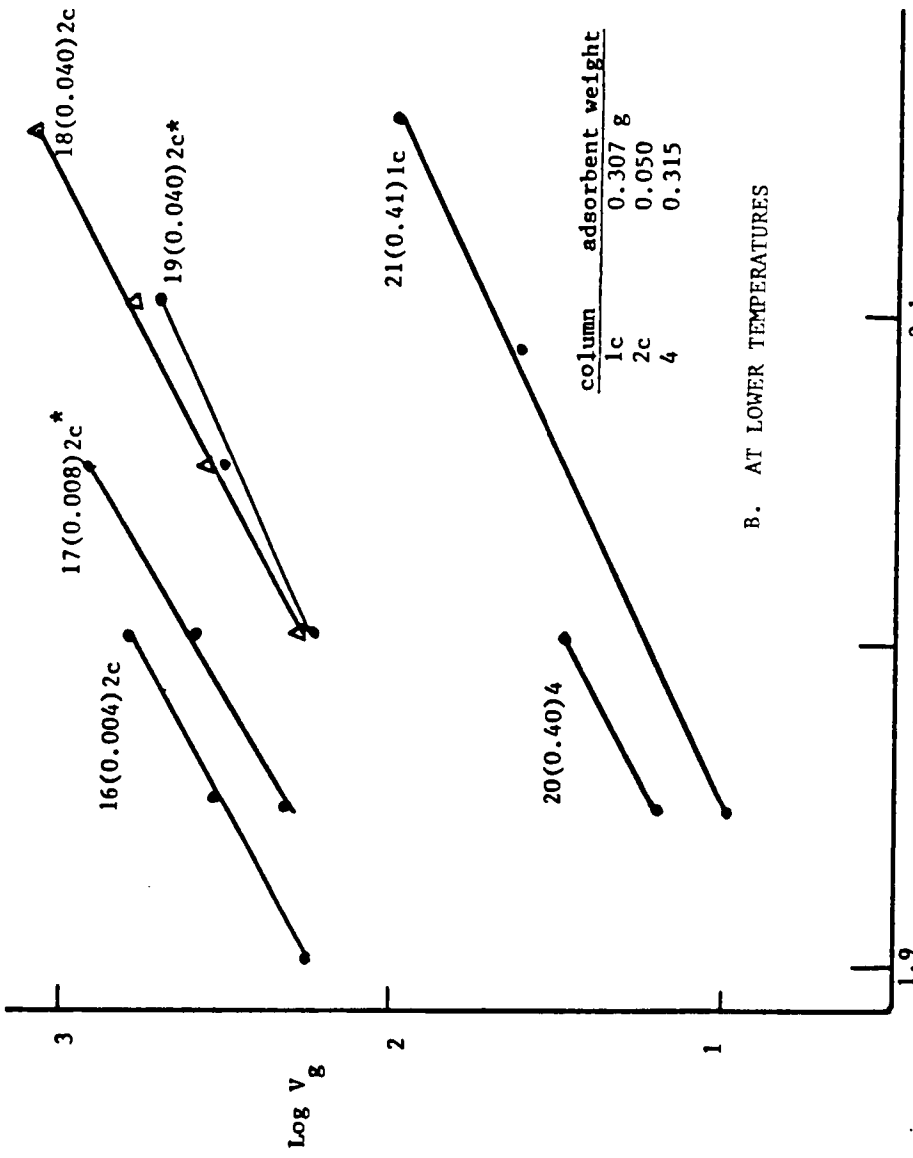

B. AT LOWER TEMPERATURES

FIGURE 4-6. (continued)

*conditioned at 400°C

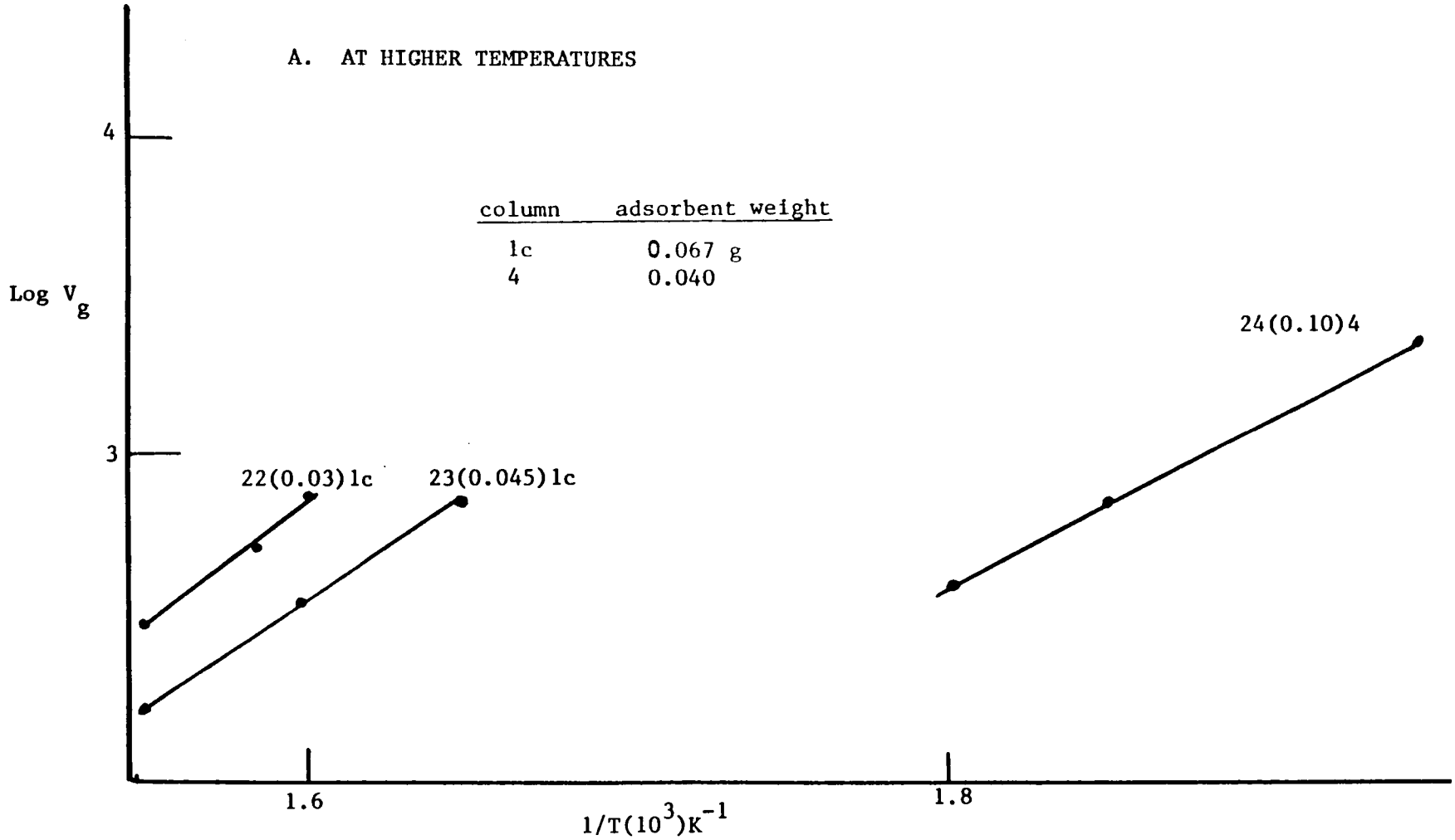

FIGURE 4-7 Log V_g versus 1/T for pyrene on KA ash

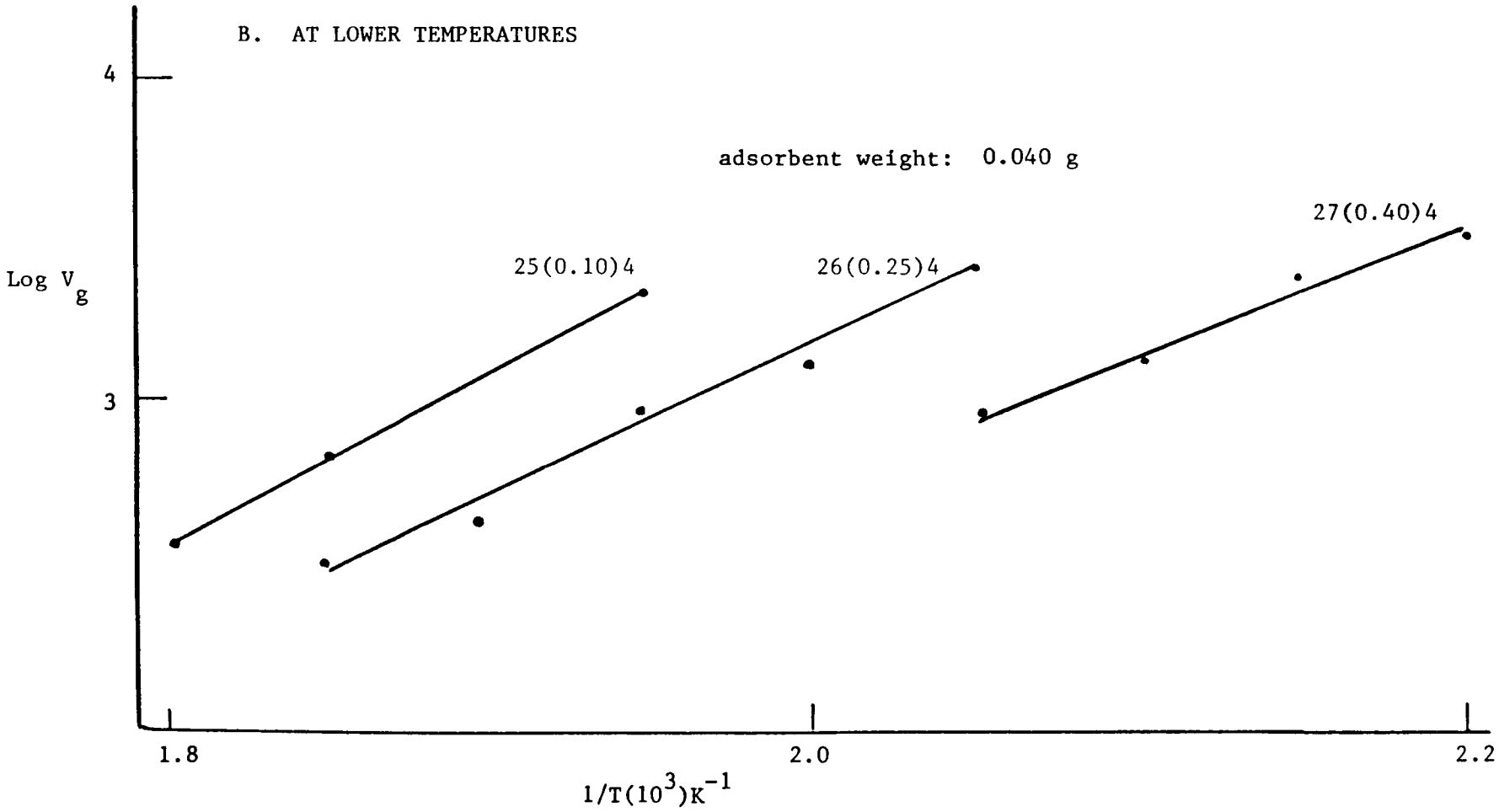

FIGURE 4-7. (continued)

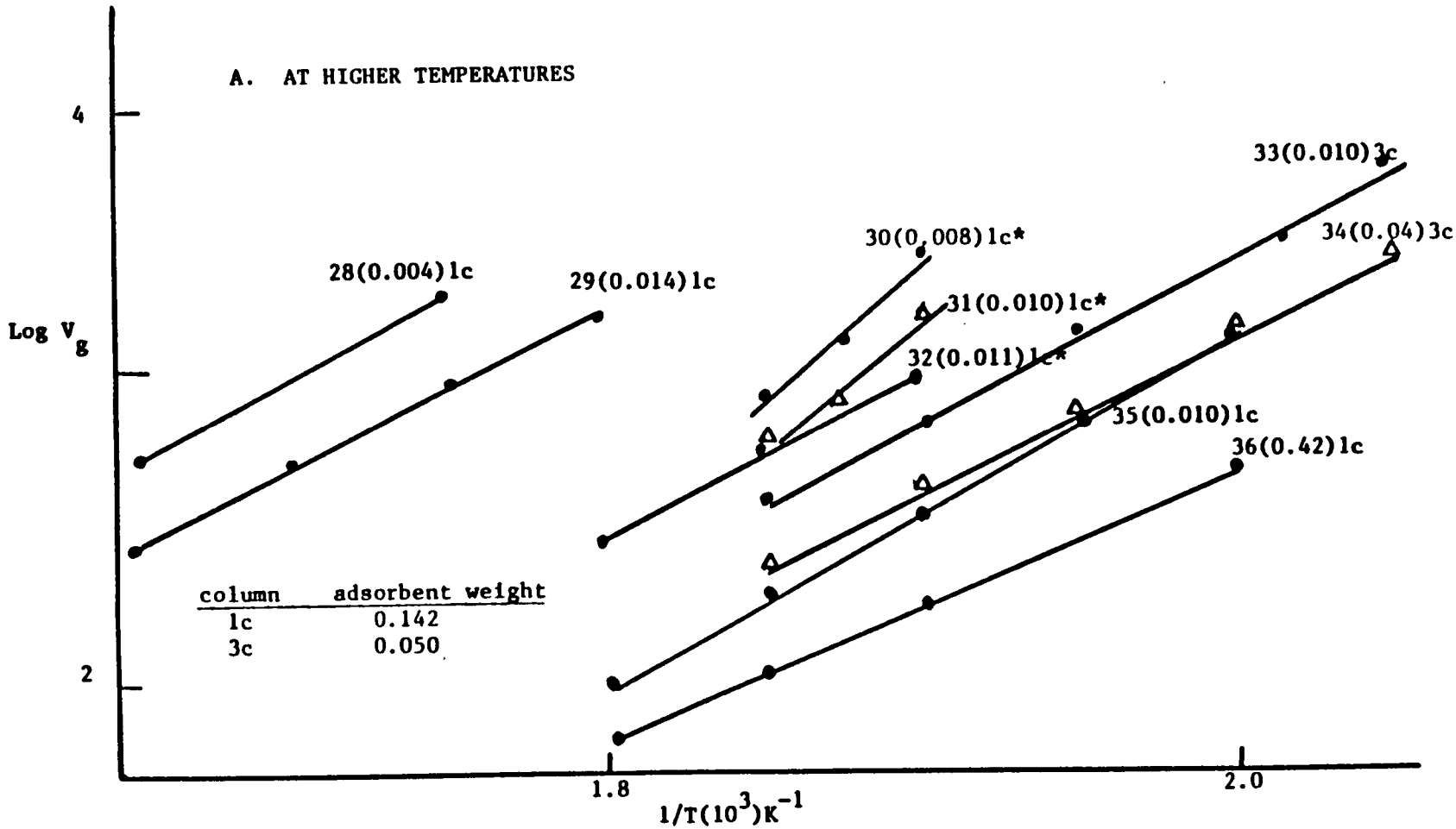

FIGURE 4-8. Log V_g versus 1/T for pyrene on ET ash

*conditioned at 400°C

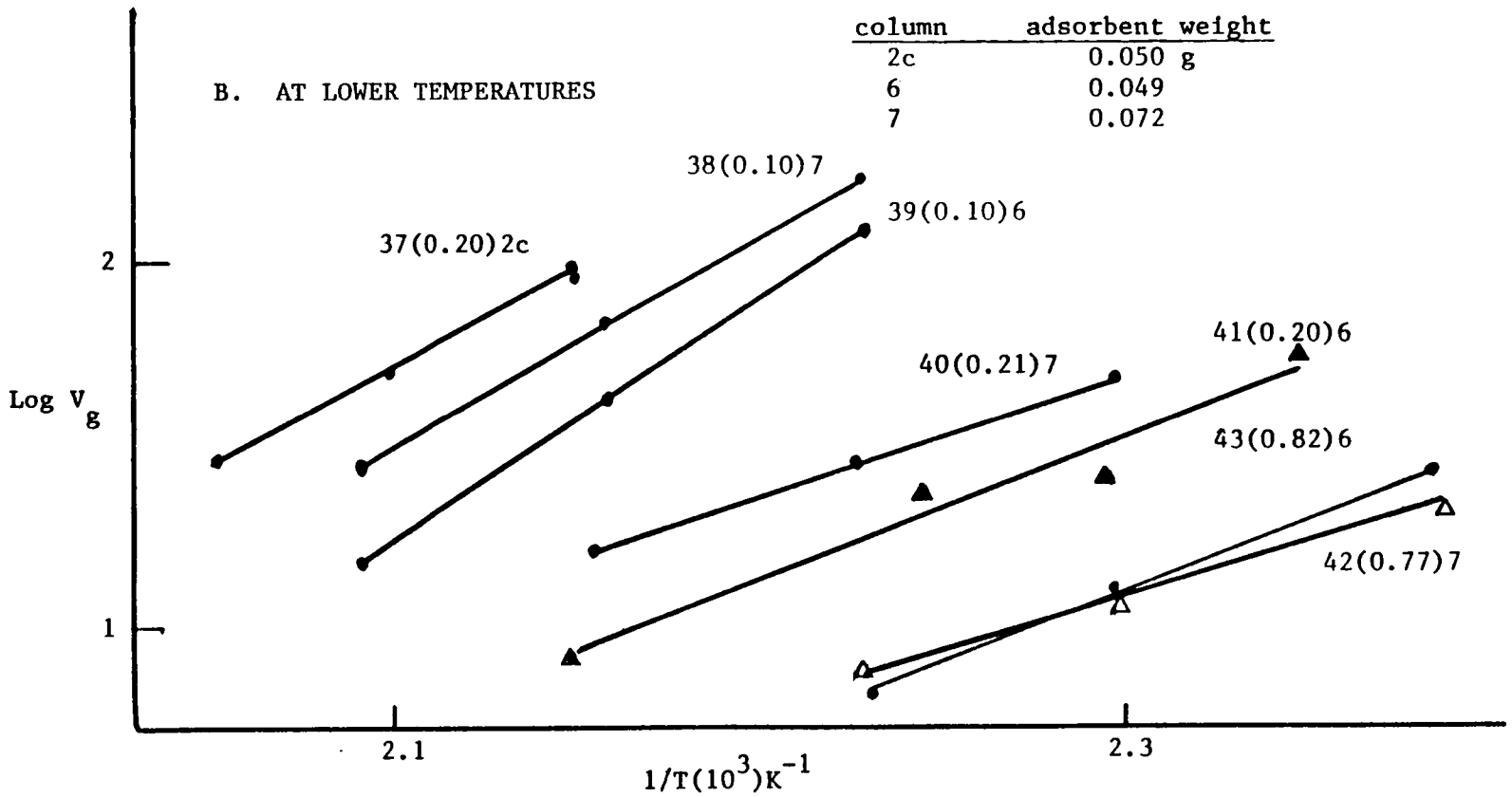

FIGURE 4-8. (continued)

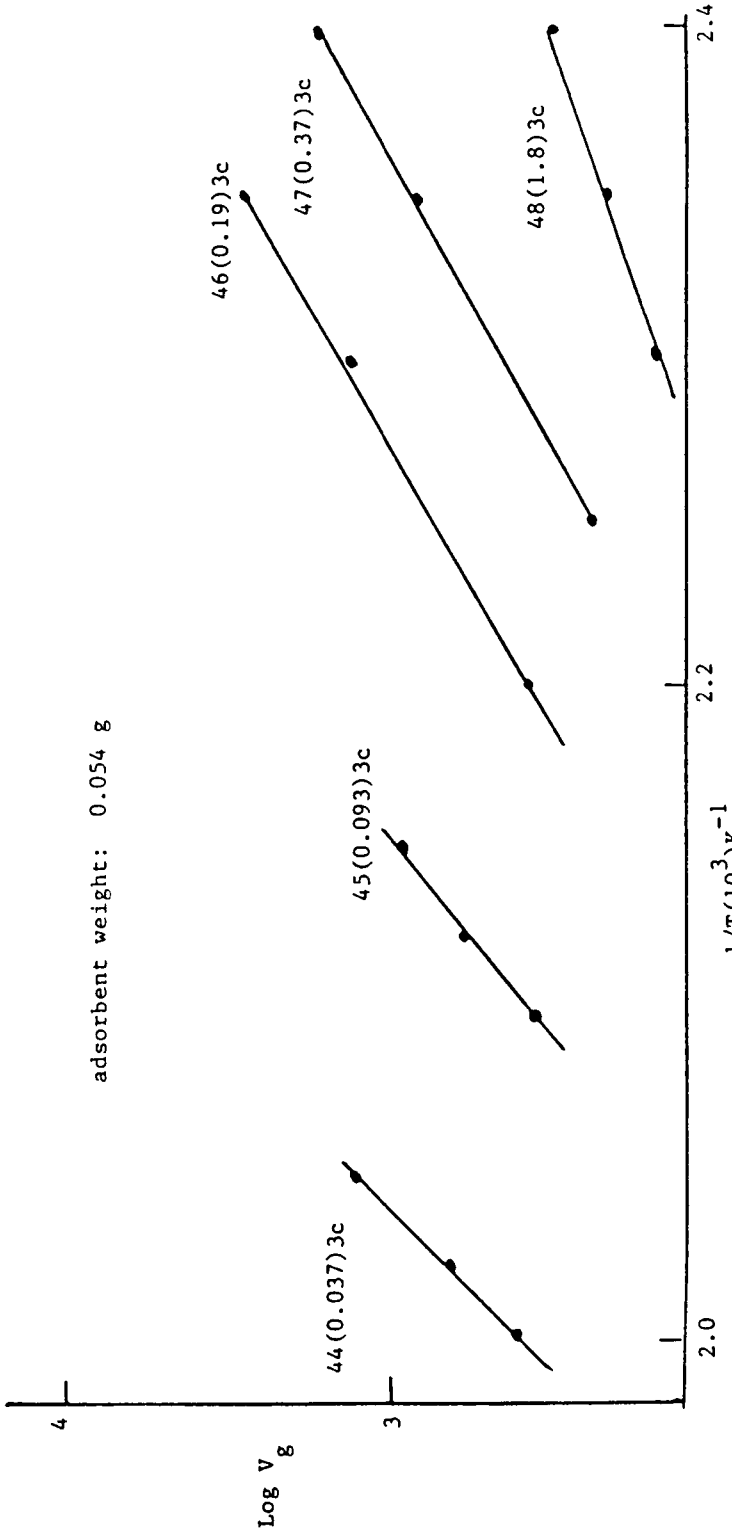

FIGURE 4-9. Log V_g versus 1/T for pyrene on AR ash

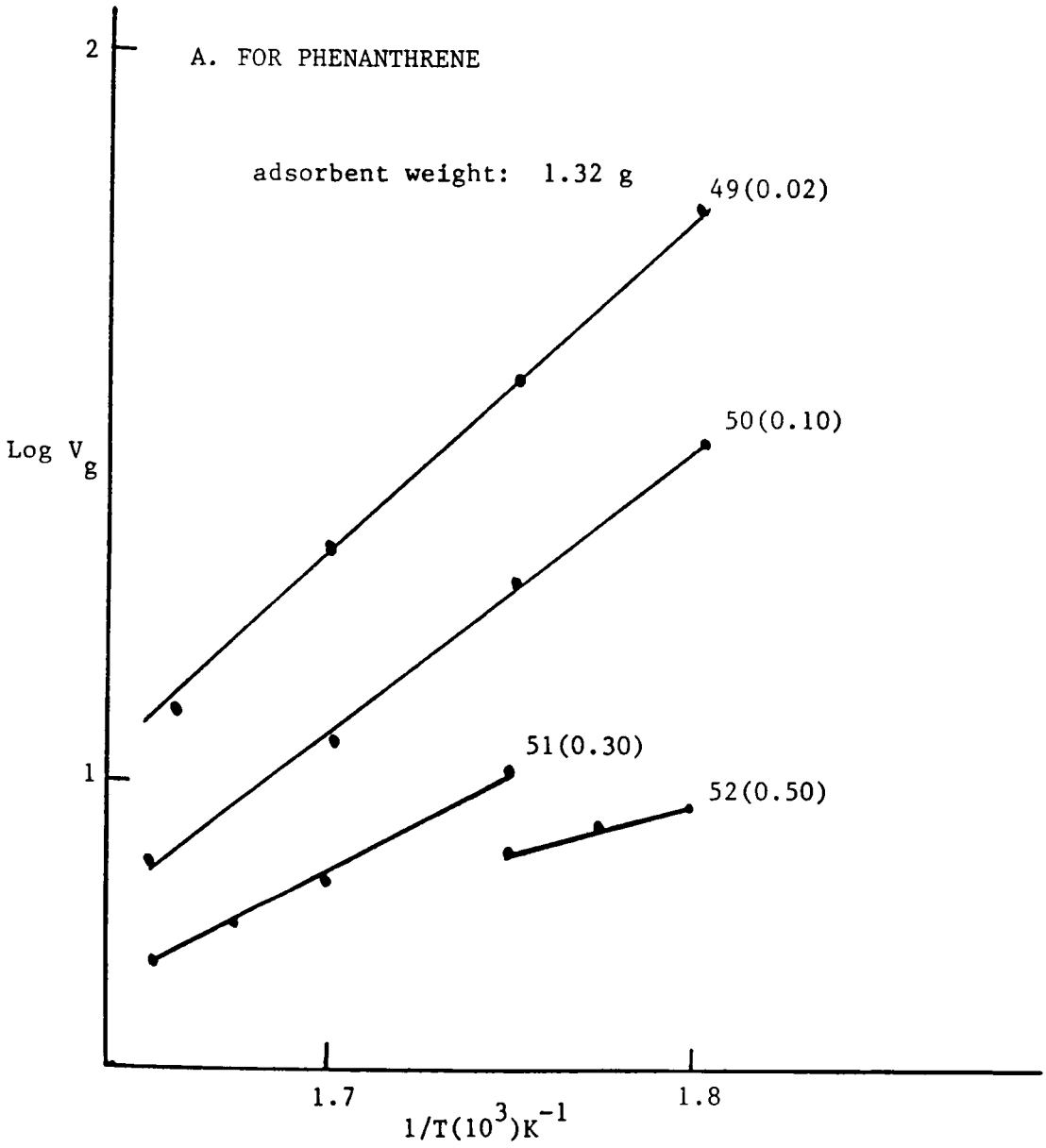

FIGURE 4-10. Log V_g versus 1/T for PAHs on TX ash

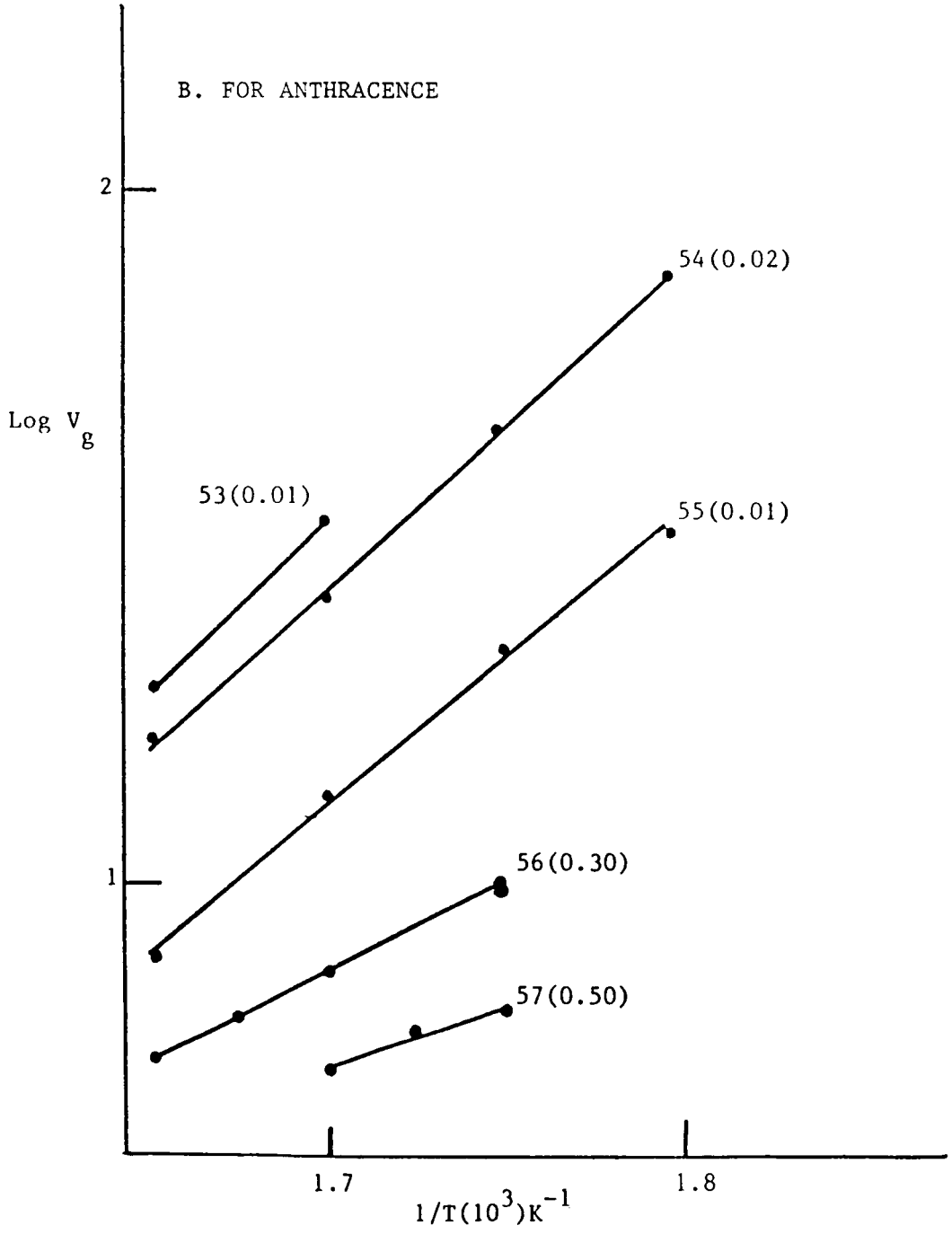

FIGURE 4-10. (continued)

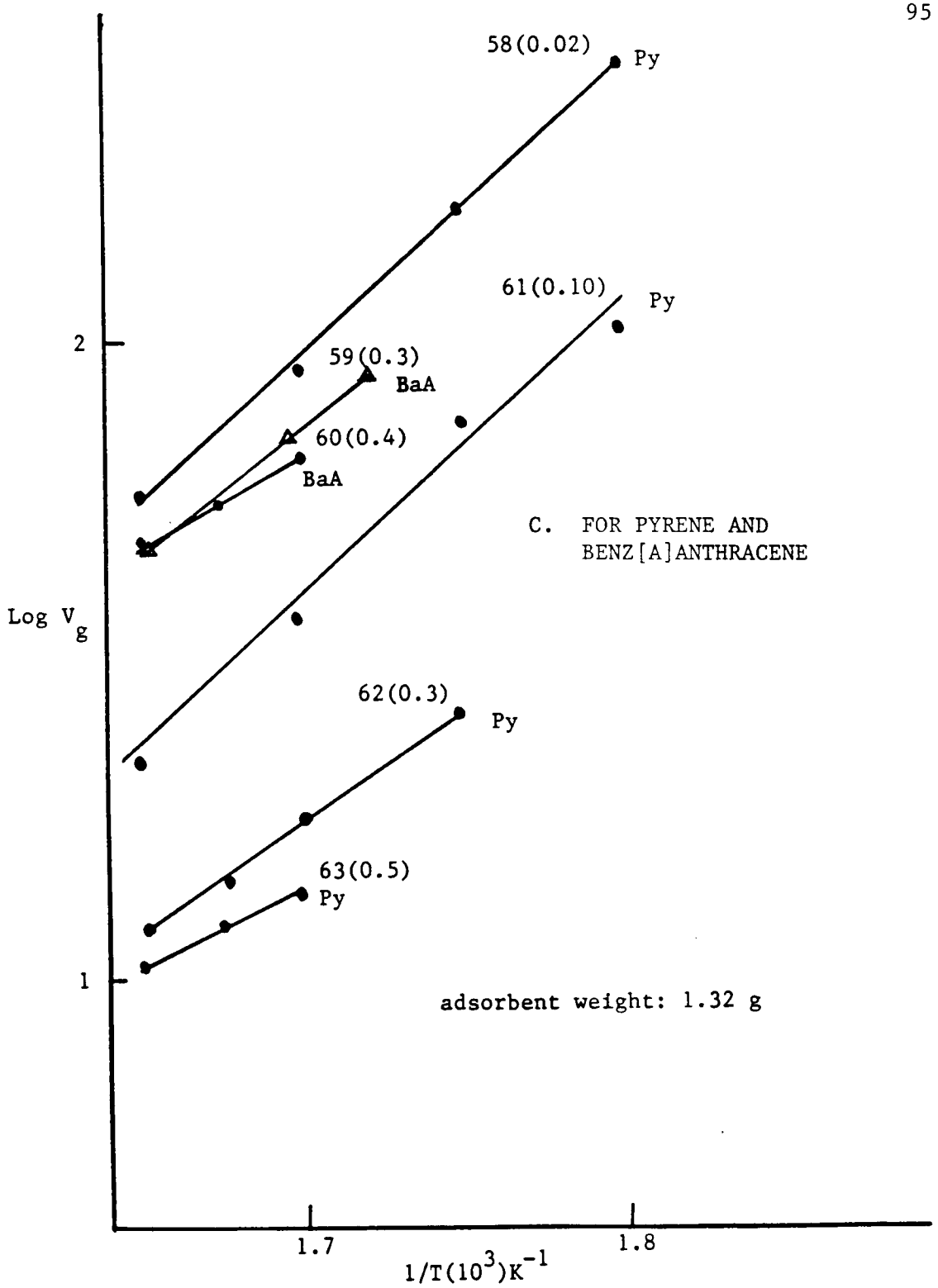

FIGURE 4-10. (continued)

TABLE 4-1

Heats of adsorption calculated from log Vg versus 1/T plots

Figure	Page num.	Plot num.	Substrate	PAH cmpd.	conc. (μmol/g)	$-\Delta H^{\circ}_{ST}$ (kJ/mol)	Corr. coef.	Column	Ads. wt. (g)	CW wt. (g)
4-4	84	1	WK	Py	0.004	103 ± 0.2	0.9686	1	0.8512	none
4-4	84	2	WK	Py	0.0176	88 ± 0.5	0.9921	1	0.8512	none
4-4	84	3	WK	Py	0.0403	69 ± 0.1	0.9998	1	0.8512	none
4-4	84	4	WK	Py	0.117	53	0.9975	1	0.8512	none
4-4	84	5	WK	Py	0.229	37 ± 0.2	0.9926	1	0.8512	none
4-4	84	6	WK	Py	0.403	32 ± 0.6	0.9955	1	0.8512	none
4-5	85	7	NM	Py	0.21	149	--	3C	0.073	0.30
4-5	85	8	NM	Py	0.20	159 ± 0.4	0.9897	4C	0.109	0.30
4-5	85	9	NM	Py	0.18	152	--	1C	0.307	0.30
4-5	85	10	NM	Py	0.41	137	--	3C	0.073	0.30
4-6A	86	11	TX	Py	0.002	125 ± 0.4	0.9992	1C	0.307	0.30
4-6A	86	12	TX	Py	0.004	120	0.9995	1C	0.307	0.30
4-6A	86	13	TX	Py	0.015	98	--	4	0.315	none
4-6A	86	14	TX	Py	0.041	108	0.9995	1C	0.307	0.30
4-6A	86	15	TX	Py	0.016	96	0.9999	4	0.315	none
4-6B	87	16	TX	Py	0.004	104	0.9999	2C*	0.050	0.30
4-6B	87	17	TX	Py	0.008	130	--	2C	0.050	0.30
4-6B	87	18	TX	Py	0.040	100 ± 0.5	0.9999	2C*	0.050	0.30
4-6B	87	19	TX	Py	0.040	91	0.9968	2C	0.050	0.30
4-6B	87	20	TX	Py	0.40	100	--	4	0.315	none
4-6B	87	21	TX	Py	0.41	96	0.9981	4	0.315	none
4-7A	88	22	KA	Py	0.03	140	0.9976	1C	0.067	0.30
4-7A	88	23	KA	Py	0.045	128	0.9995	1C	0.067	0.30
4-7A	88	24	KA	Py	0.10	99	0.9984	4	0.040	none
4-7B	89	25	KA	Py	0.10	99	--	4	0.040	none
4-7B	89	26	KA	Py	0.25	95 ± 0.4	0.9913	4	0.040	none
4-7B	89	27	KA	Py	0.40	94	--	4	0.040	none
4-8A	90	28	ET	Py	0.004	110	--	1C	0.142	0.30
4-8A	90	29	ET	Py	0.014	92 ± 0.8	0.9997	1C*	0.142	0.30
4-8A	90	30	ET	Py	0.008	165	0.9958	1C*	0.142	0.30
4-8A	90	31	ET	Py	0.010	170	0.9891	1C*	0.142	0.30
4-8A	90	32	ET	Py	0.011	116	--	1C	0.142	0.30
4-8A	90	33	ET	Py	0.010	104	0.9998	3C	0.050	0.30
4-8A	90	34	ET	Py	0.040	94	0.9997	3C	0.050	0.30
4-8A	90	35	ET	Py	0.010	102	--	1C	0.142	0.30
4-8A	90	36	ET	Py	0.42	85	--	1C	0.142	0.30
4-8A	90	37	ET	Py	0.20	103	0.9972	2C	0.050	0.30
4-8A	90	38	ET	Py	0.10	108	0.9999	7	0.072	none
4-8B	91	39	ET	Py	0.10	127	0.9994	2C	0.050	0.30

TABLE 4-1 (Continued)

Figure	Page num.	Plot num.	Substrate	PAH cmpd.	conc. (μmol/g)	$-\Delta H^{\circ}_{ST}$ (kJ/mol)	Corr. coef.	Column	Ads. wt. (g)	CW wt. (g)
4-8B	91	40	ET	Py	0.21	58	0.9990	7	0.072	none
4-8B	91	41	ET	Py	0.20	95	0.999	6	0.049	none
4-8B	91	42	ET	Py	0.77	61	0.9997	7	0.072	none
4-8B	91	43	ET	Py	0.82	77	--	6	0.049	none
4-9	92	44	AR	Py	0.037	196	--	3C	0.054	0.30
4-9	92	45	AR	Py	0.093	164	--	3C	0.054	0.30
4-9	92	46	AR	Py	0.019	98 ± 1.4	0.9980	3C	0.054	0.30
4-9	92	47	AR	Py	0.037	97	--	3C	0.054	0.30
4-9	92	48	AR	Py	1.8	71	0.9999	3C	0.054	0.30
4-10A	93	49	TX	Ph	0.02	91	--	1	1.32	none
4-10A	93	50	TX	Ph	0.10	76 ± 0.2	0.9983	1	1.32	none
4-10A	93	51	TX	Ph	0.30	58	0.9936	1	1.32	none
4-10A	93	52	TX	Ph	0.50	28	0.9999	1	1.32	none
4-10B	94	53	TX	An	0.01	92 ± 3.6	0.9988	1	1.32	none
4-10B	94	54	TX	An	0.02	87	0.9976	1	1.32	none
4-10B	94	55	TX	An	0.10	78	--	1	1.32	none
4-10B	94	56	TX	An	0.30	50	--	1	1.32	none
4-10B	94	57	TX	An	0.50	33	--	1	1.32	none
4-10C	95	58	TX	Py	0.02	89	0.9989	1	1.32	none
4-10C	95	59	TX	BaA	0.3	76	0.9964	1	1.32	none
4-10C	95	60	TX	BaA	0.4	57	--	1	1.32	none
4-10C	95	61	TX	Py	0.10	91	0.9931	1	1.32	none
4-10C	95	62	TX	Py	0.3	65	--	1	1.32	none
4-10C	95	63	TX	Py	0.5	50	--	1	1.32	none

*conditioned at 400°C.

where R is the gas constant equal to 8.3144($JK^{-1}mol^{-1}$) and the factor 2.303 is a conversion factor from natural logarithms to base 10 logarithms. In addition, the standard deviation in the heat of adsorption (calculated from the standard deviation of the slope) and the linear correlation coefficient is shown.

As is evident in Figure 4-4, the slope (and thus the heat of adsorption) increased with decreasing adsorbate concentrations. This was typical of all fly ashes. In addition, the temperature interval over which retention measurements were made decreased with decreasing adsorbate concentration, as explained later.

At higher adsorbate concentrations, temperature intervals of 50-70°C were sufficient to obtain three or four data points, from which $-\Delta H^{o}_{ST}$ could be calculated with a reasonably small degree of statistical uncertainty (less than ±2 kJ/mol standard deviation). Enough data points were usually taken to obtain a minimum linear correlation coefficient of 0.990.

Retention times of one to five minutes were generally required to separate the solute peaks from the solvent peaks. Beyond retention times of about 10 minutes, peak broadening prohibited accurate determination of retention times in most cases, since the peak maxima became more difficult to pinpoint. Occasionally, at the higher surface coverages, retention times as high as 40 minutes were observable.

The requirement of a retention time window of 1-10 minutes resulted in a narrowing of the temperature interval over which peaks could be observed at lower surface coverages. This is because, in approaching lower surface coverages, the slope of the log V_g vs. 1/T plot became

larger, so that a change in log V_g corresponding to a retention time window of 1-10 minutes occured within a change in temperature which became smaller.

For most substrates the difference in retention time for duplicate runs was within ten percent. Eventually the temperature interval became too small, given this variation in retention time, to obtain a statistically significant value of of $-\Delta H^{o}_{ST}$; thus a minimum adsorbate concentration was established for each ash, below which $-\Delta H^{o}_{ST}$ could not be measured. However, for two substrates, NM and KA, the variation of retention time for duplicate runs increased rapidly as the adsorbate concentration decreased, so that the minimum adsorbate concentration was more a result of approaching a large standard deviation (greater than ±15%) in the retention time measurement rather than a result of a shrinking temperature interval. The minimum adsorbate concentrations observed for each substrate are shown in Table 4-2.

4.3.3 Heats of Adsorption Versus Adsorbate Concentration

In order to compare $-\Delta H^{o}_{ST}$ for a particular PAH on different adsorbents, it was necessary to verify that minor changes in adsorbent weight from column to column did not affect the results. Similarly, it was necessary to check whether differences in the temperature interval over which measurements were made from column to column influenced these results and whether the presence of the nonadsorbent substrate CW had any effect.

Experiments were initially performed using long columns filled with large quantities of pure adsorbent. However, only a limited number of

TABLE 4-2

Minimum adsorbate concentration at which ΔH^{o}_{ST} could be determined

Data for pyrene on 6 coal fly ashes

ash	minimum conc. (μmol/g)
NM	0.10
AR	0.037
KA	0.030
ET	0.006
TX	0.002
WK	0.004

adsorbents yielded observable chromatographic peaks when packed in this manner: namely TX, AR, silica, and WK substrates. NM and KA ashes were so retentive that no peaks were observed after hours of elution from these types of columns. In the case of ET ash, this substrate had such a high pneumatic impedance that a flow rate above 5 ml/min could not be established. Thus for these three ashes the elution time was prolonged beyond the limit in which the peak would be observable. Eventually, a technique employing a smaller amount of adsorbent was developed. This was done by either using a shorter column or by diluting the adsorbent with nonadsorbent CW in a long column; peaks from all seven of the aforementioned adsorbents were observable using these columns and therefore data from these columns were used to obtain major comparisons of $-\Delta H^{o}_{ST}$ and K_D. Some data from the columns containing larger adsorbent weights were also used: namely, for comparing $-\Delta H^{o}_{ST}$ for several PAHs on the same column, for comparing $-\Delta H^{o}_{ST}$ on silica verses TX ash, and for indicating the effect of adsorbent weights on $-\Delta H^{o}_{ST}$.

Because the supply of WK ash ran out before a column containing a small adsorbent weight could be prepared, and because the adsorbent weight was found to affect the $-\Delta H^{o}_{ST}$ measurement at higher surface coverages, WK ash was excluded from comparisons with the other substrates. However, plots for WK were shown in Figure 4-4 for the purpose of showing the progression of slope increase with decreasing adsorbate concentration.

4.3.3.1 Columns with Large Adsorbent Weights

From the first round of experiments using 50-cm columns filled with 0.5-1.3 grams of pure adsorbent, plots of $-\Delta H^{o}_{ST}$ vs. adsorbate

concentration for pyrene adsorbed on TX, AB, WK, and silica are shown in Figure 4-11A. Data for substrates for which BET (N_2) surface areas were known (page 33) were replotted using "percentage surface coverage" as the abscissa in Figure 4-11B.

Similar plots for four PAHs on TX ash are shown in Figure 4-12A and B. Percentage surface coverages were calculated using molecular areas of 86.7 $\mathring{A}^2$ for anthracene and phenanthrene, 90.9 $\mathring{A}^2$ for pyrene and 104.5 $\mathring{A}^2$ for benz[a]anthracene,[36,46] assuming that in each case, the ring system was parallel to the adsorbent surface for an adsorbed PAH molecule.

There is no known experimental evidence that describes the geometry with which PAH molecules adsorb on fly ash surfaces. If some geometry other than the parallel arrangement assumed here prevailed, the percentage coverage would be smaller than those calculated here, which represents the largest possible percentage surface coverage for a particular weight of adsorbed PAH. It was also assumed that the BET (N_2) surface area was valid for adsorption of PAHs, which may, of course, be an invalid assumption.

Table 4-3 lists $-\Delta H^{o}_{ST}$ versus adsorbate concentration for anthracene and pyrene on silica.

4.3.3.2 Columns with Small Adsorbent Weights

The second series of experiments, conducted on columns containing about 0.05g of adsorbent mixed with 0.30g of nonadsorbent CW, produced the plots of $-\Delta H^{o}_{ST}$ vs. adsorbate concentration shown in Figure 4-13A and B. In Figure 4-13C and D, data for substrates with variable BET (N_2)

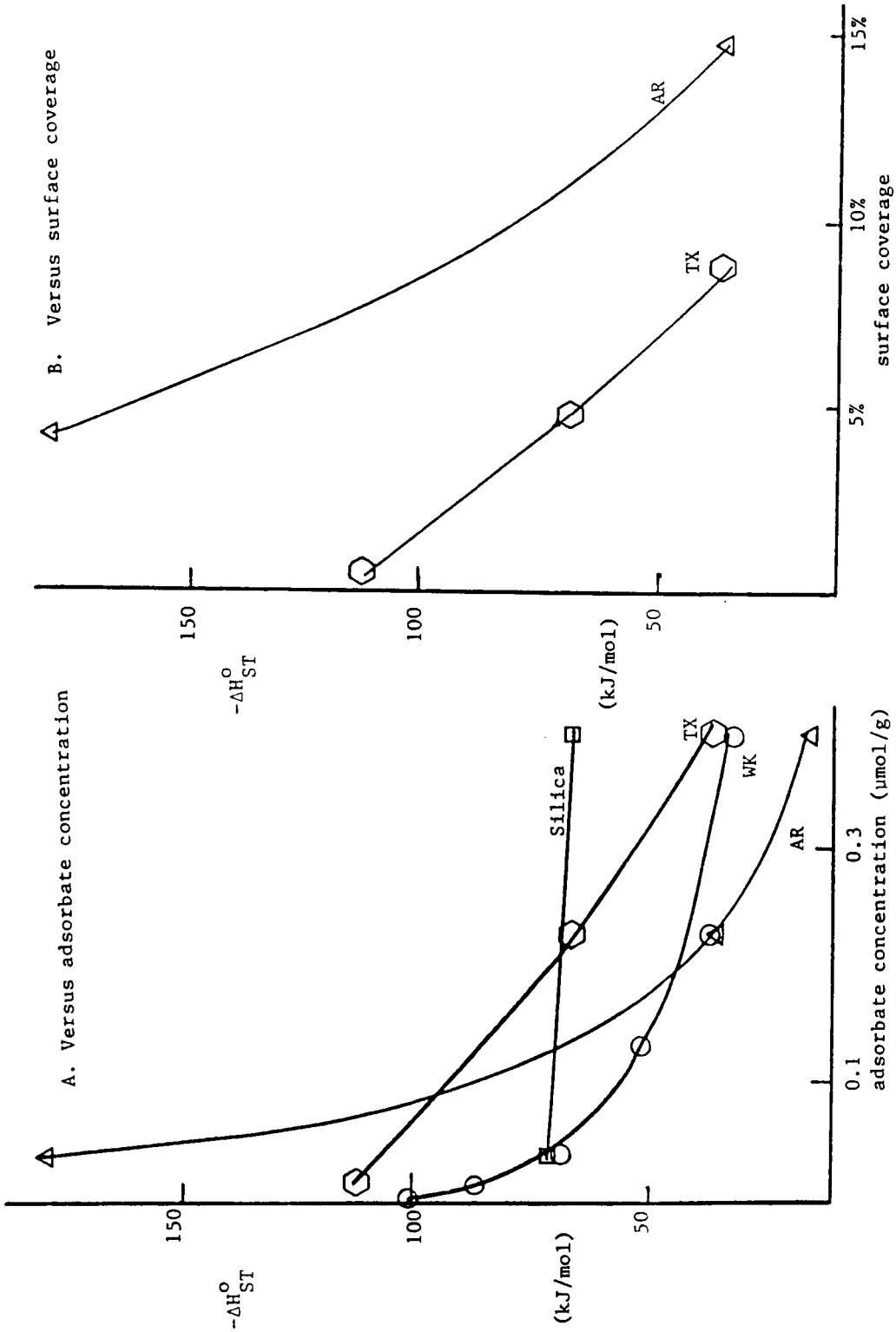

FIGURE 4-11. Heats of adsorption for pyrene on various substrates using large adsorbent weights

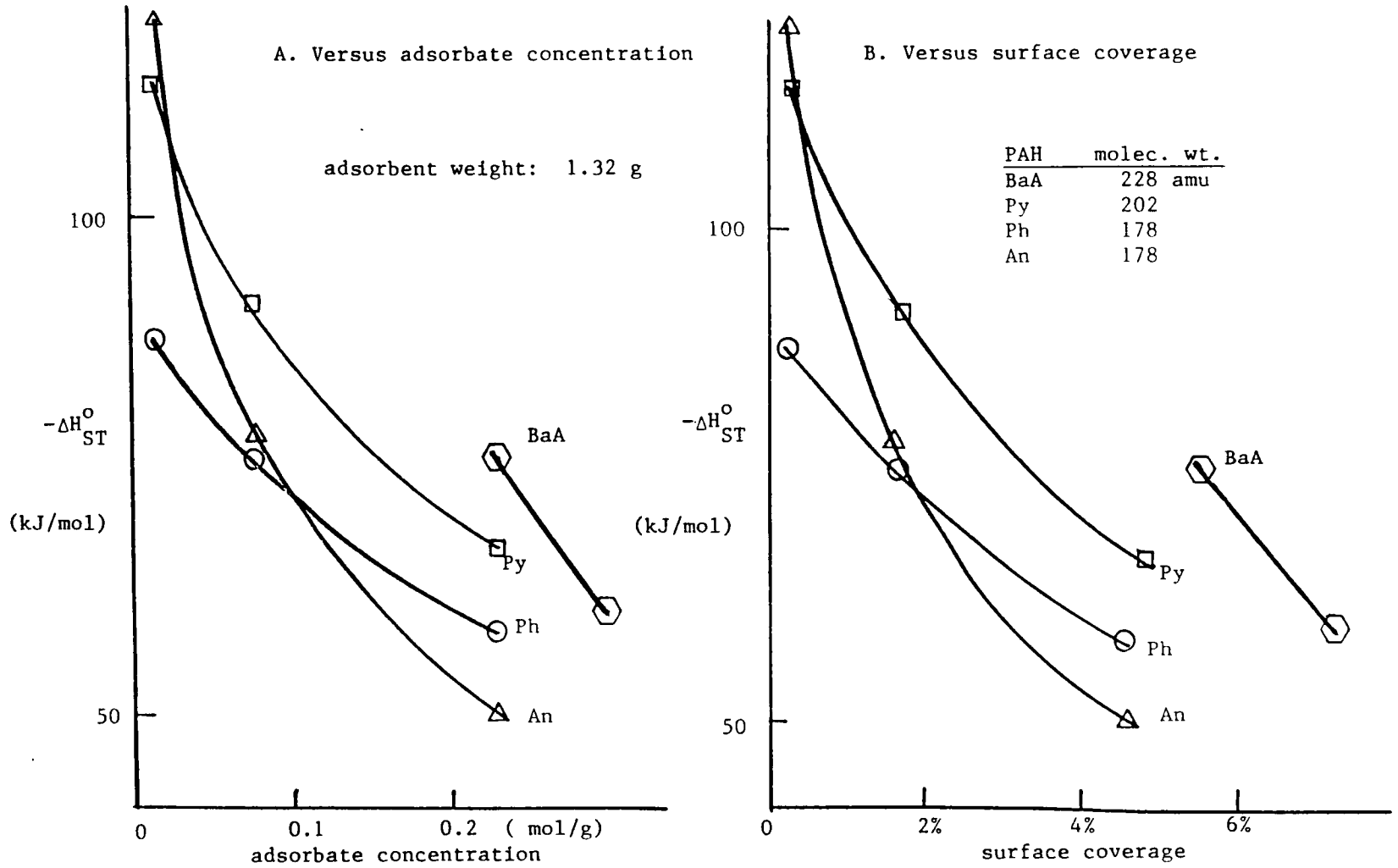

FIGURE 4-12. Heats of adsorption for PAHs on TX ash

TABLE 4-3

Heat of adsorption of pyrene and anthracene on silica

Concentration (μmol/g)	$-\Delta H^{o}_{ST}$ anthracene (kJ/mol)	$-\Delta H^{o}_{ST}$ pyrene (kJ/mol)
.0348	68	72
.5220	63	67
1.392	59	67
1.740	60	66

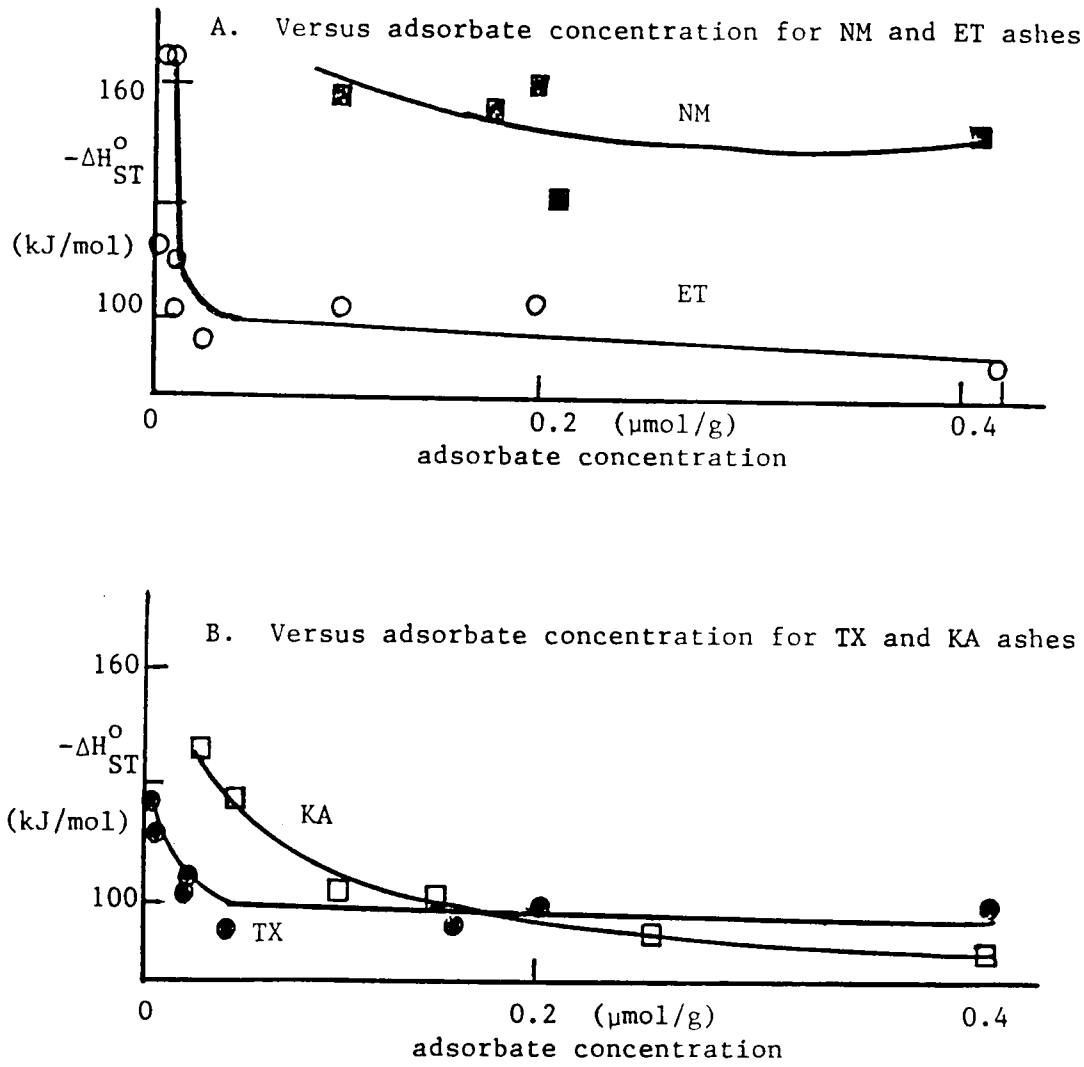

FIGURE 4-13. Heats of adsorption for pyrene on various substrates using small adsorbent weights

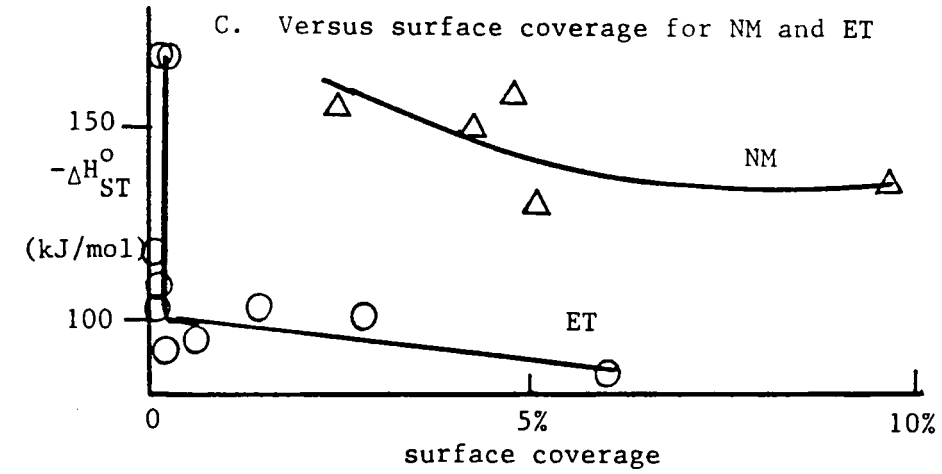

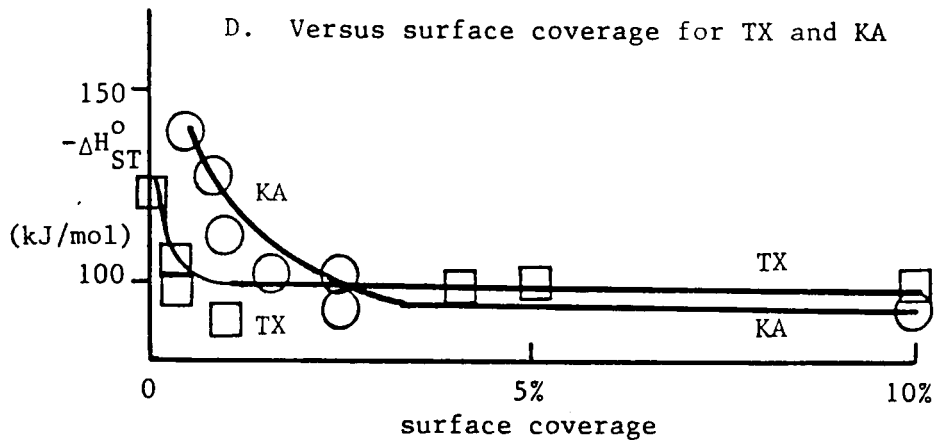

FIGURE 4-13. (continued)

surface areas have been replotted using percentage surface coverage.

In Figures 4-14A, B and C, plots of $-\Delta H^{o}_{ST}$ vs. adsorbate concentration for small amounts of pure adsorbent appear on the same graph of plots for small amounts of adsorbent mixed with nonadsorbent CW. The purpose of this was to see whether adding the nonadsorbent CW changes the observed $-\Delta H^{o}_{ST}$. Since data points for columns with or without nonadsorbent CW fall along the same plot, it was concluded that nonadsorbent CW substrate did not affect $-\Delta H^{o}_{ST}$. Further evidence for the nonadsorptive nature of CW was obtained by injecting pyrene onto columns containing only pure CW; no separations of solute and solvent peaks were observed.

4.3.3.3 Variation of $-\Delta H^{o}_{ST}$ with Adsorbent Weight

Figure 4-15 shows that for columns containing 0.3g or less of TX ash, $-\Delta H^{o}_{ST}$ was constant with changing adsorbent weight. For the column containing 1.3g of TX ash, $-\Delta H^{o}_{ST}$ was lower at surface coverages greater than 0.7%, compared to the value of $-\Delta H^{o}_{ST}$ for the other columns containing less ash. This drop in $-\Delta H^{o}_{ST}$ at higher adsorbate concentrations when the adsorbent weight was large may have resulted from an increase in the "effective adsorbate concentration" as the column length increased.

By our definition, adsorbate concentration is the amount of PAH injected divided by the adsorbent weight. However, note that a plug of injected solute does not distribute itself evenly over the entire adsorbent surface, but moves along the column and broadens with time. For two 1/4 inch i.d. columns with radically different weights of the

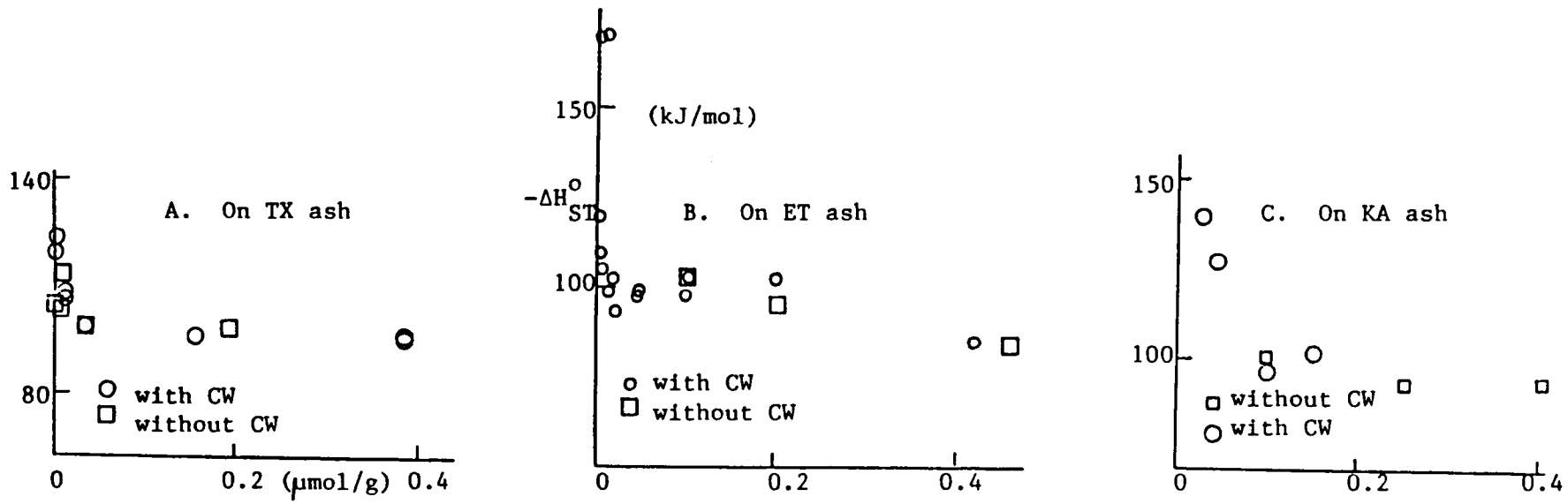

FIGURE 4-14. Heats of adsorption for columns with and without nonadsorbent CW

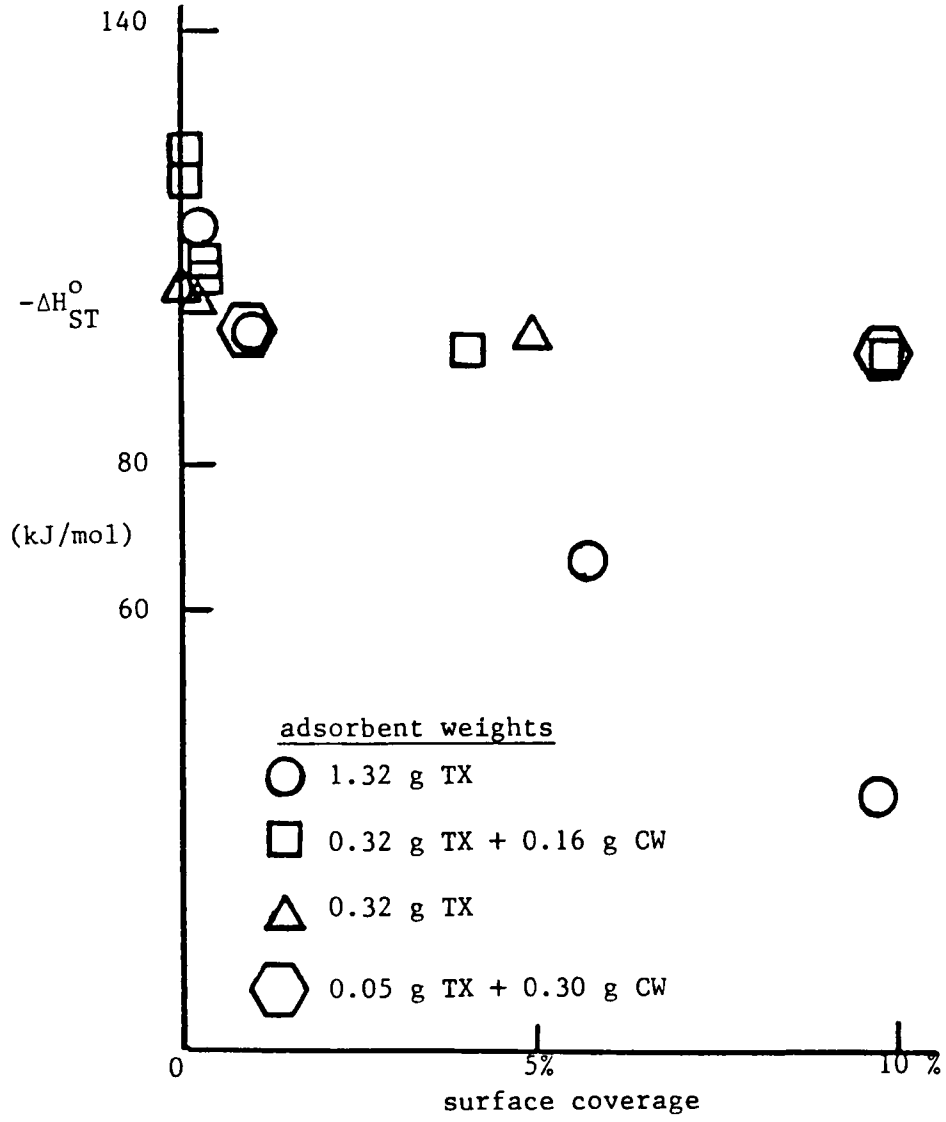

FIQURE 4-15. Variation of the heat of adsorption with adsorbent weight on TX ash

same adsorbent, a more concentrated plug must be injected into the column with the larger weight of adsorbent in order to obtain the same adsorbate concentration. The more concentrated plug makes the "effective adsorbate concentration" (that is, the concentration in a short segment of the column in which the plug is centered) larger than in the other columns. Because $-\Delta H^{o}_{ST}$ decreases with increasing adsorbate concentration, the result is that $-\Delta H^{o}_{ST}$ is higher for the column with the larger weight of adsorbent. For a given adsorbate concentration, this effect would not show up as much for columns in which the adsorbent weight was small because the solute would be able to spread through the entire mass of adsorbent more evenly.

It was apparent from the data that effects due to adsorbent weight were negligible over the entire surface coverage range (up to 10%) for adsorbent weights of 0.3g or less. For columns containing much less than 0.05g of adsorbent, reproducibility of elution times became very poor (standard deviation greater than ±30%). Therefore, an adsorbent weight of about 0.05g was chosen as the optimum and used for important comparisons of $-\Delta H^{o}_{ST}$ for pyrene on various substrates.

It should be noted that, for these columns with such small adsorbent weights, reproducibility of elution times was improved by mixing the adsorbent with nonadsorbent CW. It is believed that such dilution of the adsorbent through a nonadsorbent matrix improved reproducibility of contact between the solute and individual adsorbent particles. Thus, with improved reproducibility it was possible to obtain data at lower adsorbate concentrations by mixing the adsorbent with nonadsorbent CW.

4.3.3.4 Variation of $-\Delta H^{o}_{ST}$ With Temperature

Since some substrates were more retentive than others, it was not always possible to obtain data for $-\Delta H^{o}_{ST}$ in the same temperature ranges for all substrates. This is true because the more retentive substrates required higher temperatures to elute the solute peaks within twenty minutes. Beyond this elution time, peaks were usually too broadened to measure their maxima. It was therefore necessary to check whether the temperature range in which $-\Delta H^{o}_{ST}$ was measured affected the observed experimental value of $-\Delta H^{o}_{ST}$ significantly; otherwise, comparisons of $-\Delta H^{o}_{ST}$ obtained at different temperature ranges might not be valid.

In Table 4-4 the temperature dependence of $-\Delta H^{o}_{ST}$ for pyrene adsorbed on TX ash is examined at three different adsorbate concentrations. It is apparent that for TX ash, there is little dependence of the experimentally observed $-\Delta H^{o}_{ST}$ on temperature, so that the temperature factor was not considered a source of experimental error in comparing $-\Delta H^{o}_{ST}$ in the sections that follow.

Because of the extensive amount of data obtained on TX ash for columns of different weights, etc., it was possible to extract the data for Table 4-4 after most retention experiments had already been done. However, not enough data were available for other substrates to check the temperature dependence of $-\Delta H^{o}_{ST}$ on them. It is assumed that $-\Delta H^{o}_{ST}$ values on these other substrates are similarly independent of temperature.

4.3.4 Heats of Adsorption for Different PAHs

The heats of adsorption of anthracene, phenanthrene, pyrene, and

TABLE 4-4

Temperature dependence of the heat of adsorption of pyrene on TX ash

Heat of adsorption in kJ/mol (temperature range in parentheses)

	Adsorbent weights		
Conc. (μmol/g)	1.3g	0.3g	0.05g
0.012		108 (167-315°C)	103 (192-240°C)
0.040	100 (267-333°C)	98 (240-267°C)	100 (192-203°C)
0.18		96 (240-267°C)	99 (161-181°C)

benzo[a]anthracene on TX ash are related as a function of adsorbate concentration in Figure 4-12 (pg 104). A fifth PAH, benzo[a]pyrene, was retained too strongly on this ash to obtain useful data. The same problem for benz[a]anthracene allowed only two data points to be obtained.

At surface coverages above four percent the order of increasing heats of adsorption was as follows:

anthracene < phenanthrene < pyrene < benz[a]anthracene

This order is in the same direction as increasing molecular weight and increasing boiling point. At lower surface coverages, there was a dramatic increase in the heat of adsorption for anthracene compared to the other PAHs, causing a rearrangement in the order to

phenanthrene < pyrene < anthracene

at a coverage of about 0.03%.

The heats of adsorption for anthracene and pyrene on silica shown in Table 4-3, (pg. 105) are fairly constant with concentration, with anthracene having a consistently lower $-\Delta H^{o}_{ST}$ than pyrene.

The behavior of PAH on these two substrates was consistent with the "patch model" of adsorption (see pg. 73), wherein fly ash, being a heterogeneous substrate having a large distribution of adsorption sites, would be expected to have a heat of adsorption that gradually decreases as higher energy sites are filled. The relatively homogenous silica, on the other hand, should have a large number of sites of equal energy,

resulting in a virtually constant heat of adsorption as these sites are filled.

The change in the relative order of the heats of adsorption of different PAHs on TX ash as a function of surface coverage suggests that, at higher concentrations, the heat of adsorption may depend on molecular weight similar to dependence of boiling point on molecular weight; but at lower concentrations the PAH structure may influence adsorption via specific adsorbate-surface interactions. Further speculations in this direction at the present time are not warranted by the available data.

4.3.5 Heats of Adsorption and Distribution Coefficient

This section, which discusses the differences in the observed values of the heats of adsorption of pyrene on various fly ashes, is the most important section in this chapter. Comparisons of the distribution coefficients for pyrene adsorbed on the various ashes are also presented in this section because these data confirm conclusions drawn from the heat of adsorption comparisons.

Recall from Chapter 2 that there were significant differences in the photochemical reactivity of pyrene on a series of fly ashes which could not be explained on the basis of substrate reflectance alone. For instance, in Table 2-5 (pg. 31) we were interested in finding explanations for the extremely low overall photochemical reactivity of pyrene on ET and NM ashes, compared to the high overall photochemical reactivity on TX ash which had about the same average reflectance as the other two.

To facilitate comparisons of $-\Delta H^{o}_{ST}$, data from plots in Figures 4-11 (pg. 103) and 4-13 (pg. 106) has been condensed into Table 4-5, which contains heats of adsorption of pyrene on various coal fly ashes at three surface coverages. The values of K_D corresponding to these surface coverages have also been calculated from retention data and are shown in Table 4-6.

It is evident from both tables that the affinity of pyrene for fly ash surfaces increases in the order

$$ET < TX < KA < NM < AR$$

except at the lowest surface coverage where the affinity for ET ash increases substantially to become equivalent to the affinity for NM or AR.

The high affinity for NM ash relative to TX ash may account for the greater suppression of photochemical decomposition on the NM ash. This conclusion is based on the assumption that a PAH which is more strongly bound to an ash surface would be less susceptible to photochemical decomposition, which is highly conceivable, although not unequivocally established.

A similar rationalization for the suppression of photochemical reactivity of pyrene on ET ash, relative to TX ash, is more difficult to establish than is the previous case for NM ash, since a large difference in $-\Delta H^{o}_{ST}$ between ET and TX only occurred at very low surface coverage, whereas the suppression on ET was observed at higher surface coverages of about 5%. Assuming that the $-\Delta H^{o}_{ST}$ measurements were accurate and that a high affinity for the surface does cause suppression of

TABLE 4-5

Heats of adsorption of pyrene on coal fly ash at three surface coverages

Column adsorbent	Surface Coverage		
	0.07%	0.7%	7%
AR	>181	>181	152 (kJ/mol)
NM	>150	>150	133
KA	>140	130	95
TX	120	100	98
ET	170	98	87

TABLE 4-6

Distribution coefficient "K_D" at 200°C for various concentrations of pyrene on coal fly ashes

Column adsorbent	surface coverage		
	0.07%	0.7%	7%
NM	--	--	3.1×10^5
KA	--	2.2×10^4	5.0×10^2
TX	2.5×10^3	8.7×10^2	2.8×10^2
ET	7.0×10^4	4.8×10^2	2.5×10^2

photochemical reactivity as in the case for NM ash, then the suppression in the case for ET ash probably involved a different mechanism than affinity for adsorption sites as measured by $-\Delta H^{o}_{ST}$ and K_D. The low affinity for ET ash, despite the extraordinarily low extraction recovery of pyrene from ET reported in Chapter 3, suggests that extensive irreversible adsorption may have occurred on ET ash. Such irreversible adsorption would have been undetected by the GC method used in these experiments, since these adsorption sites would have been covered up during preliminary injections of pyrene before $-\Delta H^{o}_{ST}$ measurements were actually made (referring to procedure described on page 77, top). It is conceivable that PAH adsorbed on irreversible sites would be resistant to photochemical decomposition. Thus ET would be associated with a low affinity for reversible sites but a high resistance to photochemical decomposition due to irreversible adsorption. Accurate techniques for measuring the amount of irreversible adsorption should be developed to verify whether such adsorption is actually occurring on ET ash (see page 124 for further comment).

It is possible to rationalize the suppressed photochemical reactivity on AR ash, relative to TX ash, on the basis that their extraction efficiencies (see pg. 63) and reflectances (see pg. 31) nearly match, but the affinity for AR ash is much higher than for TX ash. However, the higher photochemical reactivity on AR ash, relative to NM and ET ashes, cannot be explained by the measured affinities, since the affinity on AR ash is equal to or higher than on NM and TX ashes. Since the reflectances of AR, NM and TX ashes approximately match, we may again surmise that some other mechanism, such as

irreversible adsorption, accounts for the greater photochemical resistance on ET and NM ashes.

In the case of KA ash, which appears to have intermediate values for $-\Delta H^{o}_{ST}$ and K_D compared to the other substrates, it is difficult to draw any conclusions about the effect of affinity for the KA ash surface in suppressing photochemical reactivity. This is because the reflectance of KA is much lower than for the other substrates (see pg. 31) for which affinities were measured. Therefore the low reflectance of KA ash is expected to be a major factor in causing suppression on KA. The extent to which each individual factor -- reflectance, affinity, and extraction recovery -- contributes to the overall photochemical reactivity on any particular substrate is a matter that is taken up in Chapter 5.

We can conclude from the data that the affinity of PAH for the fly ash surface is probably a contributing factor to the total suppression of photochemical reactivity. This explains the suppression on NM and AR ashes relative to TX ash. However, other adsorbate-adsorbent interactions, such as irreversible adsorption, may be contributing to suppression; these are not taken into account by the measurement of affinity using the GC technique applied in these experiments.

4.3.6 Reliability of Results

Table 4-7 shows the reproducibility in determining $-\Delta H^{o}_{ST}$ for several PAHs over a concentration range from 0.03 to 0.40 μmol/g on three separate ashes. The differences between the first and second determinations were less than a few kJ/mol in each case. These

TABLE 4-7

Reproducibility of heat of adsorption measurements via GC

PAH	fly ash	conc. (μmol/g)	ΔH^{o}_{ST}	% difference	comment
An	AR	0.30	65.3, 63.0	3.5	repeated immediately
An	AR	0.030	82.3, 87.3	5.7	repeated next day
Phen	AR	0.30	60.0, 60.0	0.0	repeated next day
Phen	AR	0.030	82.3, 87.3	5.7	repeated next day
Py	WK	0.40	34.1, 36.7	7.1	repeated after 50 days
Py	TX	0.23	68.6, 67.5	1.6	repeated on 2nd column

differences were small compared to the 10-100 kJ/mol differences in $-\Delta H^{o}_{ST}$ used to distinguish different levels of affinity among the fly ashes and changes in affinity with concentration in Table 4-5. The distinguishing levels of affinity were therefore statistically significant in view of the good reproducibility in measuring $-\Delta H^{o}_{ST}$.

It has been assumed that, because experiments were performed at close to zero surface coverage, the heats of adsorption observed in these experiments approximated the isosteric heats of adsorption at finite surface coverage. However, if the adsorbate concentration becomes large enough so that the adsorption isotherm begins to deviate substantially from linearity, this approximation may become very poor. Since calculation of the possible error incurred is not possible with the information available, it is advisable to select one of the GC techniques designed to measure the isosteric heats of adsorption at finite surface coverage and apply this technique to the measurement of $-\Delta H_{ST}$ on at least one substrate, and compare with $-\Delta H^{o}_{ST}$ measured previously. Elution at Characteristic Point[37,38] (ECP) is one such technique that would require little modification of existing GC apparatus.

Although it is not yet certain that the heats of adsorption and distribution coefficients obtained by experiment were absolutely accurate, it is assumed that because the surface coverages were close to zero, that the reported values of $-\Delta H^{o}_{ST}$ and K_D were still useful for the purpose of comparing relative affinities of pyrene for the various substrate surfaces.

4.3.7 Topics for Further Study

One topic recommended for further study is the stability of column retention. Columns were observed to completely lose all retention of PAHs when exposed to air at 350°C overnight. Because subsequent degassing with helium at 350°C did not restore retention on these columns, it is not likely that loss of retention was due to simple hydration. More likely it was caused by oxidation, perhaps of strongly retentive carbonaceous particles.

If oxidation is the case, then the adsorption of PAHs onto retentive particles in a coal plant may be influenced by the oxygen content of the effluent. Normally, this effluent would be considered to be depleted of available oxygen, in much the same way that the reducing zone of a bunsen burner flame is depleted of oxygen. It would be interesting to see if mixing the effluent with a stream of hot fresh air would deactivate adsorption onto retentive particles.

More generally, the relevance of measured adsorption parameters for PAHs to the chemistry of these PAHs in the environment presumes that the properties of the fly ash samples studied in the laboratory are similar to those for fly ash particles in the ambient atmosphere. The possibility that this condition may not be satisfied and that retention of coal ashes for PAHs may be modified severely by relatively minor changes in the laboratory handling of the ashes requires additional scrutiny.

A second topic worth pursuing is irreversible adsorption. We have observed that, for injections on a column that had not been previously used, several preliminary injections were often required before any

solute peak could be observed. In the next few injections after a peak appeared, the peak usually increased in area and decreased in retention volume, until finally a reproducible chromatogram was established. This observation was attributed to gradual filling of irreversible sites. It is not possible to accurately determine the amount of irreversible adsorption simply by examining the forementioned series of injections; however, a GC technique known as Frontal Analysis[37] (FA) does allow accurate determination of irreversible adsorption and should be explored. FA, however, would require extensive modification of the GC apparatus in order to introduce a continuous stream of PAH into the column, as required by this technique. It is possible that with accurate measurement of irreversible adsorption, we might obtain a more definite explanation for the mysteriously low photochemical reactivity and low extraction recovery associated with ET ash, despite the measured affinity of pyrene for its surface being relatively small.

CHAPTER 5

OVERVIEW

5.1 Overall Evaluation of Instrumental Techniques

The vapor deposition apparatus was successful in producing samples of PAHs adsorbed on fly ashes that could be used for further study. The quantification technique using a flame ionization detector allowed the original concentration of PAH adsorbed on the ash to be measured. A less sophisticated vapor deposition technique has been described by Taskar, et al.[47] which used a modified gas chromatograph, but has not been applied to fly ash. Bjorseth, et al.[48] has also described a vapor phase coating technique in which substrate and solid PAH are enclosed in a glass tube; this device is evacuated below 0.1 torr and the temperature maintained at 50-60^{o}C. Neither of these latter techniques was used in conjunction with direct determination of original adsorbate concentration. Instead, adsorbate concentrations have typically been measured after completion of deposition by extracting with a solvent, a technique shown in this research to be far less than 100% efficient for the majority of coal fly ashes tested.

The low extraction recoveries of PAH on many fly ashes imply that the use of solvent extraction to measure photochemical decomposition of adsorbed PAHs will cause error if the unextractable PAH is photolyzed. Therefore, further investigation of the unextractable fraction is recommended. This may include developing superior extraction techniques (perhaps using supercritial fluids) and in situ analysis of adsorbed molecules (for instance, direct probe mass spectroscopy).

Heats of adsorption were measured via gas chromatography in the range of surface coverages from 0.07 to 7%. These calculations were based on the assumption that the plane of the pyrene molecule was positioned parallel to the adsorbent surface. However, Daisey[49] has estimated that the adsorbent surface area occupied by a pyrene molecule, solution-deposited on fly ash, was about one fourth of the geometric area of the pyrene molecule. She interpreted this observation as meaning that the plane of the pyrene molecule was perpendicular to the surface. If this is also true for vapor-deposited pyrene, then the surface coverages mentioned previously may be as much as four times greater than the actual surface coverages.

The precision in determining the heats of adsorption was sufficient to distinguish important trends in this parameter with the natures of the PAH and fly ash, and surface concentrations of PAH. Differences between duplicate determinations were less than ±5 kJ/mole. The standard deviation obtained by Eiceman and Vandiver[5] was 12kJ/mole for pyrene on coal fly ash. The accuracy of this chromatographic technique at higher surface coverages is expected to decrease, in which case more sophisticated chromatographic techniques are recommended.

5.2 Factors Controlling Photochemical Decomposition

Observations indicated that at least three observable parameters were associated with differences in photochemical reactivity -- substrate reflectance, extraction recovery, and heat of adsorption. In Table 5-1, the approximate relative intensity of these parameters for each substrate is listed in columns one, two, and three. The relative values -- "low," "medium," and "high" -- were assigned within a given

TABLE 5-1

Relative intensities of substrate reflectance, ΔH^{o}_{st} and extraction recovery

	1	2	3	4	5
Sub-strate	Substrate reflect.	ΔH^{o}_{st}	Extract recov.	Project react.	Observed react.(OR)
Silica	high	high	high	9	10
TX	med	med	high	7	8
AR	med	low	high	6	4
NM	med	low	na	5±1*	2
ET	med	med	low	5	1
WK	low	na	med	5±1*	2±2
KA	low	med	low	4	0
Carbon	low	na	low	4±1*	0

na: data not available
*: a value of 2±1 was substituted for missing parameter value

column according to data from Table 2-5 (pg. 31), Table 3-3 (pg, 65), and Table 4-5 (pg.117). In this Table, both the sign and magnitude of ΔH^{o}_{st} were considered, so that a "high" value refers to a more positive value and a correspondingly lower affinity of PAH for the substrate. All three parameters are thus expressed in a manner such that an increase in the parameter corresponds to an increase in photochemical reactivity.

To a first approximation, suppose that the increase in photochemical reactivity is roughly proportional to an increase in each parameter. Also suppose that the contributions from each parameter to the resulting total photochemical reactivity of a given substrate were equally weighted. Then the combined affect of the three parameters on the photochemical reactivity can be obtained by "adding" the effect of column one, two and three. This was done by substituting numerical value of "1" for "low," "2" for "med" and "3" for "high." The resulting total appears in column 4, from which the predicted order of photochemical reactivity of PAH on the various substrate is,

predicted Silica > TX > AR > NM, ET, KA

The relative photochemical reactivities observed in the photochemical decomposition experiments (referred to as "OR" in Chapter 2) are listed in column 5. From these, the observed order of photochemical reactivity is

observed Silica > TX > AR > NM, ET > KA

The good agreement between predicted and observed reactivities suggests that these three parameters involve most of the major factors that influence photochemical decomposition.

Since the order of reactivities in each column is different from the other two, we do not have the situation in which two parameters, measured differently, involve exactly the same effects. Rather, the three parameters must be at least partially independent of each other.

The substrate reflectance can be assumed to be fairly independent of the other two parameters. The extraction recovery is expected to be partially dependent on the heat of adsorption because molecules more strongly bound to the substrate surface would be more difficult to separate from the surface. However, some factors that are independent of the heat of adsorption may also affect the extraction recovery. For instance, irreversible adsorption would naturally decrease extraction recovery, but may not affect the heat of adsorption measurements because the irreversible adsorption sites would be presumably filled by preliminary injections according to the procedures in Chapter 4. Microporosity is another factor which may decrease extraction recovery over a 24-hour extraction period because microporosity is known to severely decrease the rate of desorption;[35] but during the short time span of a heat of adsorption measurement, microporous adsorption sites may appear to behave like irreversible adsorption sites, thus having little effect on the measurement. Thus microporosity and/or irreversible adsorption may be factors which do not strongly affect the observed heat of adsorption, but are responsible for a low extraction recovery. As explained in Chapter 2, microporosity may also be

responsible for a decrease in photochemical reactivity. It is therefore possible that the low extraction recovery and low photochemical reactivity associated with ET ash are a consequence of microporosity, particularly since microporosity may have been one of the three possible causes for the large "C" constant observed for ET.

In the case of AR ash, the extraction recovery and photochemical reactivity of adsorbed PAHs were both high, despite the fact that the heat of adsorption was very exothermic. AR ash was also unique in that its surface area was relatively small and its low "C" constant indicated a high degree of nonlocalization of adsorbate. Strong adsorption is usually accompanied by localization of adsorbate on the surface.[35] Knowing why AR ash was an exception to this trend would probably help explain why extraction recovery and photochemical reactivity of adsorbed PAHs were high. The small surface area of AR ash is a distinguishing characteristic of this ash that may be linked to this unusual behavior, although it is not obvious how this might occur.

The low photochemical reactivity of PAH on NM ash was attributed to a highly exothermic heat of adsorption. The high photochemical reactivity on TX ash was attributed to high reflectivity. We may also attribute the relatively high photochemical reactivity of PAHs on the very nonreflective WK ash to factors connected with its high extraction recovery, and the relatively low photochemical reactivity on ET ash to its low extraction efficiency. Thus the photochemical reactivity on each fly ash can be attributed to factors associated with one or more of the three observable parameters. The exceptions to trends between

photochemical reactivity and the parameter in question (in each chapter) are assumed to result from the effect of one or more of the remaining parameters.

5.3 Final Comments

In summary, the extent of apparent photochemical decomposition of adsorbed PAHs was observed to vary with the nature of coal fly ash substrates. Apparent decomposition on the fly ashes was generally faster than on graphitic carbon but slower than on many common laboratory adsorbents, such as aluminum, glass and silica gel. The extent of decomposition appeared to be related to substrate reflectivity and the affinity of PAHs for substrate surfaces (as measured by the heat of adsorption and percentage recovery by solvent extraction). The chemical composition of the substrate was also suspected of directly influencing decomposition, although more data concerning the concentration of elements on the ash surface and their oxidation states are needed to draw more definite conclusions.

More research on the biological aspects of adsorbed PAHs must be done before many of the conclusions discussed in this dissertation can be of practical value. For instance, knowing the factors which influence the processes of decomposition and adsorption may eventually help control these processes through more intelligent selections of coals and conditions for combustion. However, it is not yet certain how the rate of decomposition of adsorbed PAHs affects the environment. It would be naive to assume that, just because a carcinogenic PAH decomposed more rapidly on one fly ash than on another, the resulting biological risk would be diminished; rather, the biological risk

contributed by adsorbed decomposition products must also be taken into account. In addition, it is not established whether more strongly adsorbed PAHs are less biologically harmful; if a preliminary step in the formation of tumors is indeed extraction of PAH off the fly ash by physiological fluids, then more strongly adsorbed PAHs would certainly be less available for such formation. More testing of mutagencity of adsorbed PAHs is needed to answer these questions.

The discovery that solution-deposited PAHs have generally higher extraction recoveries than vapor-deposited PAHs should serve as a warning; artificially prepared samples should be produced under conditions that simulate environmental conditions as closely as possible. Some conclusions concerning adsorbed PAHs made previously by many authors using solution-deposited samples may not be valid for environmental conditions.

Some practical applications for the instrumental methods developed in this work may also extend to other types of adsorbates and adsorbents. The quantification procedure for vapor-deposited compounds would be especially useful in situations in which radiolabelled tracer methods could not be used; for instance, for rare compounds for which tracers were not available. For gas chromatographic determinations of heats of adsorption, the use of small quantities of adsorbent in columns would be useful for a series of adsorbents having a large range in retention volumes. Dilution of adsorbent with a nonadsorptive substrate would also be useful in cases in which pneumatic impedances were high.

LIST OF REFERENCES

LIST OF REFERENCES

1. C.E. Chrisp, G.L. Fischer, and J.E. Lammert, Science, 199, 73 (1978).

2. D.F.S. Natusch, Environ. Health Perspect., 22, 79 (1978).

3. R.L. Davison, D.F.S. Natusch, J.R. Wallace, and C.A. Evans, Jr., Environ. Sci. Technol., 8, 1107 (1974).

4. D.F.S. Natusch, and B.A. Tomkins, in "Polynuclear Aromatic Hydrocarbons," P.W. Jones and R.I. Freudenthal, Ed., Raven Press, New York, p. 145 (1978).

5. G.A. Eiceman and V.J. Vandiver, Atmos. Environ., 17, 461 (1983).

6. C.E. Chrisp and G.L. Fisher, Mutat. Res., 76, 143 (1980).

7. J.N. Pitts, Jr., Environ. Sci. Technol., 47, 115 (1983).

8. J. Leiter, M.B. Shimkin, and M.J. Shear, J. Natl. Cancer Inst., 3, 155 (1942).

9. B.N. Ames, J. McCann, and E. Yamasaki, Mutat. Res. 31, 347 (1975).

10. G.L. Fisher, C.E. Chrisp, and O.G. Raabe, Science, 204, 879 (1979).

11. H.E. Kubitschek and L. Venta, Environ. Mutagenesis, 1, 79 (1979).

12. M.M. Ross, "Physicochemical Properties of Diesel Particulate Matter," Ph.D. Dissertation, The Pennsylvania State University (1981).

13. J.N. Pitts, Jr., D.M. Lokensgard, R.S. Ripley, K.A. Van Cauwenberghe, L. Van Vaeck, S.D. Shaffer, A.J. Thill, and W.L. Belser, Jr., Science, 210, 1347 (1980).

14. W.A. Korfmacher, E.L. Wehry, G. Mamantov, and D.F.S. Natusch, Environ. Sci. Technol., 14, 1094 (1980).

15. M.A. Fox and S. Olive, Science, 205, 582 (1980).

16. J. Peters and B. Seifert, Atmos. Environ., 14, 117 (1980).

17. K.M. Sancier and H. Wise, Atmos. Environ., 15, 639 (1981).

18. M. Katz, C. Chan, H. Tosine, and T. Sakuman, in "Polycyclic Aromatic Hydrocarbons," P.W. Jones and P. Leber, Ed., Ann Arbor Science Publishers, Ann Arbor, Michigan, p. 171 (1979).

19. R.A. Yokley, A.A. Garrison, E.L. Wehry, and G. Mamantov, Envrion. Sci. Technol., 20, 86 (1985).

20. R. Dlugi and H. Güsten, Atmos. Environ., 17, 1765 (1983).

21. W.A. Korfmacher, "The Decomposition of Polycyclic Organic Matter Adsorbed on Coal Fly Ash," Ph.D. Dissertation, University of Illinois, Urbana-Champaign (1978).

22. J.F. Thomas, M. Mukai, and B.D. Tebbens, Environ. Sci. Technol., 2, 33 (1968).

23. T.L. Gibson and L.L. Smith, J. Org. Chem., 44, 1842 (1979).

24. J.N. Pitts, Jr., K.A. Van Cauwenberghe, D. Grosjean, J.P. Schmid, D.R. Fritz, W.L. Belser, Jr., G.B. Knudson,and P.M. Knudson, Science, 202, 505 (1978).

25. P.A. Soltys, T. Mauney, D.F. Natusch, and M.R. Schure, Environ. Sci. Technol., 20, 175 (1986).

26. T.D. Behymer and R.A. Hites, Environ. Sci. Technol., 19, 1004 (1985).

27. H. Güsten, Z. Bozicevic, and L. Klasinc, Staub-Reinhaltluft, 44, 448 (1984).

28. A.H. Miguel, W.A. Korfmacher, E.L. Wehry, G. Mamantov, and D.F.S. Natusch, Environ. Sci. Technol., 13, 1229 (1979).

29. A.H. Miguel and D.F.S. Natusch, Anal. Chem., 47, 1705 (1975).

30. R.A. Yokley, "The Photochemistry of Polycyclic Aromatic Hydrocarbons Adsorbed on the Surface of Coal Fly Ash," Ph.D. Dissertation, The University of Tennessee, Knoxville (1985).

31. W.H. Griest and B.A. Tomkins, Environ. Sci. Technol., 20, 291 (1986).

32. R.J. Lauf, "Application of Materials Characterization Techniques to Coal and Coal Wastes," ORNL/TM-7663, Oak Ridge National Laboratory, 1981.

33. W.A. Aue, P.P. Wickramanayake, and J. Müller, Anal. Chim. Acta, 125, 175 (1981).

34. G.D. Renkes, S.N. Walters, C.S. Woo, M.K. Iles, A.P. D'Silva, and V.A. Fassel, Anal. Chem., 55, 2229 (1983).

35. S.J. Gregg, and K.S.W. Sing, "Adsorption, Surface Area and Porosity," Second Edition, Academic Press, London (1982).

36. M.R. Shure, Ph.D. Dissertation, Colorado State University, Fort Collins, Colorado, 1981.

37. J.R. Conder and C.L. Young, "Physicochemical Measurements by Gas Chromatography," John Wiley and Sons, New York (1979).

38. R.J. Laub and R.L. Pecsok, "Physicochemical Applications of Gas Chromatography," John Wiley and Sons, New York (1978).

39. S. Dal Nogare and R.S. Juvet, Jr., "Gas-Liquid Chromatography," John Wiley and Sons, New York (1962).

40. S. Ross, J.K. Saelens, and J.P. Olivier, J. Phys. Chem., 66, 696 (1962).

41. S.A. Green and H. Pust, J. Phys. Chem., 62, 55 (1958).

42. R.L. Gale and R.A. Beebe, J. Phys. Chem., 68, 555 (1964).

43. M.M. Ross, T.H. Risby, S.S. Lestz, and R.E. Yasbin, Envron. Sci. Technol., 16, 75(1982)

44. R.L. Grob, "Modern Practice of Gas Chromatography," John Wiley and Sons, New York (1977).

45. W.T. Cooper and J.M. Hayes, J. Chromatog., 314, 111 (1984).

46. L.R. Snyder, "Priciples of Adsorption Chromatography," Marcel Dekker, Inc., New York, 1968.

47. P.K. Taskar, J.S. Solomon and J.M. Daisey, in "Polynuclear Aromatic Hydrocarbons: Mechanisms, Methods, and Metabolism," M. Cooke and A.J. Dennis, Battelle Press, Columbus (1985).

48. A. Bjorseth, G. Becher, M.J.W. Chang, K.L. McNeill, and G.L. Fisher, in "Polynuclear Aromatic Hydrocarbons: Mechanisms, Methods, and Metabolism," M. Cook and A.J. Dennis, Battelle Press, Columbus (1985).

49. J.M. Daisey, M.J.D. Low, and J.M.D. Tascon in "Polynuclear Aromatic Hydrocarbons: Mechanisms, Methods, and Metabolism," M. Cook and A.J. Dennis, Battelle Press, Columbus (1985).

50. B.L. Karger, L.R. Snyder, and C. Horvath, "An Introduction to Separation Science," John Wiley and Sons, New York, 1973.

APPENDICES

Appendix 2-1

Procedures for Vapor Deposition

(1) Purge system of previous PAH.

(a) Set Oven 1 "off";

(b) Set Oven 2 at 150-200^{o}C;

(c) Cell should be empty of substrate;

(d) Valve should be in "Cell" positon;

(e) Purge system 2-5 hours with N_2;

(f) Set Oven 2 "off"; and

(g) Allow to cool.

(2) Degass sample.

(a) Place sample in adsorption cell;

(b) Set Oven 2 to 150-200^{o}C;

(c) Valve should be in "cell" position;

(d) Allow sample to degass (24 hrs); and

(e) Switch valve to "bypass."

(3) Deposit PAH on sample.

(a) Set Oven 1 to generator temperature;

(b) Allow 2-5 hours to equilibrate;

(c) Switch valve to "cell" to start deposition;

(d) Deposit PAH for estimated deposition time;

(e) Stop deposition by switching valve to "bypass";

(f) Set Oven 1 and Oven 2 "off"; and

(g) Cool and remove deposited sample.

Appendix 3-1

Calculations For Diffusion and Laminar Flow

An empirical formula[50] in equation A4-1 was used to estimate the diffusion coefficients for a mixture of methane in nitrogen and a mixture of pyrene in nitrogen. Values of the molecular diffusion volumes were calculated by summing the component atomic diffusion volumes listed in a table[50] (including a component for aromatic rings).

$$D_{AB} = \frac{1.00 \times 10^{-3}\ T^{1.75}}{P\ (V_A^{1/3} + V_B^{1/3})} \left(\frac{1}{M_A} + \frac{1}{M_B} \right) \qquad \text{(A4-1)}$$

where D_{AB} is the diffusion coefficient for a mixture of A and B

T is temperature (^{o}K)
M is molecular weight
V is molecular diffusion volume

The resulting diffusion coefficients at two temperatures for methane diffusing in nitrogen comparing to pyrene diffusing in nitrogen were

	$\frac{25^{o}C}{}$	$\frac{155^{o}C}{}$ (cm^2/sec)
Methane/N_2	0.88	3.39
Pyrene/N_2	0.36	1.37

In laminar flow, molecules at the center of a stream travel faster than molecules near the walls. The velocity at a radial distance r_x from the center is[50]

$$v_x = 2v\left(1 - \frac{r_x}{r}\right)^{1/2} \qquad \text{(A4-2)}$$

where r is the radius of the stream
v is the average velocity

For methane or pyrene traveling with the same average velocity, according to equation A4-2 the spreading of their phase boundaries with pure carrier gas due to laminar flow would be equal. How much spreading would be for both of them? We can approximate the dimensions of the vapor deposition apparatus by describing it as a 50 cm long tube with an inner diameter of 0.5 cm, having a detector at the outlet. Molecules start out simultaneously from the inlet, having a volume rate of flow of 40 cc/sec. Under these conditions, the fastest molecules (in the center of the stream) would reach the detector in 0.5 min; the molecules with an average velocity would reach it in 1.0 min; and 80% of all the molecules (within a 0.45 cm radius from the center of the tube, assuming the density is constant along the radial axis) would arrive before 2.6 min. Therefore, the effects of spreading the boundary due to laminar flow would be over within 3 min. This time period is much smaller than for the spreading effects observed for pyrene. Therefore, the observed spreading effects for pyrene were not due to laminar flow.

VITA

Robert Jay Engelbach was born in Brooklyn, New York, on October 30, 1948. He graduated from Martin Van Buren High School in Queens Village, New York in May, 1966. After completing two years of college at The State University of New York at Buffalo, he left school to explore alternative lifestyles. He soon returned to a more conventional lifestyle in New Jersey, where he worked as a food technician at T.J. Lipton, Inc. while attending evening classes at Fairleigh Dickenson University, Teaneck, New Jersey. He earned a B.S. in Chemistry in May, 1975 and then attended classes at The Ohio State University, earning an M.S. in Chemistry in August, 1978. In September, 1980, he entered graduate school at The University of Tennessee, Knoxville.